GREEN SYNTHESIS OF AgNPs DISPERSED 3-ARMED GLY-LAC MACROMOLECULE MATRIX AND PLA FILM FOR ITS ANTIMICROBIAL ACTIVITIES

Yodahe Gonfa Furgasa

A Thesis Submitted to

The Department of Chemical Engineering

School of Mechanical, Chemical and Material Engineering

Presented in Partial Fulfillment of the Requirement for the Degree of Master's in Chemical Engineering (Specialization in Process Engineering)

Office of Graduate Studies

Adama Science and Technology University

October, 2021

Adama, Ethiopia

GREEN SYNTHESIS OF AgNPs DISPERSED 3-ARMED GLY-LAC MACROMOLECULE MATRIX AND PLA FILM FOR ITS ANTIMICROBIAL ACTIVITIES

Yodahe Gonfa Furgasa

Advisor: Dr. P. Selvakumar

Co-Advisor: Dr. Melaku Tesfaye

Co-Advisor: Dr. Tatek Temesgen

A Thesis Submitted to

The Department of Chemical Engineering

School of Mechanical, Chemical and Material Engineering

Presented in Partial Fulfillment of the Requirement for the Degree of Master's in Chemical Engineering (Specialization in Process Engineering)

Office of Graduate Studies

Adama Science and Technology University

October, 2021

Adama, Ethiopia

Declaration

I hereby declare that this Master Thesis entitled **"**Green Synthesis of AgNPs and dispersed within 3-Armed GLY/LAC Macromolecule Matrix and PLA Film for its Antimicrobial Activities**."** is my original work. That is, it has not been submitted for the award of any academic degree, diploma, or certificate in any other university. All sources of materials that are used for this thesis have been duly acknowledged through citation.

Yodahe Gonfa Furgasa _____ _____

Name of the Student Signature Date

Recommendation

We, the advisors of this thesis, hereby certify that we have read the revised version of the thesis entitled **"**Green Synthesis of AgNPs Dispersed 3-Armed GLY-LAC Macromolecule Matrix and PLA Film for its Antimicrobial Activities**''** prepared under our guidance by Yodahe Gonfa Furgasa submitted in partial fulfillment of the requirements for the degree of Mater's of Science in Chemical Engineering. Therefore, we recommend the submission of the revised version of the thesis to the department following the applicable procedures.

Dr. P. Selvakumar (PhD)	_____	_____
Major Advisor	Signature	Date
Melaku Tesfaye (PhD)	_____	_____
Co-advisor	Signature	Date
Tatek Temesgen (PhD)	_____	_____
Co-advisor	Signature	Date

Approval Page of M.Sc. Thesis

We, the advisors of the thesis entitled **"**Green Synthesis of AgNPs Dispersed 3-Armed GLY-LAC Macromolecule Matrix and PLA Film for its Antimicrobial Activities**''** and developed by Yodahe Gonfa Furgasa, hereby certify that the recommendation and suggestions made by the board of examiners are appropriately incorporated into the final version of the thesis.

Dr. P. Selvakumar (PhD)	_____	_____
Major Advisor	Signature	Date
Melaku Tesfaye (PhD)	_____	_____
Co-advisor	Signature	Date
Tatek Temesgen (PhD)	_____	_____
Co-advisor	Signature	Date

We, the undersigned, members of the Board of Examiners of the thesis by Yodahe Gonfa Furgasa have read and evaluated the thesis entitled **"**Green Synthesis of AgNPs Dispersed 3-Armed GLY-LAC Macromolecule Matrix and PLA Film for its Antimicrobial Activities ''and examined the candidate during the open defense. This is, therefore, to certify that the thesis is accepted for partial fulfillment of the requirement of the degree of Master of Science in Chemical Engineering.

_____	_____	_____
Chairperson	Signature	Date
_____	_____	_____
Internal Examiner	Signature	Date
_____	_____	_____
External Examiner	Signature	Date

Finally, approval and acceptance of the thesis is contingent upon submission of its final Copy to the Office of Postgraduate Studies (OPGS) through the Department Graduate Council (DGC) and School Graduate Committee (SGC).

_____	_____	_____
Department Head	Signature	Date
_____	_____	_____
School Dean	Signature	Date
_____	_____	_____
Office of Postgraduate Studies, Dean	Signature	Date

ACKNOWLEDGEMENT

This thesis becomes a reality with the kind support and help assistance of many people. I would like to express my heartfelt gratitude to each and every one of them.

First and foremost, I would like to praise and thanks GOD Almighty, who has granted countless blessing, wisdom, peace of mind and opportunity to Study my MSc. and finally, I was able to accomplish this thesis. I wish to convey my heartful gratitude to my advisor Dr. P. Selvakumar for his intellectual guidance, valuable advice on doing the experiments and preparing my thesis. Dr. Melaku Tesfaye, my Co-Advisor, deserves my deepest and heartfelt thanks for taking the time to advise and assist me through each and every stage of this study. It was a pleasure working with him. And also, I am hugely indebted to my Co-Advisor, Dr. Tatek Temesgen, for his invaluable recommendations and wise counsel regarding the topic of my research.

Thanks to my Special Parents, Dad and Mom, for the numerous times they have helped me throughout my journey in University; I believe that all of their efforts will gain something great in the near future. When times were tough, their encouragement, financial assistance, and constant prayer were much welcomed and acknowledged.

Last but not least, I would like to thank my best friends and ASTU Classmates for always being there for me when I needed them; without them, I would never have enjoyed so many opportunities.

I'm also grateful to Adama Science and Technology University (ASTU) for providing me with this chance as well as financial help for my Master's Thesis.

Table of Contents

CHAPTER Page

LIST OF TABLES

LIST OF FIGURES

Figures Page

LIST OF EQUATIONS

LIST OF ABBREVIATIONS

AgNPs	Silver nanoparticles
ASTM	American Society for Testing and Materials
CLSI	Clinical and Laboratory Standards Institute
DW	Distilled water
E/DW	Ethanol with distilled water
E. coli	*Escherichia coli*
FTIR	Fourier-transform infrared spectroscopy
GLY	Glycerol
M/DW	Methanol with distilled water
LAC	Lactic acid
P. aeruginosa	*Pseudomonas aeruginosa*
PLA	Polylactic acid
S. pyogenes	*Streptococcus pyogenes*
UV-Vis	Ultraviolet visible spectroscopy
XRD	X-ray diffraction spectroscopy

LIST OF NOTATIONS

mM	millimolar
Mg	milligram
mL	milliliters
µg	microgram
%	Percentage
H	hour
CFU/mL	Colony-forming unit per milliliter

ABSTRACT

Green nanoparticles synthesis method from leaves extract revealed full an economical, sustainable and eco-friendly method. Here we used leaf extract of Vernonia amygdalina for the synthesis of silver nanoparticles (AgNPs) as reducing and capping agents. Mixed Methanol with Distilled Water (M/DW) was selected from different solvents used for the effective extraction process. The effect of different operational parameters (Solvent ratio of M/DW, Precursor concentration, ratio of $AgNO_3$/plant extract, Temperature, Time and pH) on the synthesis of AgNPs was carried out. Among them, the effect of pH was confirmed as the dominant one that affects the chemistry of the solution. The synthesized AgNPs were homogeneously dispersed in GLY-LAC macromolecule and used as filler to prepare PLA-based biofilms.

Greenly synthesized AgNPs were confirmed using UV-Vis spectroscopy and characterized by XRD and FT-IR. Besides, its antimicrobial activities were also evaluated. The UV-Vis spectra showed specific Surface Plasmon Resonance (SPR) absorption peaks between 411 nm- 430 nm for synthesized AgNPs at optimum conditions. It revealed that the presence of AgNPs in the reaction solution. XRD peaks observed at 2θ are in the range of (30°-80°), which corresponds to the reflection of the plane of crystallinity of AgNPs. Phytochemical screening test and FT-IR analysis of V. amygdalina leaves extract revealed the existence of phenolic, Tannin, saponins and flavonoid groups, which capped the nanoparticles during the synthesis. The antibacterial activities of synthesized AgNPs were evaluated against Gram-positive bacteria (S. pyogenes and S. aureus) and Gram-negative bacteria (E. coli and P. aeruginosa) and observed that a higher zone of inhibition. This study results finally revealed that the antimicrobial activity of GLY-LAC/ PLA biofilms enhanced with the dispersion of green synthesized AgNPs. Hence, it suggests that AgNPs dispersed GLY-LAC/PLA could be used to prepare different materials for packaging wound dressing, textile industries, etc.

Keywords

Vernonia amygdalina, Phytochemical analysis, Silver nanoparticles, AgNPs/GLY-LAC bioconjugate, AgNPs/GLY-LAC/PLA biofilm.

CHAPTER ONE

1. Introduction

1.1 Background of Study

Nanotechnology has recently made significant scientific advancements in the fields of study and technology. Nanoparticles are a crucial aspect of nanotechnology. The creation of new materials at the nano-scale range between 1 and 100 nm is what a nanoparticle entails (Alara et al., 2019). Metal nanoparticles, in particular, have lately received a lot of interest owing to their unique features, including huge surface area, high stability, ease of chemical modification, increased permeability, and ease of production (Gama & Bottoli, 2018). Metal nanoparticles are synthesized using physical, chemical and biological methods (Gahlawat & Choudhury, 2019)(Velusamy et al., 2016). Physical approaches have a number of disadvantages, including a greater energy need and a lower manufacturing yield. Although the chemical approach overcomes these disadvantages, it is ecologically dangerous owing to the usage of chemicals (hydrazine or potassium bitarate). In addition to this, chemical methods have drawbacks such as toxicity, instability, and low biocompatibility (Gahlawat & Choudhury, 2019).

Biogenic materials such as plant extracts, biopolymers, and microbial sources such as bacteria, fungi, algae, and yeast are referred to as biological or green sources to synthesize metal nanoparticles. The development of biocompatible, non-toxic, and eco-friendly methods for the synthesis of nanoparticles is a topic of concern in green biological methods (Abdelghany et al., 2018). Green synthesis of plant meditated synthesized nanoparticles has attracted extensive due to their low cost, low environmental effect, zero contamination, high reducing potential. The reduction potential is due to the presence of biomolecules, which further give stability to the nanoparticles (Bordoloi et al., 2020).

Plants have been reported to contain a wide range of antioxidants and secondary metabolites (polyphenols, flavonoids, sterols, Terpenes, alkaloids, alcoholic compounds, polysaccharides, saponins, glucose and fructose, reduced co-factors and proteins/enzymes), wherein these

biomolecules work in harmony to obstruct cellular components from oxidative damage, thereby resulting in metal ion reduction to nanoparticles..

Metal nanoparticles, particularly silver nanoparticles (AgNPs), are employed in various applications because of their catalytic characteristics, localized surface plasma resonance, high conductivity, and antibacterial characteristics. Silver ions and silver-based compounds are well-known antibacterial agents and antifungal agents with a wide range of applications (Wang et al., 2016).

AgNPs have been used in a variety of degradable and non-degradable polymers as an active component for a variety of applications, including the packaging industry (food packaging industries) and biomedical fields (artificial implantation, wound dressings, and antitumor drug specifically for infectious wound treatment), which has grown dramatically in recent decades (Carbone et al., 2016). The antibacterial activity of AgNPs in a polymer film and/or the increase of the film's mechanical characteristics are two of the many uses of AgNPs in polymer film preparations.

The particles, on the other hand, are easily agglomerated. Coagulation in particles can happen as a result of increased particles contact. The three armed GLY-LAC bio-conjugate resulted from the condensation reaction of lactic acid and glycerol used as plasticizers added to the polymer solution to promote flexibility of biofilms. Here in this thesis, GLY-LAC was used to promote a homogenous distribution of AgNPs. This may avoid the agglomeration and instability of AgNPs in the base fluid. Besides, the addition of AgNPs to the polymer matrix enhances their antimicrobial activity. The antimicrobial activity of AgNPs/GLY-LAC macromolecule base matrix and AgNPs/GLY-LAC/PLA biofilm was evaluated using Gram-positive and Gram-negative bacterial species.

1.2 Statement of the Problem

From currently existing methods of nanoparticles synthesis methods great energy is needed, high operational and equipment costs, and lower manufacturing yield are some of the drawbacks of the physical method of nanoparticle synthesis. However chemical methods overcome disadvantages with a simple, efficient, and economical way of synthesis. nevertheless, toxicity, instability, and limited biocompatibility remain concerns for this method of nanoparticle production. This might encourage many researchers to look into environmentally benign, biocompatible, and stable nanoparticle production methods.

Depending on the nature of the commodity, a wide range of bacteria, molds, and yeast contamination, and infections are known to inflict mess on various items. Different infectious diseases and the deterioration of different products due to microbial contamination in the food packaging industries are undeniably major issues, resulting in considerable economic losses and health issues. In severe burn injuries, traumatic traumas, and surgical operations, skin infections are the main cause of morbidity and mortality. As a result, the rising incidence of bacterial resistance leads to severe systematic complications. This is one of the methods to have an impact on an individual's and a country's economy.

The particle-particle system's attractive molecular interactions lead the particles to draw closer together, forming an agglomeration/lump of particles. This may limit the application of nanoparticles in different matrixes. Nano-based bio-conjugates in the biofilm preparation as fillers become ultra-efficient for various applications such as heat transmission, bio-medical applications, and packaging applications by altering their suspension. Also, the majority of packaging materials used across the world are petroleum-based polymers. Plastic polymers trash has significant drawbacks in terms of posing a threat to the environment due to higher levels of toxic emissions, changes in the carbon dioxide cycle, and composting issues. The usage of nono-based biofilms could replace these limitations.

1.3 Research Questions (RQ)

RQ1. What would be the effect of solvent type and different operational parameters on the synthesis of AgNPs?

RQ2. Is it possible to use synthesized AgNPs as an antimicrobial agent?

RQ3. Can it be possible to formulate an active 3-armed GLY-LAC bio conjugate/plasticizer in which AgNPs were homogenously dispersed?

RQ.4 Can it be possible to prepare AgNPs/GLY-LAC/PLA active biofilm?

1.4 Research Objective

1.4.1 General Objective

The general objective of this thesis is the green synthesis of AgNPs dispersed with 3-armed GLY-LAC macromolecule matrix for the preparation of active PLA-based biofilm

1.4.2 Specific Objectives

- ✓ To prepare *Vernonia amygdalina* leaves extract using the suitable solvent
- ✓ To study the effects of different operational parameters on the green synthesis of AgNPs
- ✓ To characterize greenly synthesized AgNPs and study their antimicrobial activity
- ✓ To disperse AgNPs homogenously in 3- armed GLY-LAC bio-conjugate
- ✓ To investigate antimicrobial properties of AgNPs/GLY-LAC bio-conjugate
- ✓ To analyze the antimicrobial activates of AgNPs/GLY-LAC macromolecules incorporated in PLA-based biofilm

1.5 Significance of the Study

Plant-meditated synthesis was created as a green synthesis technique due to its low cost, zero contamination, and high reduction potential and stable nanoparticles. This contributes to the development of dependable, sustainable, and environmentally friendly nanoparticle synthesis processes, which helps to prevent the creation of hazardous by-products. Because of their inherent antibacterial action, plant-medicated AgNPs are employed in a variety of applications.

Due to their physicochemical properties, AgNPs play effective antimicrobial actions. A greater surface-to-volume ratio results in more surface exposure to microorganisms, resulting in stronger antimicrobial activity. Furthermore, unique characteristics like size, shape, and phases influence bacterial inactivation or death.

Here are still some gaps towards for further use of AgNPs for different applications. Suspensions of nanoparticles in the fluid make smaller particles, high surface area, and the interaction among the particles became dominant. In this research, AgNPs were homogeneously dispersed with 3-armed GLY-LAC macromolecules, which can be used for further applications. Nanoparticles dispersed bioconjugate with PLA-based biofilms are eco-friendly packaging materials and could replace petroleum-derived films.

1.6 Scope of the Study

The scope of this research was explained as follows. This research is mainly focused on the,

- Green synthesis of AgNPs using leaves extract of *Vernonina amygdalina*, locally known as Grawa.
- Effect of solvent and different operational parameters (solvent ratio, precursor concentration, volume ratios of $AgNO_3$ solution to plant extract, temperature, time and pH) on greenly synthesized AgNPs was clearly investigated.
- Characterization of greenly synthesized AgNPs and their antimicrobial activity were investigated.
- The antimicrobial activity of prepared thee-armed AgNPs /GLY-LAC bio-conjugate and as a filler in PLA-based film was also investigated.

CHAPTER TWO

2. Literature Review

2.1 Nanotechnology

Over time, Nanotechnology has gained a lot of attention. Nanoparticles are the most important aspect of nanotechnology. A nanoparticle incorporates the production of novel materials at the Nano scale range between 1 and 100 nm. Nanoparticles can be classified according to their functionalization, chemical nature, surface morphology, physic chemical property, dimension, crystallite and magnetic property (Shabina et al., 2020).Generally nanoparticles can be classified as organic, inorganic and carbon based nanoparticles as shown in the figure 2.1

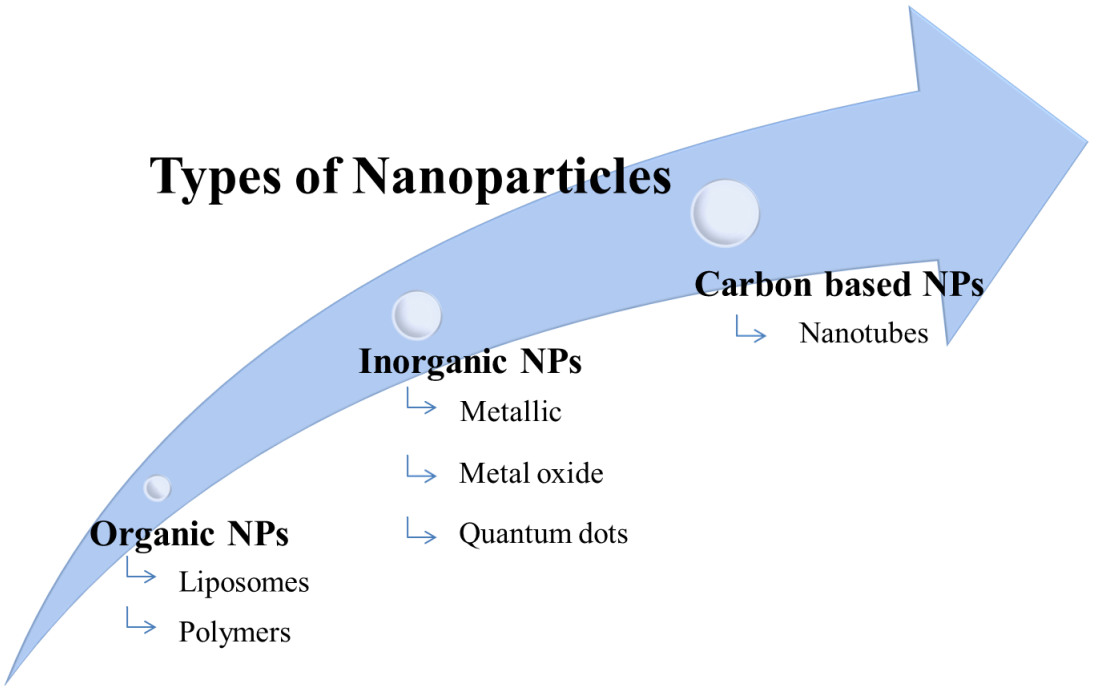

Figure 2.1 Types of nanoparticles

i. Organic Nanoparticles

Dendrimers, micelles, liposomes and ferritin, also are commonly knows the organic nanoparticles or polymers which are biodegradable and non-toxic. Liposomes are spherical vesicles made of one or more phospholipid bilayers. They are used extensively as carriers for numerous molecules in the pharmaceutical and cosmetic industries, and in the encapsulation of insoluble or unstable compounds in pharmaceutical, food, and farming industries (Akbarzadeh et al., 2013). Polymeric nanoparticles are obtained from synthetic polymers, such as polycaprolactone, polyacrylamide, and polyacrylate, or natural polymers like albumin, which improve the pharmacodynamics and pharmacokinetics properties of different drugs (Bhat et al., 2011).

ii. Inorganic Nanoparticles

From inorganic nanoparticles, Metal and Metal oxide nanoparticles are well-known types of nanoparticles. Metal-based nanoparticles are manufactured from metals to nonmetric sizes using destructive or constructive processes. Metal Nanoparticles have recently attracted a lot of attention due to their unique properties like large surface area, high stability, facile chemical modification, enhanced permeability, and easily synthesis (Gama & Bottoli, 2018). They are applicable in several areas such as drag delivery (Anderson et al., 2019)(Ivanova et al., 2018)(Siddique & Chow, 2020), Catalytic activity (Lim et al., 2016), Sensor application (Loiseau et al., 2019), energy science (X. Liu et al., 2017), cosmetic products (Lu et al., 2018), Cell imaging application (Fu et al., 2019) and antimicrobial packaging applications (Li et al., 2017).

Structurally quantum dots are made of several metal complexes such as magnetic transition metals, semiconductors, and metal. In addition to their role in a plant system, quantum dots are used in the surface coating. They also fluoresce with different colors depending on their size, and quantum dots can give a secondary coating, which improves water solubility (Nair et al., 2011).

iii. Carbon based Nanoparticles

Nanotubes are tubes in nanometer scale that belong to the fullerene structural family. They possess a hollow structure that consists of walls made of one-atom-thick sheets of carbon

(graphene). These sheets roll along at a particular angle and distinct chiral angles, the radius, and rolling angles decide the characteristics of the nanotube, that is., whether the nanotube shield is semiconductor or metal. They are classified into two types: single-walled nanotubes (SWNT) and multiwall nanotubes (MWNT) (Malik et al., 2012).

2.2 Methods of Nanoparticle Synthesis

Nanoscale structures, such as nanoparticles and nanolayers, have very high surface-to-volume and aspect ratios, making them ideal for use in various materials. There are several methods for creating nanoparticles. In general, there are three methods for preparation of metal nanoparticles, as indicated in Figure 2.2

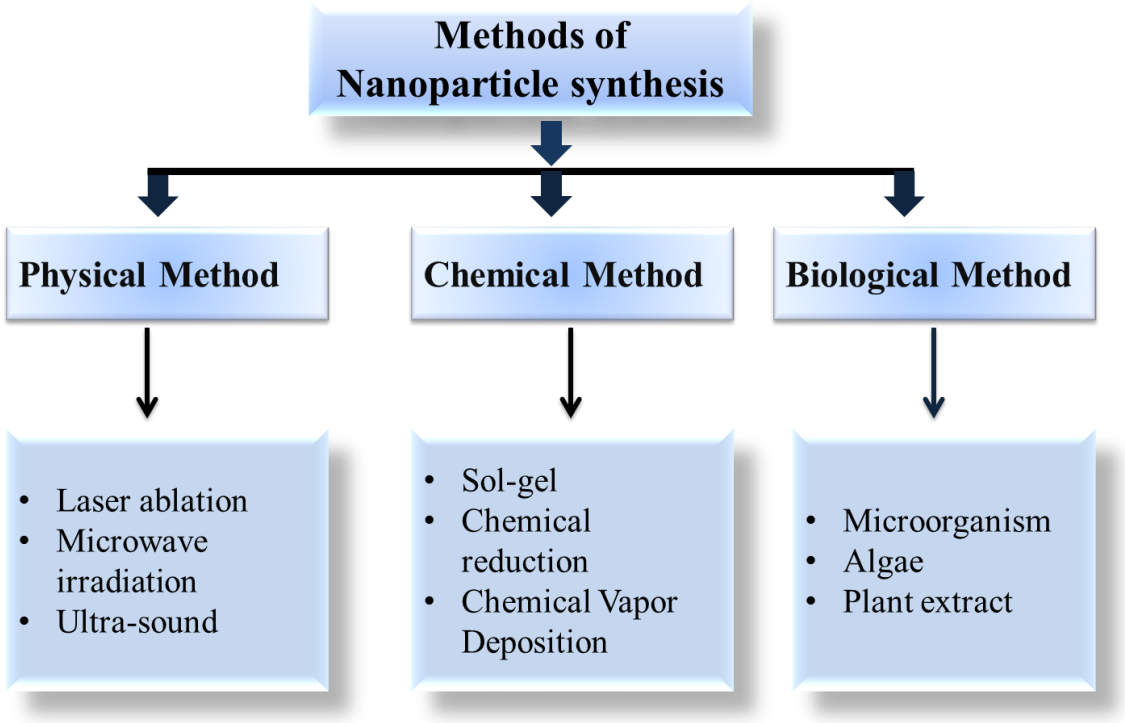

Figure 2.2 Methods for metal nanoparticle preparations

2.2.1 Physical Methods

In physical methods, metal nanoparticles like Gold, platinum, silver, titanium, zinc, cerium, iron, thallium and their compounds are synthesized by evaporation, grinding system, ultra sonication, mechanical milling and laser ablation presents as an attractive method for preparing nanoparticles. In the mechanical method ball milling system bulk powder is crushed into particle-sized by using high energy of vibrating ball mill. This method do not require several reaction steps and applicable for the large scale production of nanoparticles but requires high energy for a long period of milling (Abbasi et al., 2014).

(Rafique et al., 2019)reported Synthesis of nanoparticles using continuous wave (CW) laser has been utilize to AgNPs in the de-ionized water by comparing with pulsed laser. Pulsed laser and continuous wave diode pumped solid state laser were used for the synthesis of AgNPs in deionized water. Then the colour change was indicated formation of AgNPs. Microwave assisted organic synthesis employed in the synthesis of nanoparticles due to enhanced reaction rates, higher yields.

2.2.2 Chemical Methods

It is the most commonly known nanoparticle synthesis method; being a low cost and high yield approach. This method involves chemical reduction by using different reducing agents like Sodium citrate, Ascorbate, Sodium borohydride (NaBH4), tollens reagent elemental hydrogen. Amines, alcohols and acids are used as a surfactant to avoid particle growth and agglomeration. Toxicity, being expensive, poor reducing ability and impurity are some of its limitations of this method (Jamkhande et al., 2019).

Sol-gel method is an effective method for production of high quality of metal and metal oxide nanoparticles. This process involves conversion of monomers in to colloidal solution (sol). The solution acts as a precursor. Highly pure and transparent antimony doped tin oxide (ATO) aerogel nanoparticles successfully synthesized using sol-gel method because of it has good mechanical hardness and environmental stable. Metal nanoparticles synthesized with physica & chemical methods were discussed bellow on table 2.1.

Table 2. 1 Physical and Chemical method of nanoparticle synthesis

Synthesis method	Types of Nanoparticles	particle size (nm)	Application	Reference
Physical method				
✓ Laser ablation	AgNPs	4-14	Antimicrobial activity	(Zulina et al., 2017)
✓ Microwave assisted	PdNPs	11	Catalytic activity	(Seku et al., 2020)
✓ Ultra-sonic	AuNPs	15-40	Catalytic activity	(Bhosale et al., 2017)
Chemical Method				
✓ Sol-gel	SnO_2	13-23	Solar cell application	(Haddad et al., 2018)
✓ Chemical reduction	AuNPs	20	Water treatment	(Nebu et al., 2018)
	AuNPs	11	-	
✓ Chemical Vapor deposition	Tio_2/Ag		Antimicrobial Photo catalytic activity	(Piszczek & Radtke, 2018)

2.2.3 Biological Methods

The synthesis of metal nanoparticles may be done in a variety of ways, as shown in the above. Physical approaches have a number of disadvantages, including a greater energy need and a

lower manufacturing yield. Although the chemical technique approach overcomes these disadvantages, it is ecologically dangerous owing to the usage of chemicals (hydrazine or potassium bitarate). Chemical methods include drawbacks such as toxicity, instability, and low biocompatibility (Velusamy et al., 2016)(Gahlawat & Choudhury, 2019)

For nanomaterial manufacture, green synthesis refers to the use of biogenic materials such as plant extracts, biopolymers, and microbial sources such as bacteria, fungus, algae, and yeast. Development of biocompatible, non-toxic and eco-friendly methods for the synthesis of nanoparticles is a topic of concern in biological methods (Abdeen et al., 2018)

2.2.3.1 Plant Based Green Synthesis of Nanoparticles

Biocompatibility and huge potential of nanoparticles used for catalysts and antimicrobial agents, Plant-medicated nanoparticle production has sparked a lot of attention throughout the world. Due to their low cost, minimal environmental impact, zero contamination, high reduction potential, and stable nanoparticles, and they are more appropriate for large-scale biosynthesis than micro particles. The inclusion of biomolecules serving as a capping and reducing agent increases the rate of reduction and stability of nanoparticles, making this approach superior to others (Bordoloi et al., 2020).

Plants have been reported to contain a huge variety of antioxidants and secondary metabolites (polyphenols, ascorbic acid, flavonoids, sterols, triterpenes, alkaloids, alcoholic compounds, polysaccharides, saponins, b-phenylethylamines, glucose and fructose, reduced co-factors and proteins/enzymes), wherein these biomolecules work in harmony to obstruct cellular components from oxidative damage, thereby resulting in metal ion reduction to nanoparticles. The major portions of plants where nanoparticles are synthesized include leaves and roots, stems, fruits, and flowers. Organs/tissues of plant and parts of used for green synthesis of metal nanoparticles were described as shown in the figure 2.3.

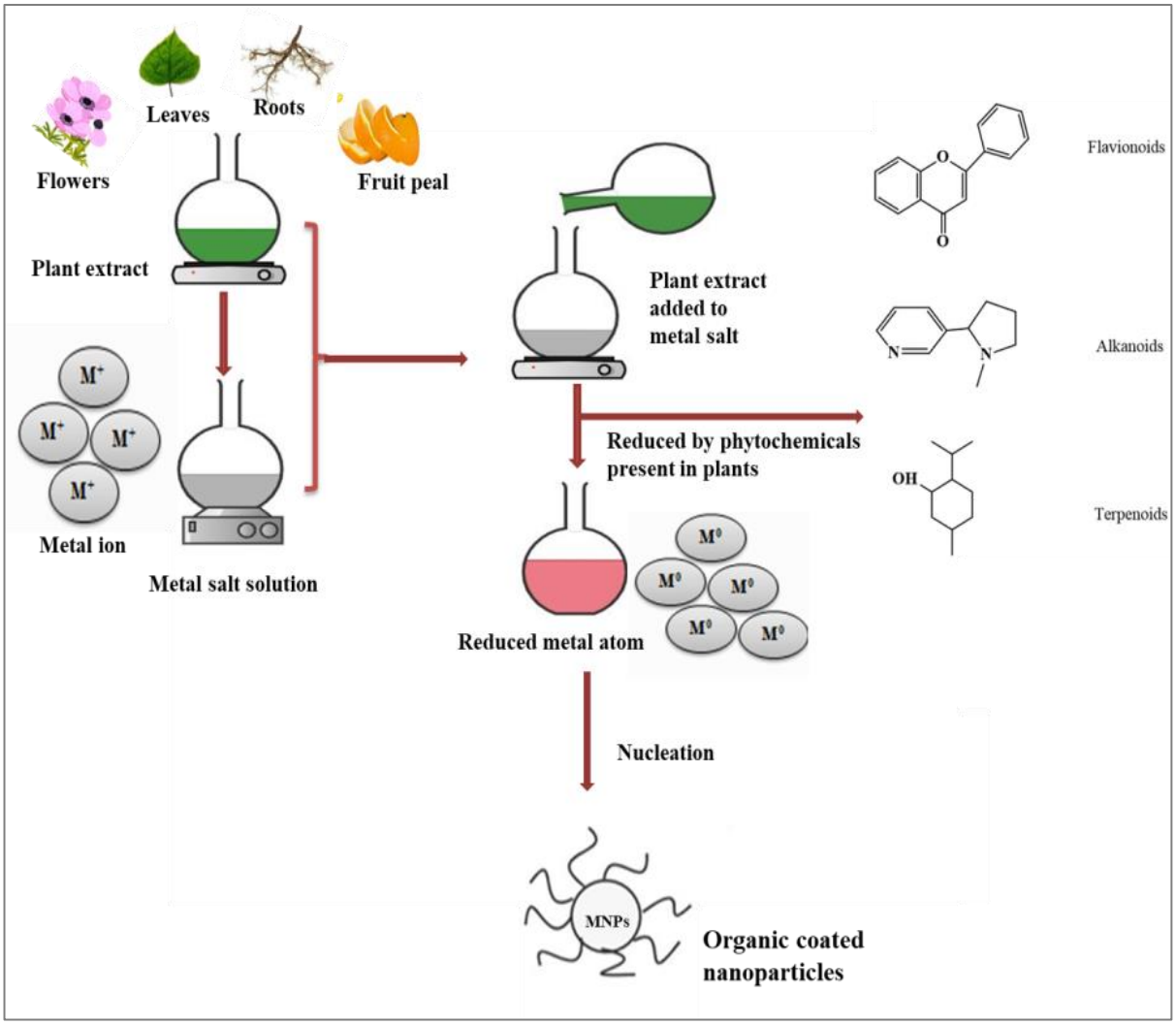

Figure 2.3 Plant based nanoparticle synthesis

Plant leaves obtained very easily and can be used as reducing and stabilizing agent to synthesis metal nanoparticles due to their high content of phytochemical components. Factors like Concentration of metal salt, Concentration of plant leaf extract, temperature, Contact time, PH are affect the synthesis and yield rate and stability of nanoparticles (El Shafey, 2020).

2.3 Green synthesis of Silver Nanoparticles

In this method presence of biomolecule acting as Capping and reducing agent and advantageous over other methods by increasing the rate of reduction and stabilization of nanoparticles (Bordoloi et al., 2020). Plant leaves have been reported to contain a huge variety of antioxidants and secondary metabolites (polyphenols, ascorbic acid, flavonoids, sterols, triterpenes, alkaloids, alcoholic compounds, polysaccharides, saponins, b-phenylethylamines, glucose and fructose, reduced co-factors and proteins/enzymes), wherein these biomolecules work in harmony to obstruct cellular components from oxidative damage, thereby resulting in metal ion reduction to nanoparticles for example for the reduction of silver nitrate salt solution to silver nanoparticles (Ag^0).

Among many metallic nanoparticles used in biomedical applications, AgNPs are one of the most important and intriguing. Physical and chemical properties of AgNPs which include optical, electrical, and thermal capabilities, as well as strong antimicrobial activates they have been utilized for a variety of applications, such as sensory application, cell imaging, textile, cosmetics, dye degradation, food packaging application, antioxidant and antimicrobial agents. AgNPs its role as a disinfectant and antimicrobial agent has been given considerable application (Shabina et al., 2020) .

2.3.1 *Vernonia amygdalina*

The presence of phytochemicals with anti-inflammatory and therapeutic effecst natural goods have long been recognized for their vital role in human health as food and medication. *Vernonia amygdalina* is a tropical African shrub belongs to Asteraceae family. it is used to make a variety of traditional remedies in West Africa (Odukoya et al., 2019). *V. amygdalina* in Ethiopia locally called Grawa in in Amharic. It is quite commonly used in Ethiopia to preparation of local beer and traditionally used in to treat various diseases. Due to its bitter test *V. amygdalina* called bitter leaf due to anti nutritional factors such as alkaloids, saponins and tannins (Habtamu & Melaku, 2018).

Figure 2.4 Fresh *Vernonia amygdalina* plant leaves

A phytochemical is phytonutrient that are naturally occurring in plants. The phytochemical studies had resulted in the isolation of Flavonoids, Saponins, Alkaloids, Tannins, Phenolic, Terpenes, Steroidal glycosides, triterpenoides and several sesquiterpene lactones. this phytochemical components are responsible for the reduction of metal salt and coating of the nanoparticles.

2.4 Silver Nanoparticles and their Application on Biofilm

Silver nanoparticles are increasingly used for several applications including antibacterial agents, in industrial, household, health care-related products, in consumer products, medical devise coating, pharmaceuticals industries, would dressing, packaging and food industries (Alaqad & Saleh, 2016).

2.4.1 Bio-Polymer Films (Polylactic acid)

Bio-polymers are long chain compounds consists of monomeric units that are covalently bonded to form larger molecules. Some of bio-degradable materials used for different applications are cellulose, starch, PLA, PHB, PHBV, and PHA (B. Hassan et al., 2018).

Recently experts have concerned on polymer materials which have significant drawbacks in terms of posing a threat to the environment due to higher levels of toxic emissions, changes in the carbon dioxide cycle, and composting issues. Basically, films and coating obtained with the use of biopolymers could maintain the quality, serve as gas and solute barriers and complement other types of packaging by improving the quality and extending the shelf-life (Kraśniewska et al., 2020).

PLA is a lactic acid-derived a linear aliphatic thermoplastic polyester. PLA with a low molecular weight is made by poly-condensing lactic acid directly. The azeotropic condensation polymerization of lactic acid has also been used to produce high molecular weight PLA. [Lactic acid is often produced by bacterial fermentation or petrochemical synthesis. PLA is made by condensation polymerizing D- or L-lactic acid or by ring-opening polymerizing lactide monomer made from lactic acid (Muller et al., 2017). Incorporating active compound and Nano fillers in PLA film helps to improve their limitations like toughness, deformation at break, thermal properties and antimicrobial properties (Li et al., 2017).

(Heydari-Majd et al., 2019) reported PLA packaging film supplemented with Zno NPs, ZEO and MEO essential oils of film. It helps to extend shelf life of O. rubber fish up to 16 day using Nano-fillers. PLA/Zno/Essential oil exhibit higher antimicrobial effect than PLA/Zno composite film. Due to hydrophobic nature of PLA polymer PLA/PEG, PLA/PEG/Zno_{100}, PLA/PEG/Zno_{50}, PLA/PEG/Ag-Cu film indicate there were no synergetic effect of nanoparticle (Ahmed et al., 2017). PLA/ AgNPs film showed strong antibacterial and antiviral activity in vitro with increasing effect at higher concentration of silver (Martínez-Abad et al., 2013)

2.4.2 Silver Nanoparticle as A Filler in Bio-Polymer

Nano-composite technology may overcome some limitations like the brittle, hydrophilic, and antibacterial properties of biopolymer-based materials. Biopolymers can be made in large quantities at relatively cheap cost, are environmentally acceptable, and form film products with low oxygen permeability. Many studies aimed at enhancing the physical, thermal, and mechanical characteristics of biopolymer-based packaging sheets have found substantial

improvements (B. Hassan et al., 2018). Weak mechanical characteristics of biopolymers and their susceptibility to moisture are generally connected with limitations in their usage.

AgNPs' antimicrobial properties have sparked interest in packaging and medicinal applications such as wound dressings, implantation, and anticancer drugs, particularly as a therapeutic option for infected open wounds (Pansara et al., 2020). AgNPs are particularly significant nanoparticles, which are novel chemicals combined into a polymer matrix to generate revolutionary Nano composites materials. Furthermore, AgNPs have antibacterial capabilities against a variety of pathogens, including bacteria, yeast, and mold. Some of application of AgNPs in the bio-polymer matrix was illustrated on Table 2.2

Table 2.2 Antimicrobial activity of various biopolymer matrix containing silver nanoparticles

Polymer Matrix	**Tasted Strain**	**Anti-microbial activates**	**Reference**
Cellulose Nano fiber /Starch	*E.coli* and *S..aureus*	Native starch film did not form an inhibition Zone. Width of CNF-AgNPs/starch 5mm and 6.3 mm for the two bacteria	(Yuan et al., 2021)
Fish skin Gelatin-	*L. monocytogenes* and *Salmonella typhimurium*	FSG shows no antibacterial activities for both bacteria, 0.5% Ag-Cu NPs showed no antibacterial activity, however 1-4% demonstrated wide variations in their antibacterial Activity	(Arfat et al., 2017)
PVA/starch/	*E.coli* and *S. aureus*	Poly-vinyl alcohol/starch with essential oil is inactive for both bacteria. PSt-AgNPs 0 wt% OEO 8.06± 0.59 for S. aureus and PSt-AgNPs 0 wt% OEO 0.87± 0.33for E.coli	(Srikhao et al., 2021)(Srikhao et al., 2021)

Chitosan	*S. aureus*, *P. aeruginosa*, Clinical strains (MRSA 10 and MRSA 11)	This shows good antimicrobial effect in all bacteria s.aureus (17.25 ± 0.96), p.aeuginosa (18.33 ± 0.93), MRSA(20.50 ± 0.58), MRSA (14.33 ± 0.29) for Quench® cream (silver sulfadiazine 1%, Q+) were used as positive control	(Shah et al., 2018)
Chitosan/mesoporous SBA-15	*S. aureus*, *P. aeruginosa* *S. epidermidis*	The film shows good antimicrobial activities with inhibition zone of Net film (0,7,7 mm), film/Ag(5) showed (7.5, 7.7 and 7 mm against *P. aeruginosa*, *S. epidermidis* and *S. aureus* respectively	(Ambrogi et al., 2014)

2.5 GLY-LAC Bio-conjugate

Three armed Glycerol-Lactic acid (GLY-LAC) are a type of evolved branching polymer with a hyper branched core and liner arms. Since the 1940s, glycerol has been produced from petroleum resources and, more recently, as a by-product of the biodiesel industry. Crude glycerol is glycerol that comes from the biodiesel business and contains varying quantities of methanol, salts, and free fatty acids (Coativy et al., 2016). Furthermore, advanced biodiesel manufacturing systems that use the best feedstock have had inconsistent outcomes, and glycerol the main waste – remains a major bottleneck in the biodiesel production chain. As a result, finding new uses for glycerol is crucial to guaranteeing the global biodiesel industry's long-term survival (Monteiro et al., 2018).

Lactic acid is a chemical platform that can be biotechnologically produced from agricultural residues, waste and byproducts. Lactic acid is the simplest 2-hydroxycarboxylic acid with chiral carbon atom exist in two optically active stereo isomers (L and D enantiomers) used for production of biodegradable and biocompatible Lactic acid polymers (Krull et al., 2020).

Glycerol is a polyol molecule with many applications in different industries, due to its non-toxic, biodegradable, colorless and highly stable. Macromolecules are a polymer that could have a branched or cross-linked structure. Subjected to the intermolecular linkage between the individual chains (Goyal et al., 2021)

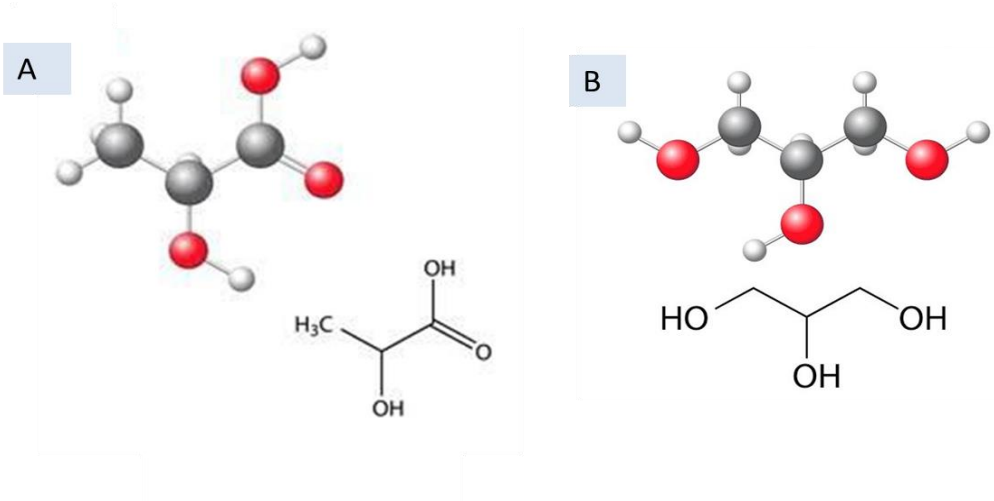

Figure 2. 5 Chemical structure of Lactic acid (A) and Glycerol (B)

The reaction between Glycerol and lactic acid is between the three OH groups of Glycerol is to react with 3-molecules of Lactic acid via condensation reaction. In this case there is possibility of ester bond formation. This bond is formed by either the reaction between the hydroxyl group of glycerol with carboxyl group of lactic acid or by the reaction between the hydroxyl groups of one lactic acid monomer. Figure bellow shows that schematic structure of 1-12 GLY-LAC bio conjugate.

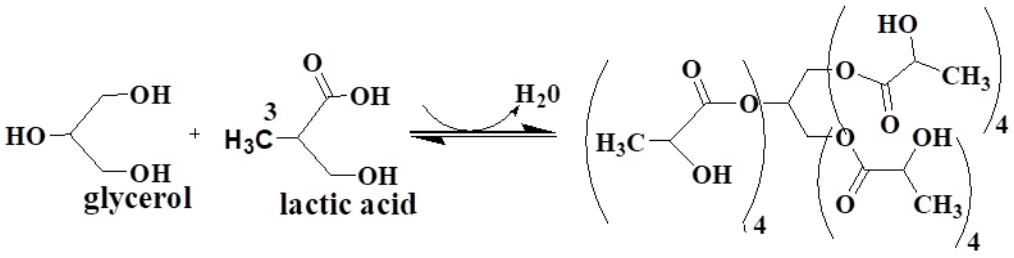

Figure 2. 6 Chemical structure for GLY-LAC (1:12 ratio) bio-conjugate

CHAPTER THREE

3. Material and Methods

3.1 Materials and Chemicals

Materials/Equipment

Vernonia amygdalina leaves were collected from Adama Science and Technology University premises, Ethiopia. The glassware such as Beakers, Measuring Cylinders, Conical Flasks, Round Bottom Flasks, Funnels, Petri Dishes, Test Tubes, Centrifuge Tubes, Samples Holder, Condenser, Cotton and Whatman No. Filter Paper and the instruments, namely Electronic Mass Balance, Blender, Sieves, Magnetic Stirrer with Hot Plate, Hot-Air Oven, Centrifuge, Cooling Incubator, Ultra-Sonicator were used for performing various experimental works in this study. For analysis purposes, UV-Vis Spectroscopy, X-RAY Diffraction (XRD) and Fourier-Transform Infrared Spectroscopy (FT-IR) have been used.

Chemicals

Silver nitrate ($AgNO_3$), ferric Chloride, Mercury (II) Chloride, potassium Iodide, ethanol (C_2H_6O, purity ≥ 99.9%), methanol (CH_3OH, purity ≥ 99.85%), ethyl acetate, n-hexane, Dichloromethane, sulfuric acid (H_2SO_4, 99%), chloroform, sodium hydroxide (NaOH, purity ≥ 97%), hydrochloric acid (HCl, 37%), L-Lactic acid (88% aqueous solution), Glycerol (99%), Film grade luming LX175 PLA and distilled water were used for different stages of this study. All the chemicals, reagents, and equipment used to carry out various procedures and characterize the samples were analytical grade and standard Laboratory tools.

3.2 Methods

3.2.1 Sample Collection and Preparation of *V. amygdalina* Powder

The fresh leaves (*V. amygdalina*) were collected from Adama Science and Technology University premises and immediately transferred to the Laboratory. The required mass of leaves was thoroughly washed once with tap water and then washed twice with double distilled water to remove debris and dust particles. Subsequently, the cleaned leaves were

shade dried at room temperature for one week to reach constant weight. The dried leaves were crushed into powder using POLYMIX® PX-MFC 90D laboratory miller, equipped with hammer grinding attachment and sieve with 0.2 mm mesh. The prepared powder was packed with an airtight container and stored under dry conditions for further use. The overall procedure of powder preparation from *V. amygdalina* leaves is illustrated in Fig. 3.1.

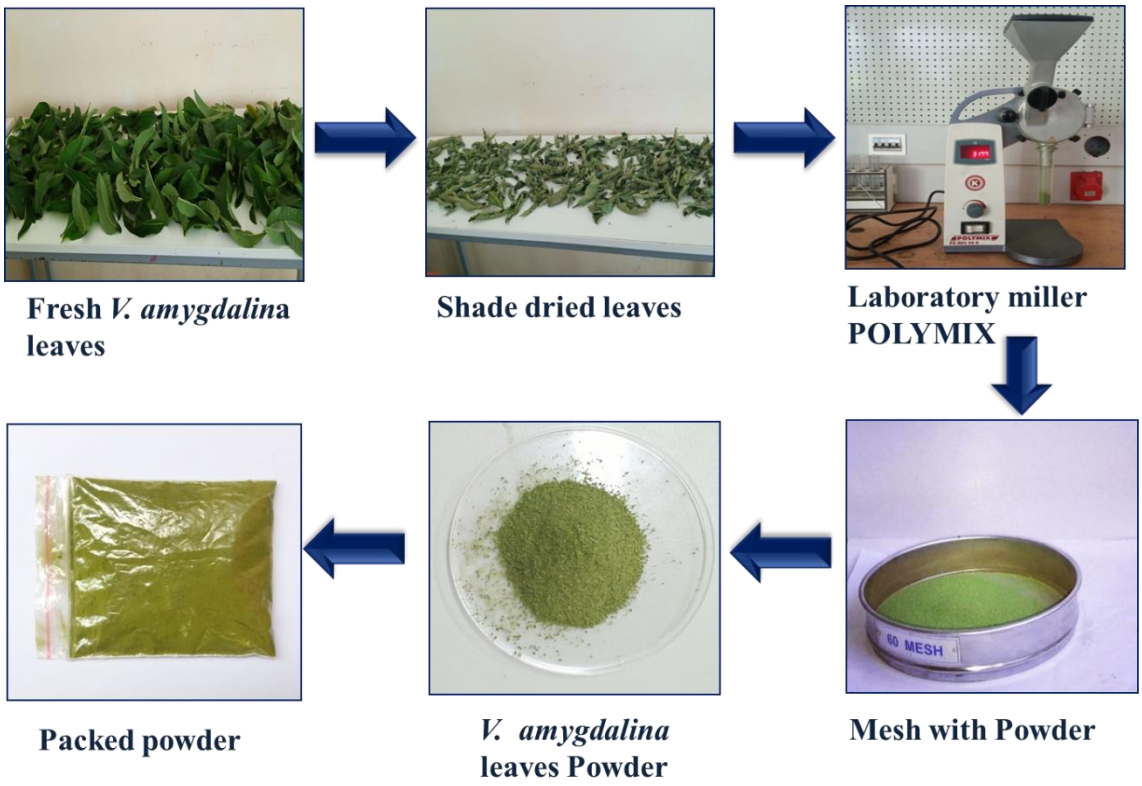

Figure 3.1 The diagrammatic representation of *V. amygdalina* leaves powder preparation

The moisture content of shade dried leaves powder was determined using a standard procedure (American Society for Testing and Materials (ASTM D4442)). For this, one gram of powder was taken in a clean, dried, and pre-weighed Petri dish. The sample plate was kept in an oven at 105 ^{o}C for 2 h. After that, the sample was cooled and reweighted. The moisture content of the powder was calculated using equation 3.1.

Moisture Content (%) = $\frac{W1-W2}{W1} * 100$ ……Equation 3.1

Where

W1 = Initial weight of the sample (g)

W2 = Final weight of the sample (g)

3.3 Green Synthesis of Silver Nanoparticles (AgNPs)

Green-based nanoparticle synthesis is a biologically mediated process in which biologically active compounds acting as a capping or stabilizing agent. In this study, the green synthesis of AgNPs was performed using leaves extract of *V.amygdalina* and metal salt ($AgNO_3$) with the help of a magnetic stirrer equipped with a hot plate. The overall procedure of synthesis of AgNPs is illustrated in Fig. 3.2

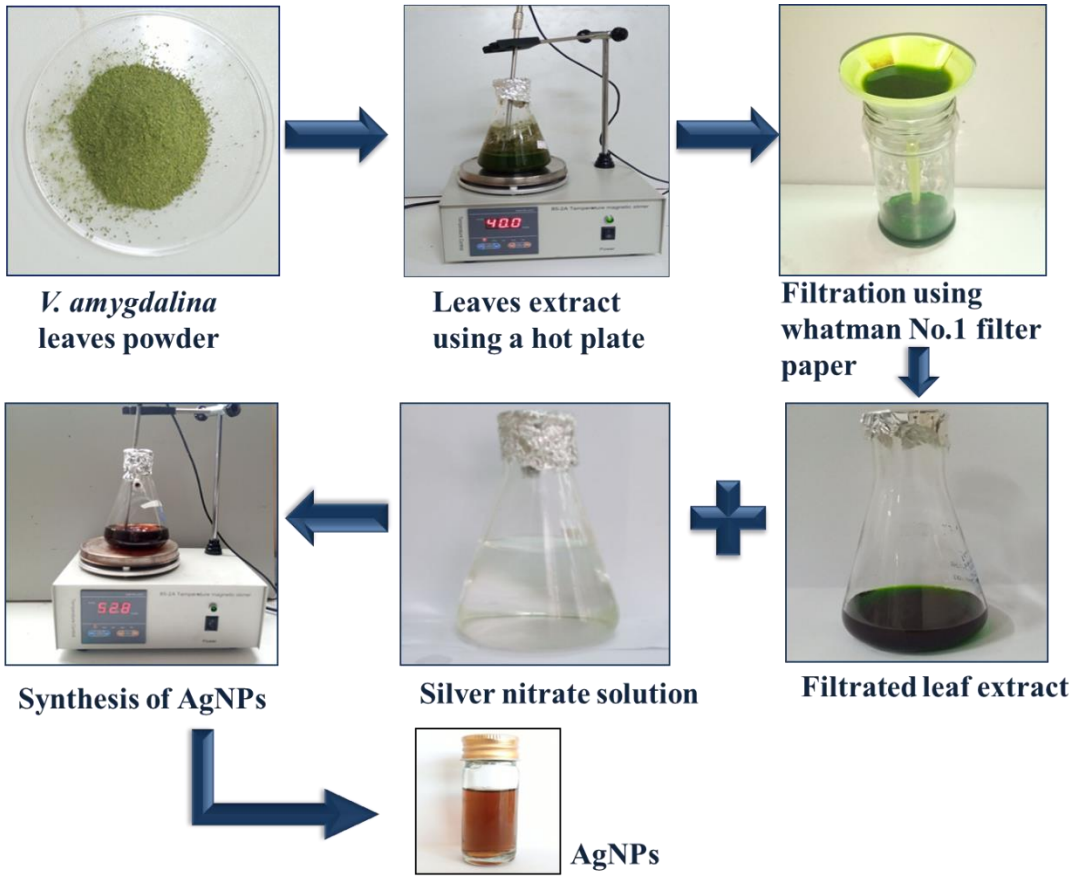

Figure 3.2 Stages in the preparation of AgNPs using *V.amygdalina* leaves extract

3.3.1 Solvent Selection for Extraction Using Plant Leaves

Different solvents exhibit different effects on the extraction of bioactive compounds of various biomasses. Hence, the extraction was carried out with different solvents such as distilled water, ethanol, methanol, ethanol with distilled water (1:1, v/v) and methanol with distilled water (1:1, v/v) using prepared *V. amygdalina* leaves powder. Two grams of dried powder were taken in a 250 mL screw-capped Erlenmeyer flask containing 100 mL of solvent to conduct the extraction. The sample flask was kept at 40 °C for 1 h under constant stirring. Then, the obtained mixture was filtered using Whitman No.1 filter paper and the obtained filtrate (extract) from each solvent was separately used to synthesize the AgNPs.

The AgNPs were synthesized by adding 50 mL of extract in 250 mL Erlenmeyer flask containing 50 mL of 5 mM $AgNO_3$ solution and the sample flask was kept at 50 ^oC for 1 h under constant stirring using a magnetic stirrer (Aisida et al., 2019). The synthesized AgNPs were confirmed using UV-Vis spectrophotometer. Based on the results observed by the UV-Vis spectrophotometer, the suitable solvent was selected and used for further experiments.

3.3.2 Study the Effect of Operational Parameters on the Synthesis of AgNPs

In the synthesis of metal nanoparticles, various factors need to be maintained at an optimum condition to attain the desired quality of products. In this study, the effect of various operational parameters such as solvent ratio, precursor concentration, volume ratios of $AgNO_3$ solution to plant extract, temperature, time and pH was analyzed for different ranges on the AgNPs synthesis.

3.3.2.1 Effect of Solvent Ratio

Methanol with distilled water (1:1, v/v) was selected as a suitable solvent mixture. Different methanol to distilled water (M/DW) ratios such as 30/70, 40/60, 50/50, 60/40 and 70/30 were used to study their effect on the AgNPs synthesis. Other parameters, namely concentration of biomass (2 g), temperature 40 ^oC and time 1 h, were kept constant while conducting the experiments for all solvents ratios. The obtained extract from each experiment was used for the synthesis of AgNPs separately using standard procedure and the synthesized AgNPs were analyzed UV-Vis spectrophotometer.

3.3.2.2 Effect of Precursor Concentration

The precursor concentration affects the NPs characteristics, namely shape, size, stability, and concentration of NPs in the sample (Saxena et al., 2016). As a result, the precursor ($AgNO_3$) concentration was varied from 1 to 10 mM to study their effect on the AgNPs synthesis. The experiment was conducted separately for each precursor concentration by adding 50 mL of extract in a 250 mL Erlenmeyer flask containing 50 mL of precursor solution and kept it at 50 ^oC for 1 h under constant stirring. The synthesized AgNPs were confirmed using UV-Vis spectrophotometer. Based on the results observed by the UV-Vis spectrophotometer, the suitable precursor concentration was selected and used for further experiments.

3.3.2.3 Effect of $AgNO_3$ Solution and Extract Volumes

The volume Reaction ratio of $AgNO_3$ to plant extract, which serves as reducing and stabilizing agent affects the concentration of Ag^+ reduced to Ag^0 (Dada et al., 2018). Due to this 5mM $AgNO_3$ solution to extract volume ratio was varied as (10/90, 20/80, 30/70, 40/60, 50/50, 60/40, 70/30, 80/20, 90/10, v/v). Then the experiment was done at 50 ^oC for 1 h under constant stirring and other parameters may kept constant. The synthesized AgNPs were confirmed using UV-Vis spectrophotometer. Based on the results observed by the UV-Vis spectrophotometer, the suitable volume ratio was selected and used for further experiments.

3.3.2.4 Effect of Temperature

Temperature is a potential controlled parameter that affects the growth of AgNPs by controlling the reaction kinetics of the synthesis process (Rose et al., 2019). Effect of synthesis temperature was studied at 30°C, 40°C, 50°C and 60 °C. The experiment was conducted separately by adding 20 mL of extract in a 250 mL Erlenmeyer flask containing 80 mL of precursor solution and kept it for 1 h under constant stirring. The synthesized AgNPs were confirmed using UV-Vis spectrophotometer. Based on the results observed by the UV-Vis spectrophotometer, the suitable temperature was selected and used for further experiments.

3.3.2.5 Effect of Synthesis Time

Most of the time, synthesis time or reaction stirring time were related to temperature and had great effects on nanoparticle synthesis. Reaction time or contact time was done by the varying time taken for the formation of nanoparticles (Adewumi et al., 2018). The reaction time of synthesis was varied as (15 min, 30 min, 40 min, 65 min, 90 min). The experiment was conducted separately at different times by adding 20 mL of extract in a 250 mL Erlenmeyer flask containing 80 mL of precursor solution and kept it at 30°C under constant stirring. The synthesized AgNPs were confirmed using UV-Vis spectrophotometer. Based on the results observed by the UV-Vis spectrophotometer, the suitable temperature was selected and used for further experiments.

3.3.2.6 Effect of pH

Another important parameter that affects the formation of AgNPs is pH of the solution. Change in pH of the solution affects the concentration of AgNPs formed by altering the charge of the bioactive components of leaves extract (Verma & Mehata, 2016). The pH of the reaction was studied using different pH where the reaction pH was maintained at 4.0, 5.0, 6.0, 7.0, 8.0, 9.0, 10.0, 11.0 and 12.0. The pH was adjusted drop-wise by using 0.1 N HCl or 0.1 N NaOH. The synthesis was performed by adding 20ml of extract into a 250 ml Erlenmeyer flask containing 80 ml of precursor solution, Then the NaOH was added drop wise under constant stirring. The synthesized AgNPs were confirmed using UV-Vis spectrophotometer. Based on the results observed by the UV-Vis spectrophotometer, the pH was selected and used for further experiments.

3.3.3 Synthesis of Powdered AgNPs

The synthesized AgNPs at the optimum conditions, the Colloidal AgNPs are needed to be purified from unconverted Silver ions and some impurities. Getting a high yield of powder AgNPs at optimum conditions were also needed to be considered. Then purification using Centrifuge were done for AgNPs synthesized at pH 7 and 5. This process is described in figure 3.3.

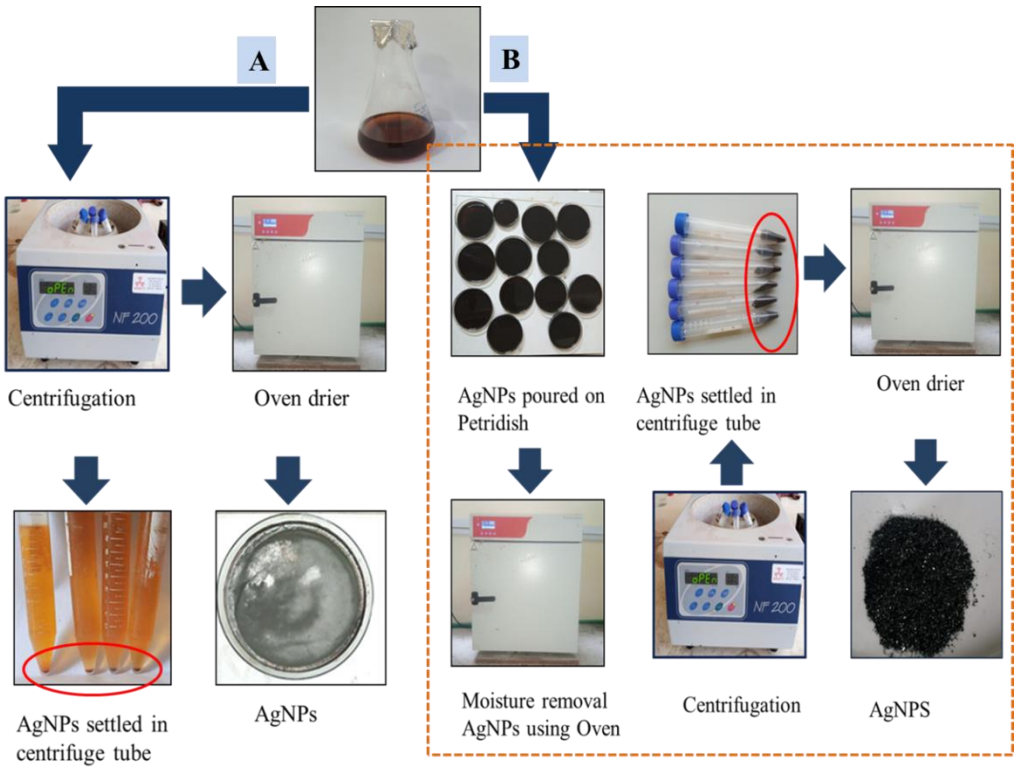

Figure 3.3 preparation and separation technique for powder AgNPs

According to figure 3.3 (A) showed that the synthesized AgNPs in the solution were transported to sterile 15 ml centrifuge tubes that had been pre-weighed. The nanoparticle-filled centrifuge tubes were put into the centrifugation machine's holes (NF 200 Bench Top Centrifuge). The particles were centrifuged for 2 h at 5000 rpm. Then, to eliminate any contamination, Petridish was rinsed with distilled water. AgNPs that had settled were put onto Petridish and dried in the oven (Moodley et al., 2018)

Anew method was proposed for getting high yield of nanoparticles as indicated on figure (B). The prepared AgNPs at the optimum conditions, first poured in to the Petridish and putted in to the Oven at 40 ^{0}C. When the solvent were evaporated after 12 h, again the solution was poured. This was repeated 5 to 10 times to collect the powder. The nanoparticles were filled in to centrifuged tube and centrifuged for 2 h at 5000 rpm. Then after centrifugation, it was dried in an oven. The image depicts our efforts to obtain or gather higher amounts of AgNPs.

3.4 Characterization of *Vernonia amygdalina* Leaf Extract

3.4.1 Phytochemical Screening of Extract

Phytochemical Screening for the extraction helps for the identification of bioactive compounds like phenolic, Saponins, Flavonoids, Tannins, and Terpenoids, alkaloids, Cardiac glycosides and Anthraquione glycosides. Phytochemical screening tests of *V.amygdalina* leaf extract were carried out on the selected 40/60 (M/DW) plant extract. The phytochemical screening was done using the following standard procedures to identify the constituents (Usunobun & Ngozi, 2016)(Gul et al., 2017).

i. Test for Phenolic Compounds

1 ml of plant extract was transferred to the test tube and diluted to 2 ml of distilled water. To this, a few drops of neutral 10% ferric chloride solution were added. The dark green color indicates the presence of phenolic compounds.

ii. Test for Saponins

The test for the presence of saponins is known as the frothing test. About 5 ml of extract, 5 ml of distilled water were added to the test tube and shaken while heating to boil. Appearance of a foam like, when frothing was mixed vigorously with few drops of olive oil showed the presence of saponins.

iii. Test for Flavonoids

The Phytochemical test for flavonoids was done by using Alkaline Reagent Test. Here, 2 ml of 2.0% NaOH mixture was mixed with aqueous plant leaves extract.a concentrated yellow color was produced, which became colorless when we added 2 drops of diluted acid to the mixture. This result showed the presence of flavonoids.

iv. Test for Tannins

1 mL of plant extract was transferred to the test tube by using a dropper. 2 mL of 5% ferric chloride was added. The formation of dark blue or greenish-black will be observed in the presence of tannins.

v. Test for Terpenoids

5ml of plant extract sample was transferred to a test tube and treated with 2ml of chloroform after and evaporated on the water bath then boiled with 3 ml of H_2SO_4 concentrated. If a grey color was formed,it showes the presence of terpenoids.

vi. Test for alkaloids

1ml of the extract was stirred with 1% HCl on a water bath for 5min and filtered. This filtrate was divided into three equal parts. To one portion of filtrate, Mayer's reagent (the mercury (II) chloride solution was added by potassium iodide) 1ml. The formation of orange-colored precipitate gives an indication of the presence of alkaloids.

Vii. Test for glycosides

According to Salkowski's Test, 1 ml of plant extract sample was added to the taste tube. Then added 2 ml H_2SO_4 concentrated to the whole aqueous plant extract. A formation of reddish-brown color is an indication of the presence of steroidal aglycone part of the glycoside.

3.4.2 Thin-Layer Chromatography (TLC)

Commercially available Thin-layer chromatography stationary phase is a thin layer of material (sorbent) was used. A Silca gel-based coated –TLC sorbent was used. A small spot of our extract solution was applied on the TLC plate 0.5 cm from the bottom marked by line ruled using pencil near one end of stationary phase with the initial zone. After the sample spotted on the plate was dried, the TLC plate was inserted into the chromatography tank (I. A. Hassan et al., 2015). The dried end of the stationary phase with the initial zone was placed into a mobile phase. The number of components was determined as the solvent moved upward using mobile phase solvents with different ratios. Ethyl acetate mixed with n-hexane and Dichloromethane mixed with methanol are solvents used. For ethyl acetate ; n-hexane (4;6, 2;8, 1;9, 7;3, 3;7 and 3;2) v/v ratios were used inside a closed chamber. Also, for dichloromethane: Methanol (3:2, 2:3, 3:7 and 7:3) was used. The chromatography was developed at the appropriate ratio on the two solvents. When the mobile phase has moved an appropriate distance, the stationary phase is removed. Then the spot or the zones were detected under UV at 360 nm light. The compound identification from TLC is based initially on a comparison of RF (Retention Factor) using equation 3.1.

$$RF = \frac{disstance\ moved\ by\ solute}{distance\ moved\ by\ mobile\ phase\ front} \quad \text{..... Equation 3. 2}$$

3.4.3 Fourier Transferred Infrared Radiation

IR spectroscopy is a characterization method deals with the vibration of chemical bonds in the molecule at various frequencies depending on the type of bonds (Zienkiewicz-Strzałka et al., 2017).

Sample preparation for plant extract was done by using 40/60 (M/DW) based extract. 500ml of filtrated plant extract was put in a beaker then placed in an oven at 40 ^{o}C for 4 days until it was dry. Then the crude extract, which is left at the bottom of the beaker, was characterized using FT-IR. Fourier examined the surface functional group of *V. amygdalina* Plant extract transferred infrared radiation (FTIR) with model name FTIR- 6600 type A and serial number A013861790. FTIR energy corresponding to these transitions corresponds to the infrared region (4000 with total reflectance (ATR) model in the range of 4000 to 400 cm^{-1} with $4cm^{-1}$ resolution and 64 scan rates.

3.5 Characterization of Green Synthesized AgNPs

Characterization study of nanoparticles has been done to characterize the size, crystal structure, shape, quantity of particles, elemental composition and physical properties of nanoparticles. The size distribution, surface charge, degree of aggregation, the surface area may affect the application of nanoparticles (Mourdikoudis et al., 2018). Here UV-Vis spectroscopy, XRD, FTIR, and antimicrobial activities of AgNPs were characterized as follows.

3.5.1 Ultraviolet-visible Spectroscopy

UV-Vis molecular absorption spectroscopy is an analytical technique based upon the absorption of electromagnetic radiation in the wave region between 200-800 nm. This technique is performed based on the measurement of absorbance (A) or transmittance (T) of solution in transparent cells with path length l (cm) (Titus et al., 2019). The absorbance of a solution is directly proportional to the concentration (C) and inversely proportional to the

logarithms of transmittance or directly proportional to the logarithmic ratio of transmitted intensity (I) to incident intensity (I_o) of the solution as shown by Beer Lambert's law equation 3.3,

$$A = log \frac{I}{Io} = \varepsilon cl = -log\, T \quad \text{..... Equation 3. 3}$$

Where ε is molar absorptivity

Accourding to Beer-Lambert law stated, the greater the number of molecules capable of absorbing light of a given wavelength, the greater the extent of light absorption. It may also, be used for estimation of metal nanoparticles formation at certain characteristic maximum wavelength absorption.

Greenly prepared Silver (Ag°) nanoparticles were characterized using a double beam UV-Vis spectrophotometer. The spectrophotometer was equipped with "UVWin lab" software to record and analyze data. Baseline correction of the spectrophotometer was carried out by using a blank reference. The AgNPs were first placed into UV- cuvette and the cuvette is placed in a spectrophotometer for testing. Due to the intensity greater than 3 it was diluted using the dilution factor. The cuvette can hold 2.5 milliliters. Then, the UV-Vis absorption spectra of all the samples and characterization were recorded and numerical data plotted in the "Origin v-18".

3.5.2 X-RAY Diffraction

X-ray diffraction is a powerful technique that helps to identify the structure, phase purity, degree of crystallinity and unit cell parameters of a given sample (Arya et al., 2019). The XRD patterns are recorded by the measurements of the angles at which the X-ray beams are diffracted by the periodicity of the sample. The relation between the distance between two planes (D-spacing) *(d)* and the angle of diffraction (2θ) is given by Bragg's equation (equation 3.4)

$$n\lambda = 2d sin\, \theta \quad \text{..... Equation 3. 4}$$

Where λ = wavelength of X-rays, n= an integer known as the order of reflection (*h*, *k*, and *l* represent Miller indices of respective planes). From the diffraction patterns, the uniqueness of the mesoporous structures, phase purity, degree of crystallinity, and unit cell parameters can be determined.

The average crystalline or grain size of nanoparticle were calculated using scherrer equation (equation 3.4)

$$D = \frac{K\lambda}{\beta cos\Theta} \quad \text{..... Equation 3.5}$$

Where D is average crystalline size: K is the shape factor (0.9), λ is the wavelength of X-ray radiation, Θ is Bragg angle of corresponding diffraction peak, β is full width at half maxima (FWHM) of main diffraction pick.

In this work, AgNPs with pH-5 (original sample) and pH-7 were performed with an X-ray diffraction technique (Philips PAN analytical, The Netherland) using Cu Kα radiation. Silver samples were scanned in the 2 θ ranges with continuous scan mode.

3.5.3 Fourier Transferred Infrared Radiation

FT-IR characterization was carried out to identify functional groups of biomolecules responsible for surface capping and reducing agents for AgNPs. The functional groups coated AgNPs were examined using FT-IR with model name FTIR- 6600 type A and serial number A013861790. FTIR energy corresponding to these transitions corresponds to the infrared region (4000 with total reflectance (ATR) model in the range of 4000 to 400 cm^{-1} with 4 cm^{-1} resolution and 64 scan rates.

3.5.4 Antimicrobial Testing

i. Preparation of Inoculums

In vitro antimicrobial susceptibility test was performed using Agar well disk diffusion method or called as Cup plate method. First the medium was prepared by dissolving 38g Mueller Hinton agar medium in 1000 mL of distilled water and autoclaved at 121 ^{0}C for 15 min. the autoclaved medium was poured in to solified under sterile condition at room temperature.

After solidification, the test bacterial species were transferred from the stock using bacterium-logical loop to autoclaved Muller Hinton agar (MHA) that cooled streaked on Mueller Hinton plates and incubated for 24 h at 37 ^{0}C the approximately 1.5×108CFU/mL by swabbing evenly onto the surface of the medium with a sterile cotton swab. Well-separated bacteria colonies were then used as inoculums (Samuel et al., 2021). The medium was then poured into sterile Petri dishes, allowed to solidify and used for the bio-test.

The antibacterial activities of synthesized compounds were done in Biology Department Laboratory, Adama Science and Technology University, Ethiopia.

ii. Preparation of Disc Controlling Synthesized Compounds

Deferent concentration was prepared from each greenly synthesized AgNPs at pH-5 and pH-7. This was done by dissolving 25 µg, 50 µg and 75 µg of AgNPs into 1 mL of Distilled water. The concentration was incubated to sterile blank discs and was dried at 37 °C. The paper disc was weighted carefully for confirming the exact amount of the synthesized compound is incorporated.

ii. Determination of Antibacterial activities by Disc Diffusion method

The antibacterial activates of prepared AgNPs at pH-5 and pH-7 were done against 4 drug-resistant bacteria Gram-negative bacteria (*E.coli* and *P. aeruginosa*) and Gram-positive bacteria species (*S. pyogen and S. aureus*) and examined by disk diffusion assay (Swamy et al., 2015. Ciprofloxacin was used as a control and pure isolated colonies from new grown bacteria were transferred from plates into sterile normal saline solution and vortexes to make bacterial homogenous suspensions. The turbidity was then adjusted to Mc Farland standard units and the suspensions will be poured in over MHA plates. Then by preparing sterile paper disks with 6 mm diameter paper, discs were cut from Whatman-No.1 filter paper were placed over this plate and Sterilized in an oven at 180 ^{0}C for 1 hour. A 25 µg, 50µg and 75µg of silver nanoparticles were dissolved in 1ml of distilled water. The solution was added to each well. Petri dishes were incubated at 37 °C for 24 h. The inhibition zones of bacteria were observed and measured in millimeters using a ruler.

3.6 Synthesis of Bio-conjugate

Bio-Conjugate is a chemical method to form a stable covalent link between two or three biomolecules. GLY-LAC bio-conjugate is an esterification process, where the three hydroxyl groups in Glycerol molecule may involve three moles of lactic acid. Hear GLY-LAC bio-conjugate is used as a plasticizer and AgNPs are incorporated to enhance their activity. First GLY-LAC conjugate was synthesized and then AgNPs were dispersed using the two-step method as follows.

3.6.1 Synthesis GLY-LAC Bio-Conjugate

A commercially available pure glycerol (99%) and Lactic acid (88%) were used for the preparation of bio-conjugate via a condensation reaction. For commercially available 99 % pure glycerol, 1mole is equal to 74 ml of liquid glycerol. Whereas the commercially available 88%, 3 moles of lactic acid is equal to 12 (84.879 ml) = 1,018.54 ml, so to prepare a 1:12 molar ratio of Glycerol: Lactic acid 74 ml of glycerol was reacted with 1,018.54 ml of lactic acid was mixed using magnetic rod stirrer at room temperature. The mixture was poured into a necked rounded bottom flask (RBF) and placed in a temperature-controlled oven (reactor) at a temperature of 190 °C for 8 h retention time. The process for the synthesis of bio-conjugate is described in figure 3.4.

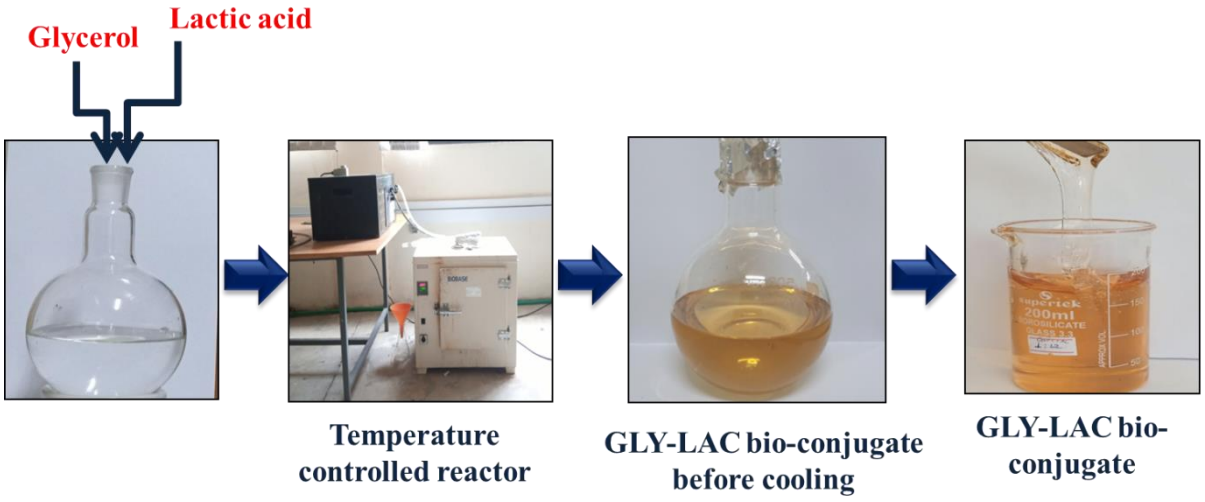

Figure 3.4 Synthesis of GLY-LAC bio-conjugate

3.6.2 Synthesis of AgNPs Dispersed with GLY-LAC Bio-Conjugate

There are two types of nanoparticle dispersion method, a one step and two step methods. Here, a two-step method of nanoparticle dispersion techniques was followed. The prepared nanoparticles were dispersed and mixed in the base matrix using a mixer or Ultra-sonication techniques (Ilyas et al., 2017). An AgNPs/GLY-LAC bio-conjugate was prepared by incorporating 0.1wt%, 1wt% and 3wt% AgNPs. First to prepare (AgNPs/GLY-LAC) 0.1wt%, 1wt% and 3wt%, AgNPs were well dispersed into 10 mL of distilled water using magnetic stirrer for 1 hr. Then well dispersed AgNPs nanoparticles were added slowly into 25 mL of 1:12 GLY-LAC three armed micro molecule solution under continuous string for quarter hour, and then Nano solution was putted into ultra-solicitor bath for 2 h at 40 ^{0}C. A sonication is used in order to assist the disruption of particles agglomerates through a process known as Cavitation. This refers to the application of higher sound energy at frequencies largely inaudible to the human ear (higher than >> 20 kHz) (Taurozzi et al., 2010).

Finally, 0.1%, 1% and 3% AgNPs/GLY-LAC bio-conjugate were placed in the oven at 105°C overnight until the solvent was evaporated. This method of dispersing nanoparticles was adopted from (Mansour & Atiya, 2016). The process of dispersion nanoparticles into GLY-LAC macromolecule is illustrated in figure 3.5. After all, the stability of the Nano fluid with time was retrieved from visual inspection.

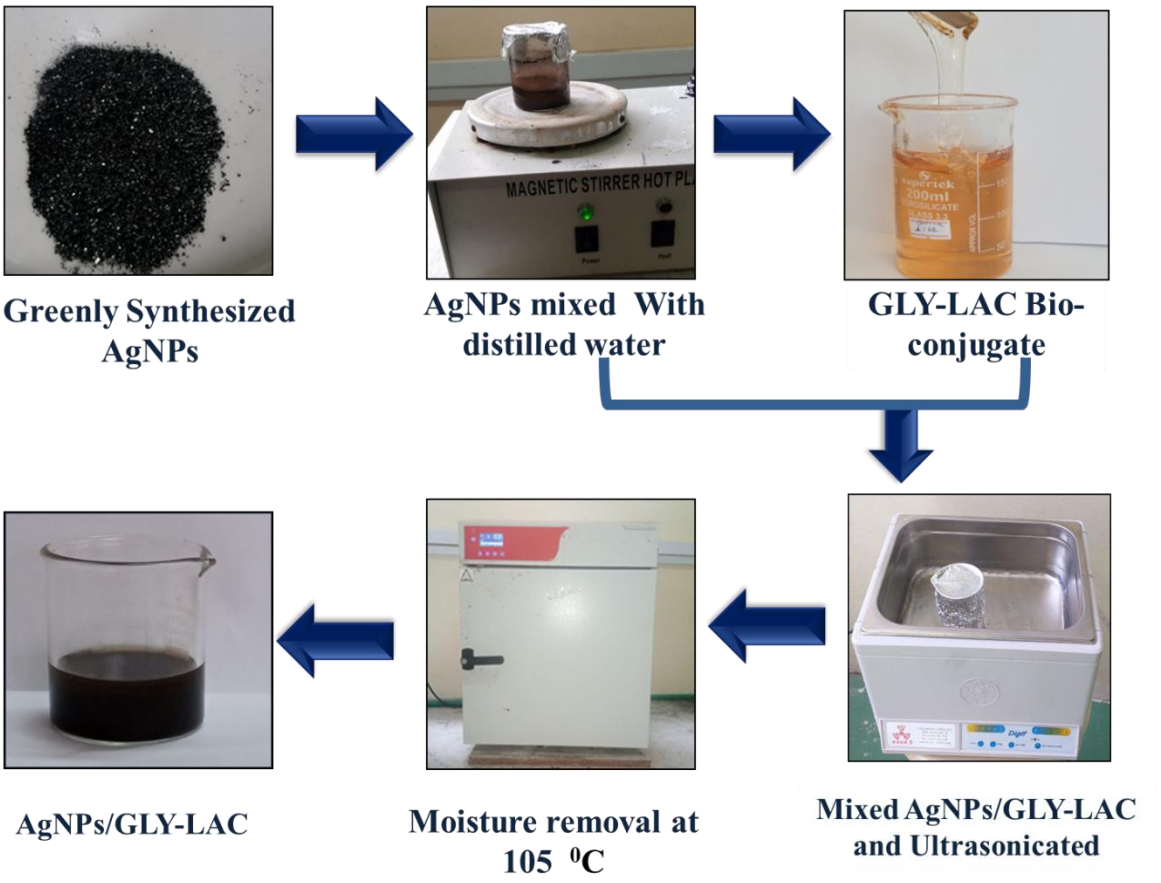

Figure 3.5 Homogenous desperation of AgNPs with in GLY-LAC bio-conjugate

3.7 Preparation of AgNPs/GLY-LAC/PLA Bio-film

PLA is a lactic acid-derived a linear aliphatic thermoplastic polyester. Form various film processing techniques Solvent Casting method is used by dissolving polymer in an organic solvent. The solution of final geometry of the mixture is formed and it can be cast onto a glass plate to make a membrane or in a three-dimensional mold to make a scaffold (Ajitha et al., 2016) (Films et al., 2018).

AgNPs/GLY-LAC/ PLA based biofilm was prepared using a solvent casting method or solvent evaporated method. Before preparation of biofilm 1wt% AgNPs/GLY-LAC bio conjugate was selected which the nanoparticles were stable and good antimicrobial activity than 0.1wt% AgNPs dispersed in GLY-LAC. AgNPs/GLY-LAC/ PLA Nano composite biofilm was prepared by incorporate with 1wt%, 5wt% and 10wt% AgNPs/GLY-LAC was

named as 10wt% (AgNPs/GLY-LAC)/PLA, 5wt%(AgNPs/GLY-LAC)/PLA and 1wt% (AgNPs/GLY LAC/PLA).

A stable Nano fluid of GLY-LAC/AgNPs with different concentration was used as filler for plasticization and enhances the antimicrobial activity of biofilm. A 3g of PLA pellets were dissolved in to 90 mL of chloroform on a magnetic stirrer at room temperature for 3 hrs. Subsequently the three products 1wt %, 5wt% and 10wt% AgNPs/GLY-LAC conjugate was added. Also the solution was mixed for further 30 min. After all the sample AgNPs /GLY-LAC /PLA, GLY-LAC/PLA film and PLA biofilm was casted in to 14 cm glass Petridish and allowed to dry for 24 h. Then the dried film was peeled with care from casting surface as indicated in the figure 3.6.

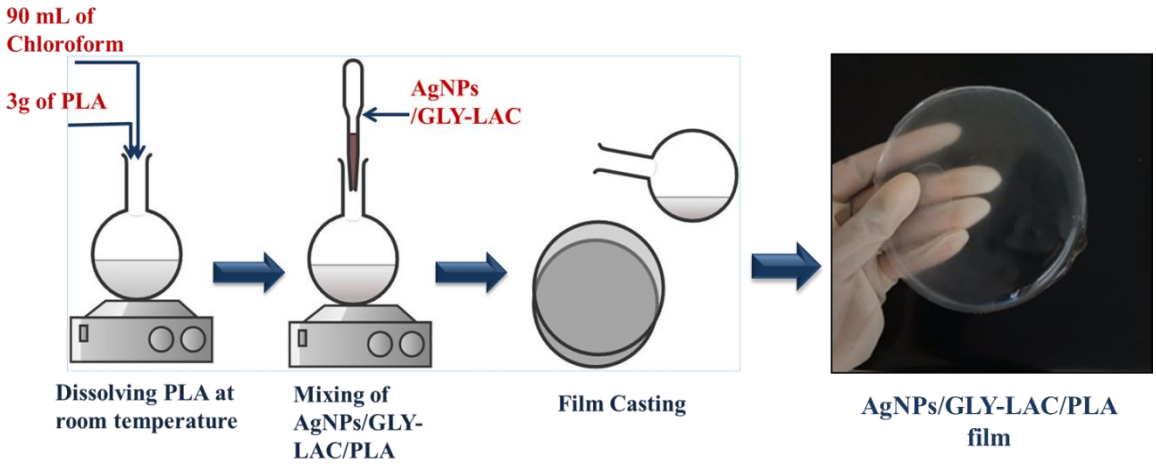

Figure 3.6 Preparation of AgNPs/GLY-LAC/PLA based biofilm

3.8 Characterization of Synthesized AgNPs/GLY-LAC Bio-conjugates

3.8.1 Ultraviolet-Visible spectroscopy

The UV-Vis spectroscopic study was done for both GLY-LAC and 1% AgNPs/GLY-LAC bio-conjugate. The spectrophotometer was equipped with “UVWin lab” software to record and analyze data. Baseline correction of the spectrophotometer was carried out by using a blank reference. The GLY-LAC/AgNPs into UV- cuvette and the cuvette is placed in a

spectrophotometer for testing. Then, the UV-Vis absorption spectra of the samples characterization were recorded and numerical data plotted in the "Origin v-18".

3.8.2 Fourier Transferred Infrared Radiation

FT-IR characterization of pure GLY-LAC and AgNPs/GLY-LAC was carried out to identify expected functional groups and there interaction. The effect of incorporation of AgNPs on the functional groups of base matrix was analyzed. The functional groups coated AgNPs were examined using FT-IR with model name FTIR- 6600 type A and serial number A013861790. FTIR energy corresponding to these transitions corresponds to the infrared region (4000 with total reflectance (ATR) model in the range of 4000 to 400 cm^{-1} with 4 cm^{-1} resolution and 64 scan rates.

3.8.2 Antimicrobial Activity

The microbial activity bio-conjugate was examined by using a gar disk diffusion method which is simple, practical and has been well standardized. This testing method is performed by applying microbial inoculums of approximately 1.5×10^{8} CFU/ml to the surface of a Mueller-Hinton agar plate. Commercially prepared with fixed concentration, paper antibiotic disks will be placed on the inoculated agar surface (Samuel et al., 2021). The antibacterial was performed first by preparing with an office paper puncher, 6 mm diameter paper discs were cut from whatman-No.1 filter paper and put in a beaker filled with aluminum foil and sterilized in an oven at 180 ^{0}C for 1 h. The discs were then pipetted with pure 1mg/ml GLY-LAC as a control, 0.1wt%, 1wt% and 3wt%. AgNPs/GLY-LAC Plates were incubated for 24 h at 35°C prior to the determination of results. Then bacteria were selected one from Gam positive bacteria and one from Gram negative bacteria in which AgNPs show higher Zone of inhibition. The zones of growth inhibition around each of the antibiotic disks against *P. aeruginosa* and *S.aureus* were measured to the nearest millimeter. The diameter of the zone is related to the susceptibility of the isolate and to the diffusion rate of the drug through the agar medium. The zone diameters of each product will be interpreted using the criteria published by the Clinical and Laboratory Standards Institute (CLSI, formerly the National Committee for Clinical Laboratory Standards or NCCLS) or those included in the US Food and Drug Administration (FDA)-approved product inserts for the disks.

3.9 Characterization of AgNPs/GLY-LAC/PLA Biofilm

3.9.1 Antimicrobial Activity

As we have been working before *in vitro* antibacterial susceptibility test for prepared film was determined by disc diffusion method (Iconaru et al., 2014). The agar medium was prepared within dissolving 38 g of Mueller Hinton agar medium (MHA) in 1000 mL of distilled water autoclaved at 121 °C for 15 min. The autoclaved medium was poured into sterile plates (20-25 mL/plate) and the plates were allowed to solidify under sterile condition at room temperature. After solidification, the plates were seeded with overnight grown culture approximately 1.5 X 10^8 CFU/mL by swabbing evenly on to the surface of the medium with a sterile cotton swab.

According to the methods described by CLSI with slight modification the synthesized Net PLA, GLY-LAC/PLA, 10wt% (AgNPs/GLY-LAC)/PLA, 5wt% (GLY-LAC/AgNPs)/PLA and 1wt% (AgNPs/GLY-LAC)/PLA Films were cut in the diameter of approximately 6 mm (as discs) using puncher. The 6mm PLA biofilm were placed and position on the surface of the medium with sterile forceps. gently pressed down to ensure contact with the MHA. Ampicillin was used as standard antibiotics and then plates were inverted and then incubated at 37 ℃ for 24 hrs. After incubation the inhibition the zones of growth inhibition around each of the antibiotic disks against *P. aeruginosa* and *S.aureus* were measured to the nearest millimeter. Zone halo of growth produced by the synthesized biofilms were evaluated by measuring the diameter (mm) of the clear zone around the disc against the test organisms using a ruler.

CHAPTER FOUR

4. Result and Discussion

4.1 Preparation of *Vernonia amygdalina* Leaves Powder

Drying or removal of water from *V.amygdalina* leaves is an early stage in the preparation of raw material for extraction. A substantial portion of biological materials is made up of water. Variations in the water content of Plant leaf powder may influence the solubility of bioactive components in plant leaves.

4.1.1 Moisture Content (%)

The proximate analysis of *V. amygdalina* leaves powder on the chemical analysis was done using standard methods American Society for Testing and Materials (ASTM D4442). The moisture compositions (%) of the dry powder sample material were calculated at approximately 1.2% ± 0.05. Dry powder leaves which have proximately 1.2% moisture content were used for the extraction process on the synthesis of AgNPs.

4.2 Green synthesis of AgNPs

4.2.1 Solvent Selection for Extraction Using Plant Leaves

Extraction process is the most common method for extracting bioactive phytochemical compounds from biomass sources. The aim of the extraction procedure is to get the greatest number of biological active compounds from the extracts while maximizing the quantity of target components. The extraction of bioactive compounds of the resultant extract is impacted not only by the extraction process but solvents used for extraction. Solvents Methanol, Ethanol, Distilled water, Mixed Methanol distilled water (M/DW) and Mixed ethanol Distilled water (E/DW) were selected as solvents.

4.2.1.1 Visual Observation

The formation of AgNPs was preliminary confirmed visually by the change of color of solution as shown (figure 4.1). Polar Solvents like 100 mL of Methanol (99.9%), 100 mL Ethanol (98%), 100 mL Distilled water, (1:1 v/v) M/DW and (1:1 v/v) E/DW was selected due to their extraction wide range of polar compounds and Cheap, less toxic (Non Toxic), have moderate boiling point and highly polar.

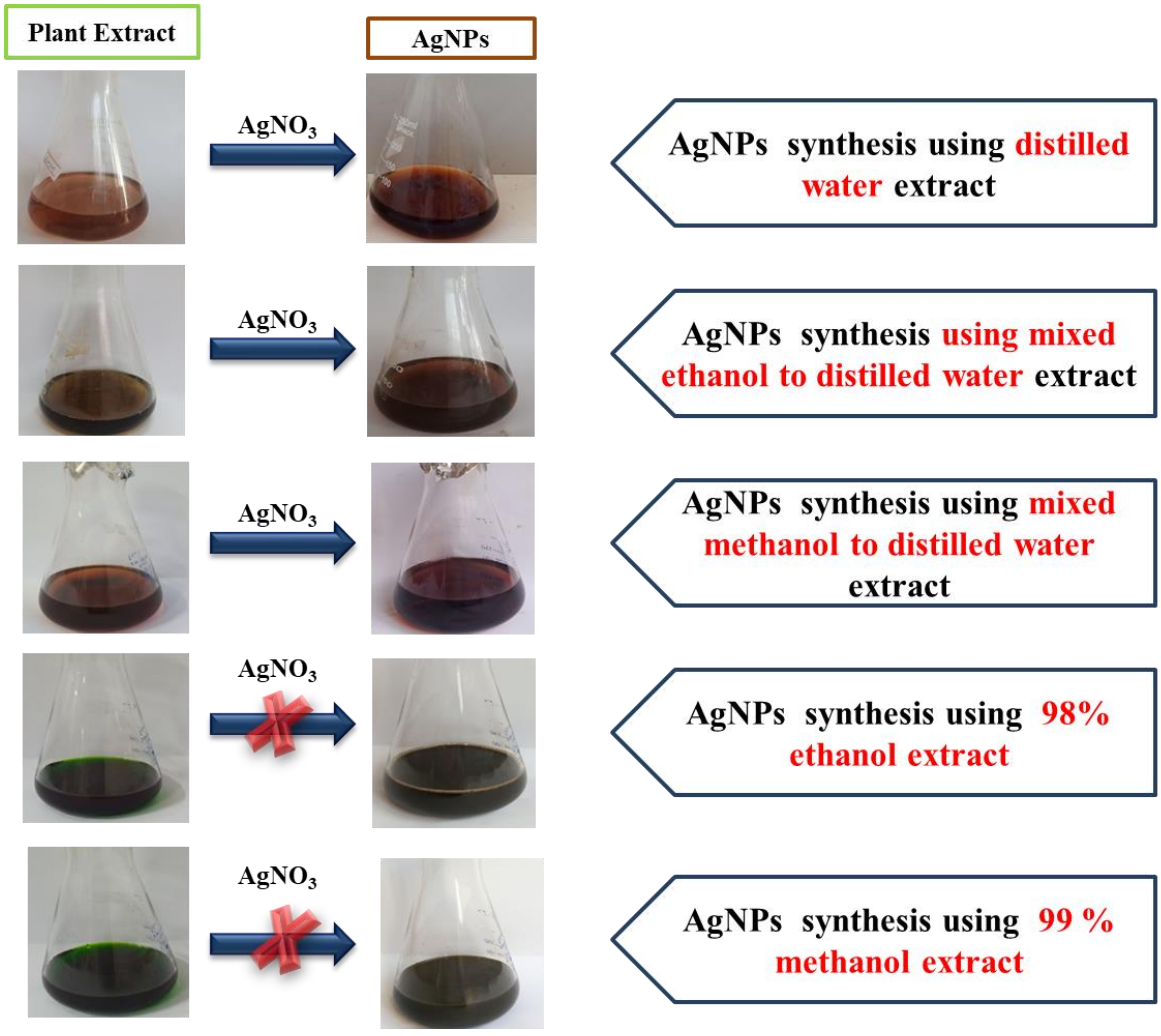

Figure 4.1 Colour change of plant extract before and after addition of $AgNO_3$

V. amygdalina leaf extraction was performed using pure 100 ml distilled water, E/DW and M/DW showed a light brown colour. After mixing the extract with 5 mM $AgNO_3$ precursor

solution (1:1) v/v showed a dark brown colour. The synthesis of AgNPs was done following a synthesis method reported by (Aisida et al., 2019).

However for the extract of *V.amygdalina* using 98% ethanol and 99% of methanol which shows a green colour were changed to dark green colour when mixed with $AgNO_3$ solution.

The formation of dark brown colour on the synthesis of nanoparticles using the above three solvents (DW, E/DW, M/DW) Showed that the formation of AgNPs (Roy et al., 2017). (Moodley et al., 2018)(Kumavat & Mishra, 2021) also confirmed that the formation of AgNPs were preliminary investigated by the color change to brown and dark brown after adding aqueous plant extract to $AgNO_3$. But 98% ethanol and 99% of methanol based extracts didn't show a colour change on the synthesized AgNPs.

The color variation is due to the presence of bioactive compounds (alkaloid, Saponins, Flavonoids, phenol, Tannin and Terpenoids) contained in plant materials that differ the solubility properties in different solvents. The color change is due to the origin of Surface Plasmon resonance in Nobel metal nanoparticles. The generation of surface Plasmon vibrations in AgNPs was generated by light interactions with suspended nanoparticles, which resulted in fascinating colors that differed from those seen in bulk materials. The metal's free electrons are unrestricted in their movement through the substance (Selvamani, 2018). The free-electron oscillation in the metal is caused by light in resonance with the surface Plasmon oscillation. The electron density in the particle is polarized to one surface and oscillates in resonance with the light's frequency as the wave front passes, creating a standing oscillation. Generally, Surface Plasmon Resonance (SPR) (for metallic nanoparticles) and quantum confinement are the main mechanisms that impart color to nanoparticle suspension (Chhatre et al., 2012)

4.2.1.2 UV-Vis Analysis for Solvent Selection

The most significant instrumental approach for the characterization of synthesis AgNPs is ultraviolet and visible spectroscopy (Murugesan et al., 2017)(Swamy et al., 2015). It's a method of determining the amount of light that goes through or is reflected from a substance under investigation. Light is made up of two energetic components that can excite electrons to higher energy levels. The visible portion of the magnetic spectrum is where electrons are

excited. Electron transition of to л- л*, n- л*, σ-σ*and n- σ* occur in atom or molecule (Adewumi et al., 2018).

The reduction of pure Ag+ ions was monitored by measuring the UV-Vis spectrum of the reaction medium after diluting a small *V. amygdalina* sample into M/DW, E/DW, and DW was mixed with the metal salt at 40°C with a 1:1 ratio. The UV absorption peak of synthesized AgNPs is in the range of 400 nm – 450 nm (Eya'ane Meva et al., 2016). The figure 4.2 shows the UV absorption peaks for AgNPs synthesized by using 1:1 v/v ratio (M/DW), 1: 1 v/v ratio (E/DW) extract based synthesis and pure 100% (DW) extracts based synthesis of AgNPs.

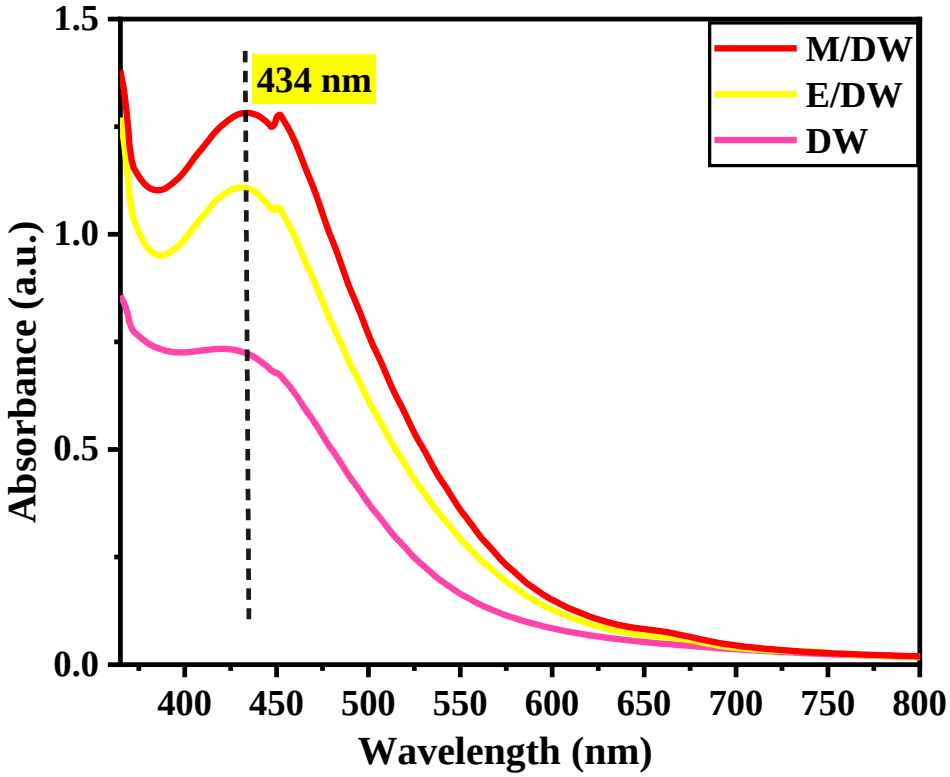

Figure 4.2 UV-Vis Spectra of AgNPs using M/DW , E/DW and DW

UV-Vis spectroscopy follows the principle of the Beer lambert law. At a particular wavelength, the absorbance of a sample is directly proportional to the concentration of the absorbing substance (Titus et al., 2019). The UV-Vis spectra of synthesized AgNPs showed peaks approximately at 434 nm. The reduction of Ag^{+} ion in the solution was observed highest absorbance by using M/DW based extract as reducing agent. Also, mixed E/DW based extract also showed higher reduction or concentration of AgNPs than DW-based extract. Distilled

water-based extract showed broad absorbance (417-431 nm). The presence of phytochemical components causes the intensity absorbance peaks to vary. DW was known as a Universal solvent for the synthesis of AgNPs since it is the cheapest, most readily accessible, and environmentally friendly solvent on the planet. A liquid phase is necessary for Ag^{+} ion reduction, nucleation, ordering of atoms into particles, growth of the particles to Nano scaled dimensions, and stability of nascent NPs in green Nano synthesis activities (Shabina et al., 2020). Mixed M/DW and E/DW have a positive impact on bioactive component extraction. When compared to E/DW, using M/DW as an extraction solvent allows for the extraction of a greater amount of bio-active components.

To confirm the peaks observed using UV-Vis spectra is AgNPs' the pure *V. amygdalina* and $AgNO_3$ solution was monitored using UV-Vis spectroscopy as showed in figure 4.3.

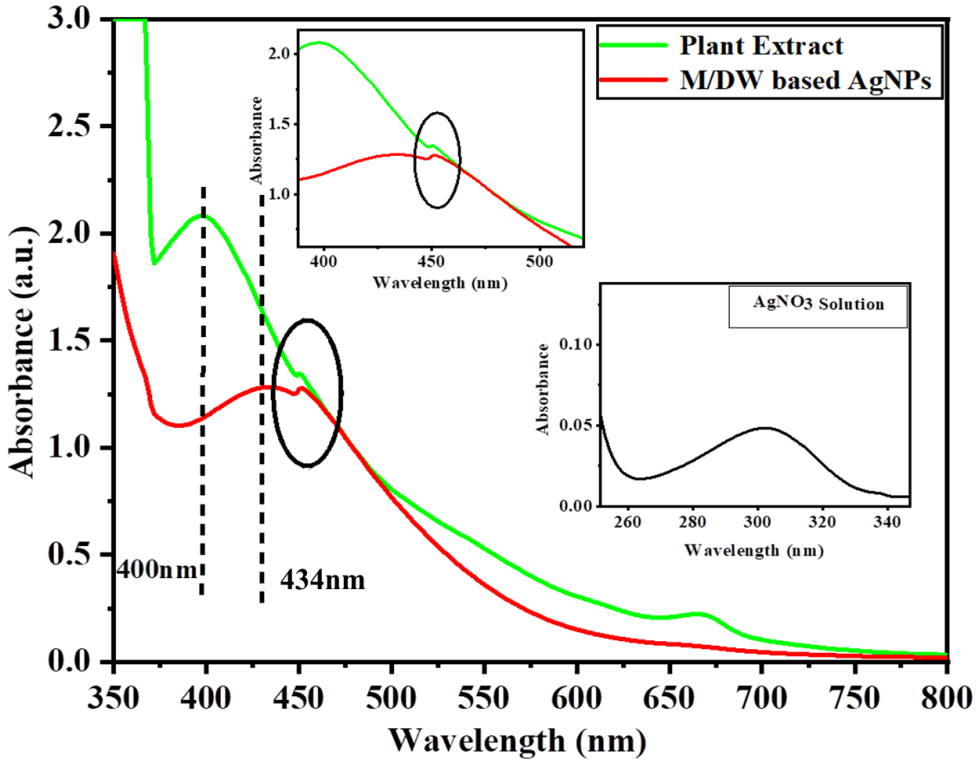

Figure 4. 3 UV-Vis spectra Of M/DW plant extract, $AgNO_3$ and AgNPs

The M/DW based plant extract showed two absorption peaks at 400 nm and 450nm, which is responsible on the reduction of Ag^{+} to AgNPs. The peaks at 450nm also observed on the synthesized AgNPs in the solution. The solution of $AgNO_3$ showed absorbance peaks at 300 nm Wavelength.

The peaks observed on the plant extract is due to $n \rightarrow \pi^*$ or $\pi \rightarrow \pi^*$ transitions of, C=O and C=C molecules. This result was confirmed later on using FT-IR. This investigation of UV-Vis for plant extract are consistent with those found in the literature (Kahsay, 2021) . Generally, the presence of water in an organic solvent, Methanol can initiate the mass transfer process by raising the relative polarity of the solvent; therefore, enhance its solubility via efficient plant swelling. Some bioactive compounds may be extracted using methanol and others may be extracted in water. A strong peak indicates a large yield of AgNPs and tighter distribution at characteristics λmax (Ashraf et al., 2013). So M/DW based *V. amygdalina* leaf extract is selected for further AgNPs synthesis.

4.2 Study the Effect of Operational parameters on Synthesis of AgNPs

Most of the important operational parameters or experimental factors, which are the solvent ratio of mixed M/DW, precursor concentration, the ratio of precursor to extract, temperature, time, and pH effect on the formation of AgNPs, were investigated and the study was monitored using UV–VIS spectrophotometer as a result of surface Plasmon resonance (SPR). The Surface Plasmon resonance was developed from the free electrons of AgNPs arising from the conduction and valance bands lying close to each other (Adewumi et al., 2018). The UV-Vis spectroscopy spectral peaks in the AgNPs synthesis provide information on the SPR at the maximum absorption wavelength.

4.2.1 Effect of Solvent Ratio of mixed M/DW

In most of the green synthesis of nanoparticles with a high concentration of nanoparticles with relatively high particle concentrations coupled with predefined shapes, organic solvents have been achieved (Dorjnamjin et al., 2008). In our case, M/DW was selected for the extraction, which helps for the reduction of high concentrations of AgNPs. Then the effect of varying extraction solvent ratios 30/70, 40/50, 50/50, 60/40, 70/30 (M/DW) on the synthesis of AgNPs was examined using UV–Vis spectrophotometer, as shown in Figure 4.4.

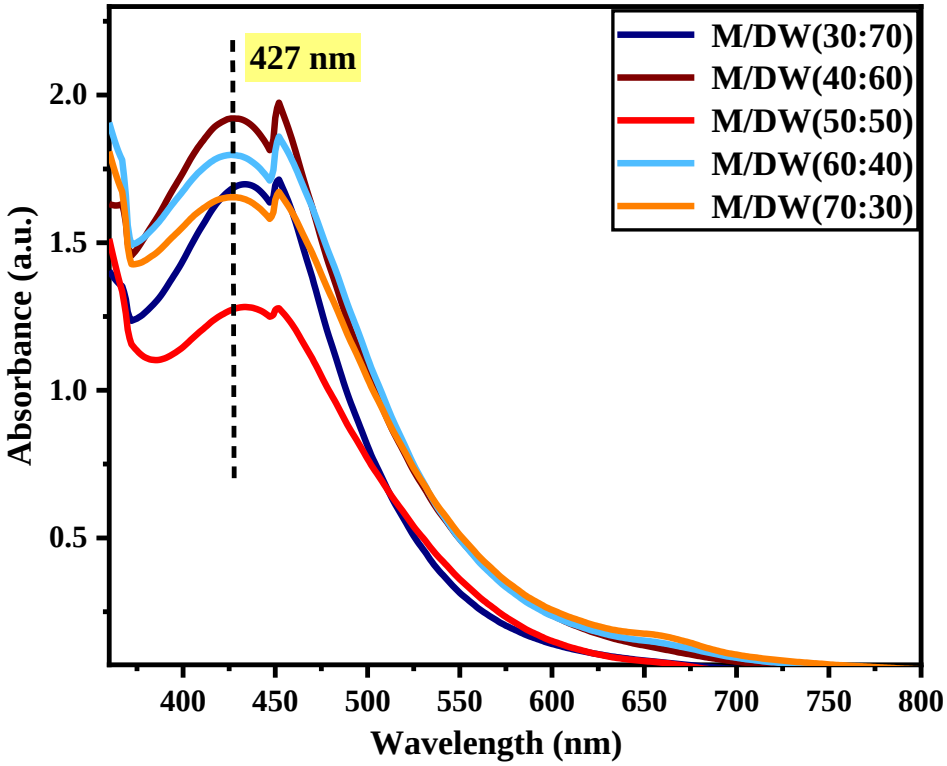

Figure 4.4 UV-Vis spectra of AgNPs synthesized using different mixing ratio of M/DW

UV-Vis spectrophotometer analysis for mixed M/DW ratios the absorbance increased from 50:50 < 70:30 < 30:70 < 60:40 < 40:60 on the synthesis of AgNPs. 40/60 mixed M/DW shows higher absorbance of UV-Vis spectra, which means a higher concentration of AgNPs. Various concentrations of the methanol solvent with the addition of tiny amount of water to the methanol solvent may vary the degree of polarity in the solvent. This is the ratio that affects the yield of phytochemical components, indirectly the concentration of synthesized AgNPs. This activity helps to create a more polar medium with improved solubility for bioactive compounds. Variation of solvent ratio exemplifies the 'like dissolve like' or 'polarity versus polarity' principle. An attraction between the mentioned chemical compounds and the different methanol solvent concentrations occurs due to the almost similar polarity (Tham & Liew, 2014). So for further analysis 40/60 (v/v) (M/DW) based extract were used to for the synthesis of AgNPs.

4.2.2 Effect of Precursor Concentration

The Concentration of $AgNO_3$ (precursor) or silver ion was majorly affects synthesis of AgNPs (Saxena et al., 2016). This parameter was investigated for identification amount of silver ion most suitable for generation of AgNPs. To investigate the effect of precursor concentration, 50 mL of 40:60 (M/DW) extract was mixed with 50 mL different molar concentration of $AgNO_3$ solution. The Effect of concentration of silver salt (1mM, 2 mM, 3 mM, 4 mM, 5 mM, 6 mM, 7 mM, 8 mM, 9 mM and 10mM) was investigated and shown in figure 4.5 using UV-Vis spectra. The UV-Vis spectra help identifies a suitable concentration for synthesizing a number of AgNPs, which shows better surface Plasmon resonance.

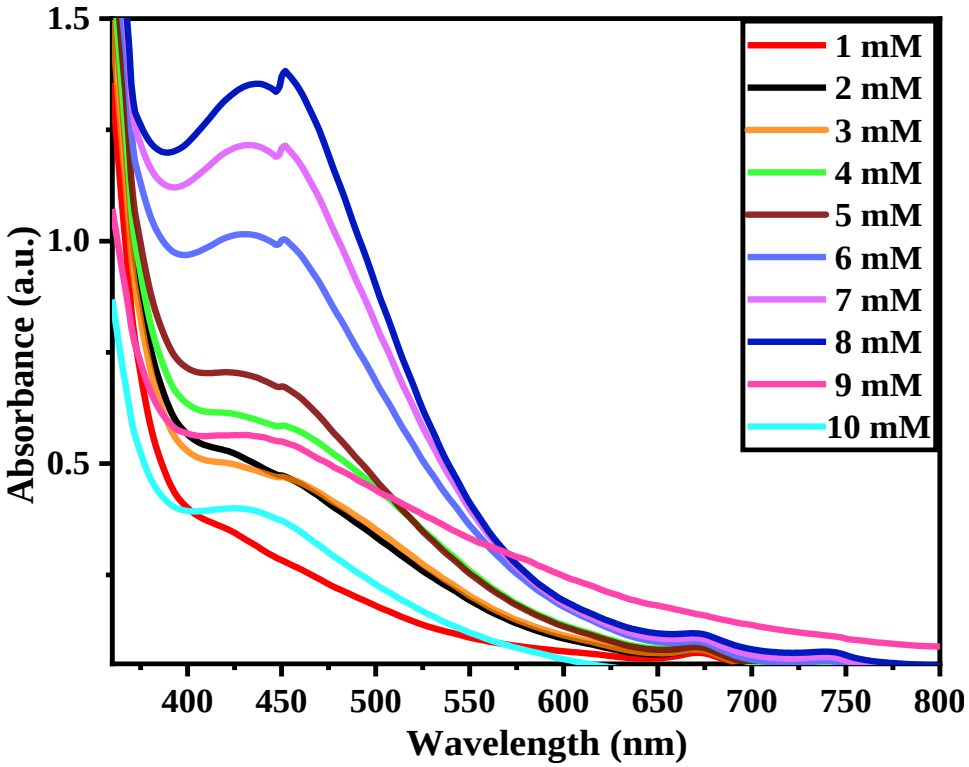

Figure 4.5 UV-Vis spectra of AgNPs synthesized at different precursor concentrations

At a low concentration of $AgNO_3$ from (1mM – 5mM), the absorption peaks of AgNPs were broad and less intense. The absorption peaks were centered between 415 – 440 nm. However, the absorbance intensity increases gradually from 6mM – 8mM, the absorbance peak becomes sharper and more intense by shifting of SPR peak to a longer wavelength direction. At 8 mM

the absorbance was maximum and the SPR at 431 nm. The AgNPs absorbance peaks get relatively smaller as the $AgNO_3$ solution concentration increases to 9 mM and 10 mM.

The increase in the intensities of SPR peaks from 1mM to 8mM might be due to an enhancement in the nuclei formation that resulted in the synthesis of a larger number of nanoparticles (Islam et al., 2019)**.** The decrease absorbance intensity of peaks at 9 mM and 10 mM may be caused due to the increase in the destabilization of AgNPs and increased agglomeration of Nanoparticles or not enough reducing agents.

This result was agreed with the green synthesis of AgNPs using spent 10 mL of black Tea Leaves Extract. Then the extract was mixed with 90 mL of $AgNO_3$ solution of different concentration (1, 3, 5, 7 & 9 mM) at room temperature shows increasing absorbance from 1mM -7mM. However, with increasing the molarity to 9 mM the SPR peak is shifted toward the shorter wavelength with a decrease in the absorbance. Possibly this may cause by increasing in destabilization of the particles as indicated by the decreased absorbance due to increased particle aggregation and precipitation (Moosa et al., 2015). (Ahmed A. Moosa1, 2015) reported synthesized AgNPs using $AgNO_3$ as a metallic salt and Aloe Vera Plant leaves extract as reluctant, Increasing $AgNO_3$ concentration (1, 3, 5, 7 & 9 mM) resulted in a gradual increase of absorbance peak between 422 – 447 nm due to its surface Plasmon resonance absorption band. According to our study, 8mM $AgNO_3$ concentration was selected for further studies due to larger amount of AgNPs synthesized. This was done at 50 °C for 1 h using 50 mL of plant extract as reducing agent

4.2.3 Effect of $AgNO_3$ Solution and Extract Volumes

The effect of 8mM $AgNO_3$ solution mixed with extract volumes were done using in the range 10/90, 20/80, 30/70, 40/60, 50/50, 60/40, 70/30, 80/20 and 90/10 (v/v) ratio and other parameters were kept constant. The experiment was conducted using UV-Vis spectrophotometry as shown in the figure 4.6 in order to find out the highest composition of AgNPs.

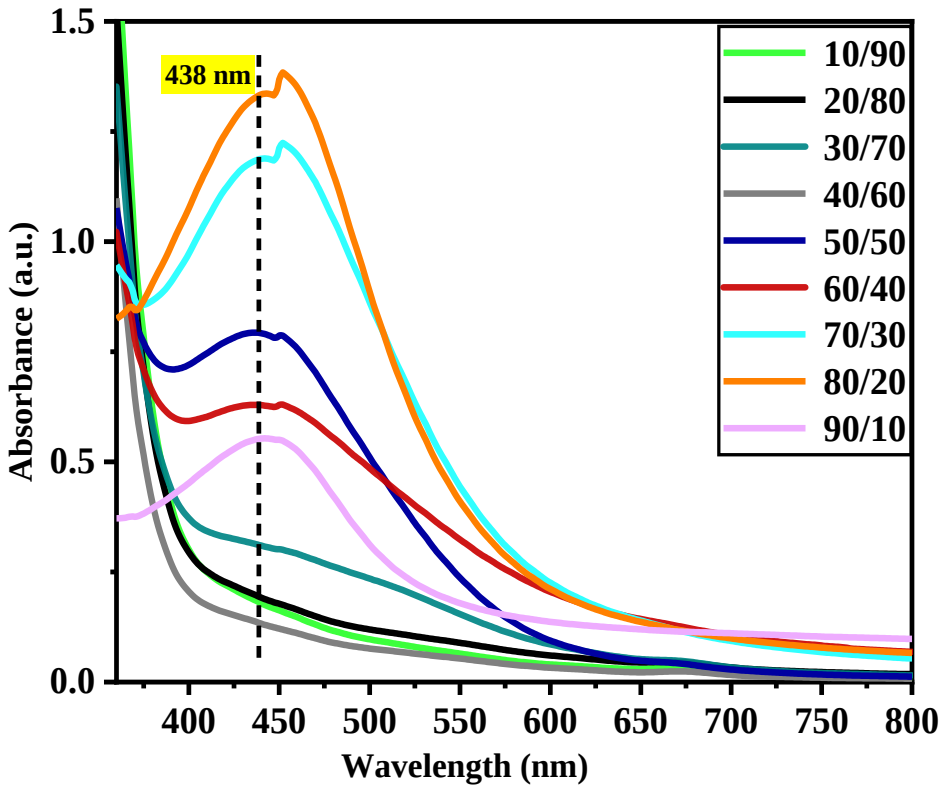

Figure 4.6 UV-Vis spectra of AgNPs synthesized at different ratios of $AgNO_3$/ plant extract

The effect of the volume ratio of $AgNO_3$ to plant extract was performed at 9 different proportions. As demonstrated in the above figure, when the volume ratio of $AgNO_3$ solution was reduced from 40 to 10 mL and by increasing reducing agents the absorption peaks showed a decreasing intensity, Due to less amount of Ag+ concentration. In addition, the surface Plasmon peaks were shifted towards shorter wavelengths from 450 to 438 nm. This result indicated a reduction in the mean diameter of AgNPs. However, increasing $AgNO_3$ solution from 60 to 80 mL shows the increased intensity of absorbance peaks. This showed an increased amount of reduced Ag+ to AgNPs. However, 90 mL of $AgNO_3$ indicates decreasing surface Plasmon peaks, due to agglomeration of nanoparticles. Excellent SPR was recorded with 80 mL of 8 mM $AgNO_3$ solution to 20 mL of plant extract using UV-Vis spectra.

Similar results were also reported on the synthesis of AgNPs from *P. bracteosa* (1:1-1:10) v/v ratios with constant plant extract volume. This might result from the synthesis of AgNPs by speeding up the reduction of Ag ion. 1:10 ratios show high absorbance at 420 nm(Press,

2016). (Vivehananthan & De Silva, 2021) also confirmed that the effectiveness of the reaction ratio with the selected concentration was at the highest silver salt concentration to plant extract.

4.2.4 Effect of Temperature

Effect of reaction temperature was varied from 30 °C, 40 °C, 50 °C, 60 °C using UV-Vis absorption spectra as shown in the figure. 4.7. 20 mL of plant leaves extract was added in to 80 mL of $AgNO_3$ containing Erlenmeyer flask. The reaction was performed at different temperature for 1h under continuous stirring.

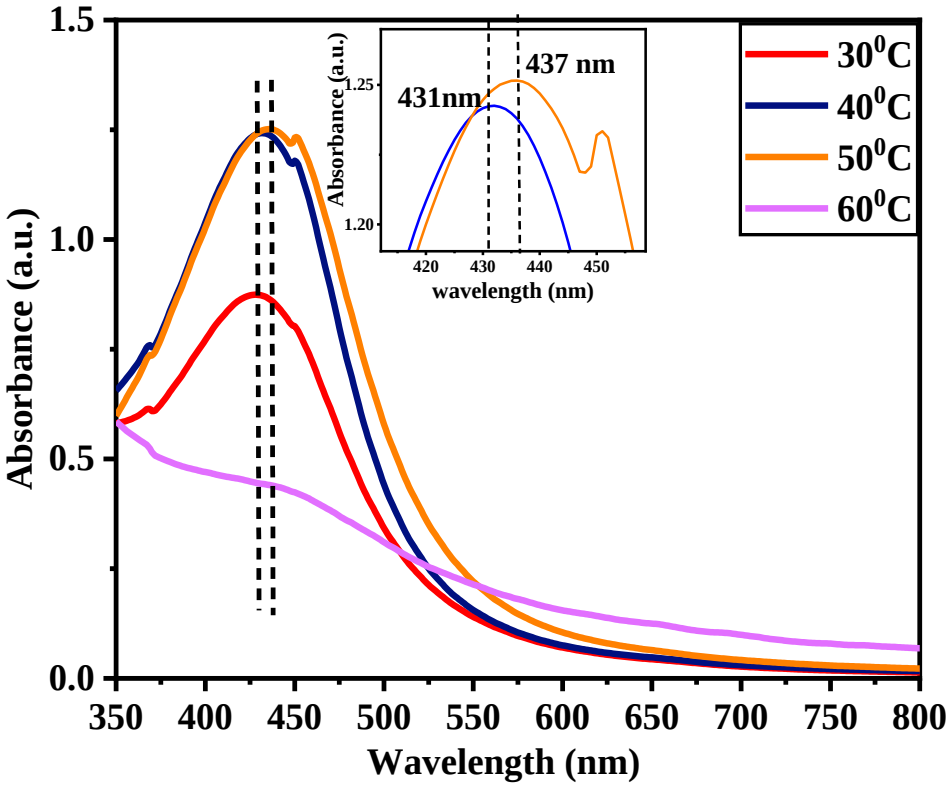

Figure 4.7 UV-Vis spectra of AgNPs synthesized at different Temperatures

When the reaction temperature increased from 30°C - 50°C the absorption peak was shifted towards a lower wavelength (437-431 nm) and increased in the intensity of the absorption Plasmon band. As the temperature increased to 60°C the absorbance peaks were decreased. The change in the absorption peak was caused by the AgNPs' surface Plasmon resonance

becoming localized. The UV-Vis spectra at 40°C and 50°C showed higher absorbance peaks which suggest that the concentration of AgNPs increased with increasing temperature, which was probably due to the faster reaction rate at a higher temperature. At higher temperature, the kinetic energy of the molecules increases and silver ions gets consumed faster leaving less possibility for particle size growth. Thus, smaller particles of nearly uniform size distribution are formed at higher temperatures (Verma & Mehata, 2016). As the temperature increased to 60°C the absorbance was decreased. This is maybe due to the agglomeration of nanoparticles were due to the degradation of bioactive components coated with the nanoparticles.

Previous works of literature try to relate this with particle size. At higher temperatures conductivity of nucleation was observed. A lower temperature is conducive to growth. With increasing temperature the intensity of plasmon band increased. So that generally nanoparticles grow better and larger at a lower temperature(H. Liu et al., 2017). This result were agreed with synthesis of AgNPs using Bilberry and red currant waste extract increases the SPR as the temperature increases from 20 to 60°C green synthesis of AgNPs using Bilberry and red currant waste extracts. A positive effect of temperature on the kinetics of AgNPs was frequently observed (Rose et al., 2019)(Saxena et al., 2016).

4.2.5 Effect of Synthesis Time

Effect of reaction time was investigated starting from the reactant is added in the flask to occur reaction. This was monitored plant extract added in to $AgNO_3$ at 15 min, 30 min, 45 min, 60 min, 75 min and 90 min. varying the time taken for the formation of AgNPs was examined using UV-Vis spectrophotometer as shown on the figure 4.8. The synthesis of silver nanoparticles was at 40°C and other parameters were kept constant.

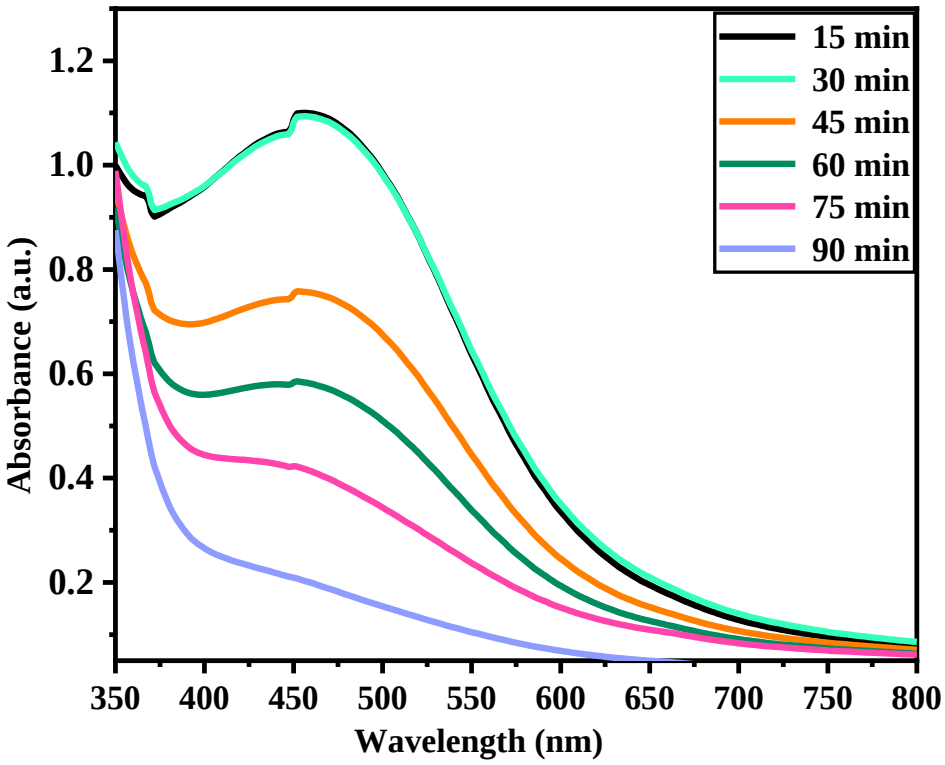

Figure 4.8 UV-Vis spectra of AgNPs synthesized at different times

The intensity of the peak is a function of the contact time that decreases as increasing time. At the early stage of contact time (15 min - 30 min) it shows excellent Plasmon band formation because a large amount of Ag^{+} has been converted to Ag^{0}. After the reaction is performed at 40°C for 15 min and 30 min the AgNPs obtained the UV-Vis absorption peaks showed at 441 nm. However, further increase in contact time from 45 min- 90 min leads to a noticeable decrease in absorption intensity. A decrease in absorbance peaks at 40°C with the reaction time increased indicates that the concentration of AgNPs decreased. This is due to the aggregation of AgNPs, which leads to an increase in particle size and settling of AgNPs that can't be detected through UV-Vis spectroscopy. This also confirmed the green synthesis of AgNPs using Tithonia diversifolia from 10 min to 90 min at room temperature. UV-Vis spectra showed rapid synthesis was obtained at a lower time. But excellent SPR was observed as the reaction time increased due to the large amount of Ag+ being converted to Ag^{0} (Dada et al., 2018). green synthesis of AgNPs using *E.japonica* leaf extract began to generate within 5

min after addition of $AgNO_3$. As the reaction time was prolonged for 60 min, the intensity of the SPR peak observed at 435 nm was increased (Rao & Tang, 2017) .

4.2.6 Effect of pH

Like other parameters pH also influences the reduction of AgNPs. The effect of pH as one of the operational parameters may influence the chemistry of the solution. The pH of the solution was adjusted from pH 4 - pH 12 the reaction process for the formation of AgNPs was examined by UV-Vis spectrophotometry as shown on figure 4.9. 20 mL of extract was mixed with 80 ml of the precursor solution. Then NaOH was added drop wise and the reaction was controlled for 30 min at 40°C

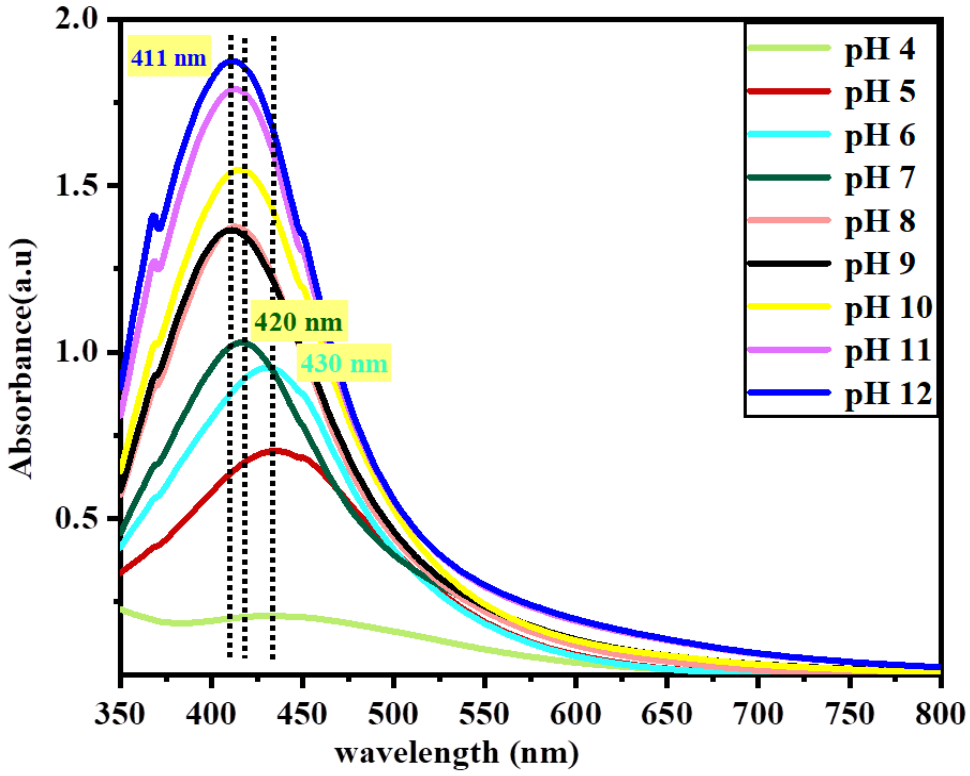

Figure 4.9 UV-Vis spectra of AgNPs synthesized at different pH

The UV-Vis spectra showed as increasing pH value from 4 to 12 was increase the absorption of intensity. Also with the increasing of pH, the absorption peaks shifted towards a lower wavelength, for pH 6, pH 7, pH 12 it was 430nm, 420 nm, and 411 nm respectively. The poor rate reduction seen in the acidic medium might be due to electrostatic repulsion of anions

present in the reaction mixture, and this could be linked to the ionization of functional groups at increased pH.

The shifting of wavelength may be due to reduced particle size of AgNPs. As the diameter of the particle decreases the energy required to excite the surface Plasmon electrons increases. As a result, the absorption maximum shifted toward a lower wavelength (Jain & Mehata, 2017). This result was also agreed with a green synthesis of AgNPs using *Tragopogon Collinus* leaves extract. At pH values 9 and 10 a sharp and symmetric increasing peak was observed, whereas absorption declined at a pH of 11. This can be attributed to the hydrolysis of silver ions causing the production of stable types of hydroxide and preventing their entry (Seifipour et al., 2020). Here the original pH of synthesized AgNPs was 5 without the addition of base or acid. Synthesized powder AgNPs greater than pH-8, formed like sticky in which the oil of plant extract was covers the powder sample. Due to this pH-7 and Ph-5 were selected for further studies.

4.3 Synthesis of Powder AgNPs

Using method (A) and method (B), the yield of converted AgNPs was estimated by assuming that all silver atoms in the stack solution were converted to AgNPs using the extract as a reducing agent. The first technique (A) is a frequently used or well-known method for producing nanoparticles. Only 7% of ANPs were generated using this technique. This might be because a greater number of AgNPs were washed away with unconverted silver ions and contaminants. A newly approach method (B) were proposed to solve this problem. 77% of AgNPs were produced by using this method. This is because a large number of nanoparticles collected or aggregated on the Petri dish before centrifugation makes it easier to sediment the nanoparticles by increasing the weight of nanoparticles in the centrifugation tube.

4.4 Characterization of *Vernonia amygdalina* Leaf Extract

4.4.1 Phytochemical Analysis

Phytochemical screening tests were done to determine the class of compounds present in the extract. Phytochemicals are large number of secondary metabolites or bioactive compounds found in plants. A phytochemical screening of Methanol with Distilled water (M/DW) based

extracts followed standard protocols were described as showed in Table 4.1.The Phytochemical Screening gives positive results with in ferric chloride test of phenols, frothing test, and alkaline test of flavonoids and Tannin preliminary phytochemical Tests.

Table 4.1 Phytochemical screening of methanol to distilled water extract

RUN	Phytochemical Compounds	Tests performed	M/DW extract
1	Phenolic	Ferric chloride test	+
2	Saponins	Frothing test	+
3	Flavonoids	Alkaline test	+
4	Tannins	Ferric chloride test	+
5	Terpenoids	Salkowski's test	-
6	Alkaloids	Meyers reagent test	-
7	Glycosides	Salkowski's Test	-

(+, present); (-, absent)

The phytochemical screen for secondary metabolites revealed the presence of phenolic, saponins, flavonoids, tannins in the M/DW extract. Phenolic compounds have been reported, which are split into phenolic acids and polyphenols are the major class of secondary metabolites. These molecules can be discovered in combination with mono and polysaccharides, connected to one or more phenolic groups, or as derivatives such ester or methyl esters (Minatel et al., 2017). (Ogidi et al., 2019) also shows phenolic phytochemical components in vernonina amygdalina. Saponins are a complex and chemically diverse group of bitter-tasting surface active agents (surfactants) that may cause a lot of foaming activity in aqueous solutions. (Kregiel et al., n.d.). Saponins are starch glycosides with three hydroxyl groups connected to complicated sugar components. Flavonoids are a class of natural

chemicals with a phenolic structure that varies. Flavonoids occurring in *V. amygdalina* have been identified with luteolin, luteoiin 7-O- β glucuronoside and luteolin 7-O-β glucoside (Igile et al., 1995). Tannins commonly denoted to as tannic acid due to they are drive from phenolic acid. Tannins are water-soluble polyphenols that are present in *V. amygdalina* (Ali et al., 2020). according to literatures Methanol based extract of *V.amygdalina* shows positive results for phenolic, saponins, flavonoids, tannins, alkaloids in the presence with in high level (Ekam et al., 2010)

4.4.2 Thin Layer Chromatography (TLC)

Thin layer chromatography is a form of liquid chromatography where the stationary phase is thin layer of chromatographic material flat support of metal. After the crude extract of *V.amygdalina* was treated by methanol solvent applied on to the origin and it moves upward with the solvent ratio. The sample under UV florescence lamp at 366 nm, used to visualize the spots didn't show any spot when ethyl acetate: n-hexane with (2:3, 1:4, 1:9, 3:7 and 3:2 mL) where used as a mobile phase, and for dichloromethane: Methanol (2:3) was used as a mobile or developing solvents. TLC of component mixture which shows a spot were indicated as shown in figure 4.10

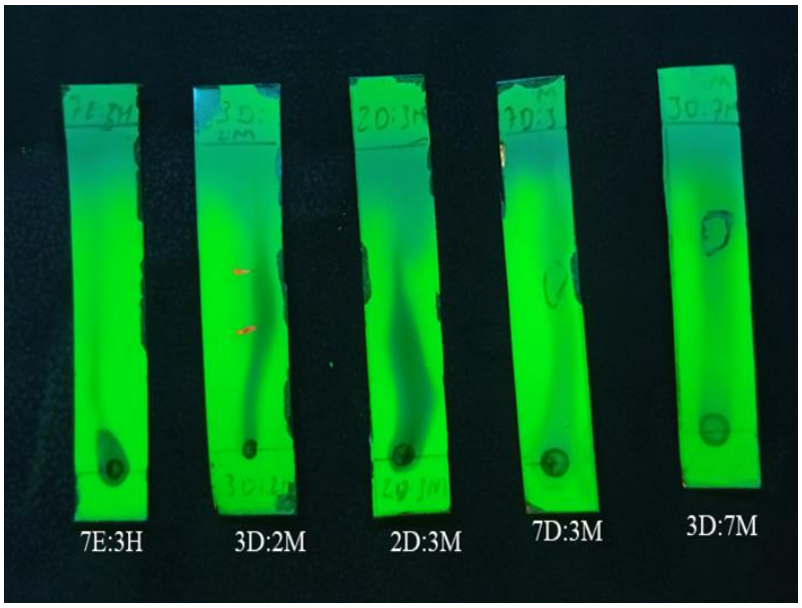

Figure 4.10 TLC picture under UV light using various mobile phase systems

Chromatography has validated the presence of several types of phytochemical components like saponins, flavonoids, phenolic and Tannins, according to previous phytochemical screening data. The R_f value for the selected solvents (7E:3H, 3D:2M, 7D: 3M and 3D:7M) are 0.15, 0.485, 0.55, 0.66 respectively. This difference in R_f values gives an essential hint in determining their polarity and assisting in selecting an appropriate solvent system for column chromatography separation of pure chemicals included in various fractions. 3D:2M showed two spots, which indicates at least there are two components in the extract. Specially 2D:3M, 7D: 3M and 3D:7M did not Show a separate movement of components. The R_f value also too large this indicate that all components of the mixture was moved along with the solvents, due to the high polarity of solvents.

4.4.3 Fourier Transferred Infrared Radiation Analysis

FTIR is tool for identification for functional groups within organic compounds. The bio-active molecules present in 40/60 (M/DW) based *V. amygdalina* leaves extract were showed on the figure 4.11 using FT-IR spectra.

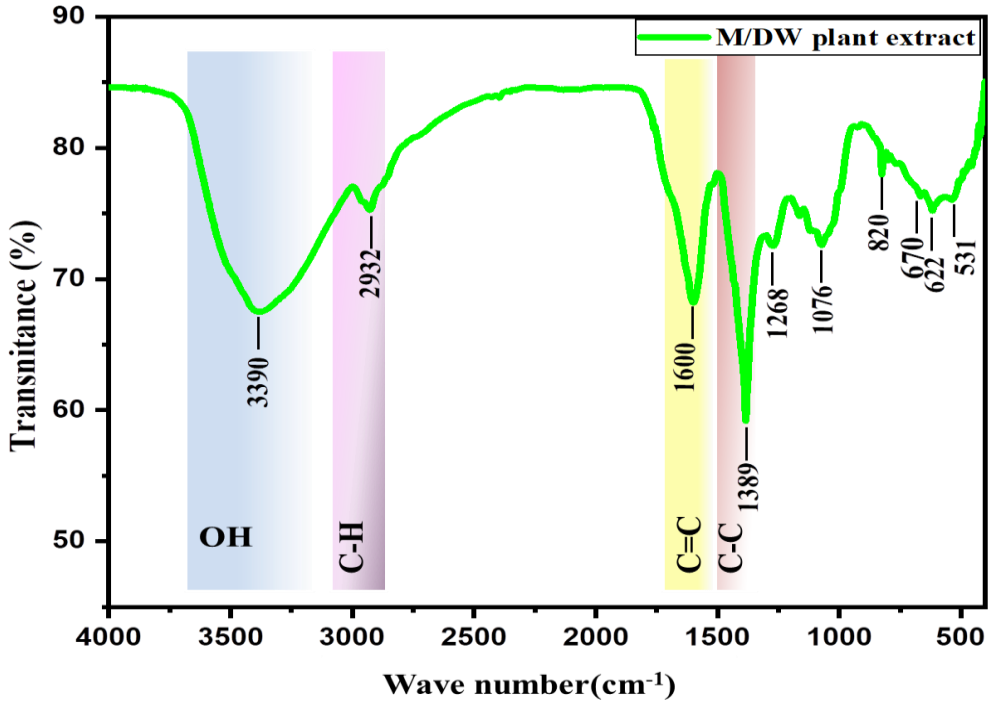

Figure 4.11 Functional group analysis of plant extract prepared with M/DW(40/60 ratio)

The presence of different compounds was confirmed according to spectra showing the identity of O-H stretching of intermolecular bonded alcohol at 3390 cm^{-1}. The peak 2932 cm^{-1} indicates the presence of CH_3 asymmetric and symmetric stretching of alkanes. The C=C starching of ester takes place at 1600 cm^{-1}. The peak at 1389 cm^{-1} elucidates the occurrence of C-C stretching. The fingerprint region of the spectra accounts for the presence of OH stretching and C-O ester stretching at 1268 cm^{-1} and 1076 cm^{-1} respectively. The outcome of this result was confirmed as the presence of phytochemical components Phenol, Saponins, Flavonoids, and Tannins as indicated before.

The above hydroxyl group indicates the presence of phenolic groups from phytochemical results. The functional groups characterized as C-H absorption from alkene/alkyl groups confirm the presence of Saponins bioactive molecule. Generally, the functional groups were indicate the result aligned with the synthesis of Ag_2O Nanoparticles using *V. amygdalina* as reducing agent (Widyaningtyas et al., 2019). These results were agreed with methanol based *V. amygdalina* extract which shows the presence of alkanes, alkenes, amines, carboxylic acids and alcohols with peaks of frequency at 3436.69, 2928.2, 2861.80, 1743.75, 1644.48, 1462.26, 1376.92, and 1212.97 cm^{-1} (aBashir et al., 2020).

4.5 Characterization of Green synthesized Powder AgNPs

4.5.1 UV-Vis Spectrophotometery

UV-Vis spectroscopy is preliminery technique that comfirms the formation of nanoparticles. Here, the optimized AgNPs at pH 7 in the solution before centrifuagation process and the powdered AgNPs, which dissolved in to distilled water when exmined using UV-Vis spectroscopy as shown in the figure 4.12

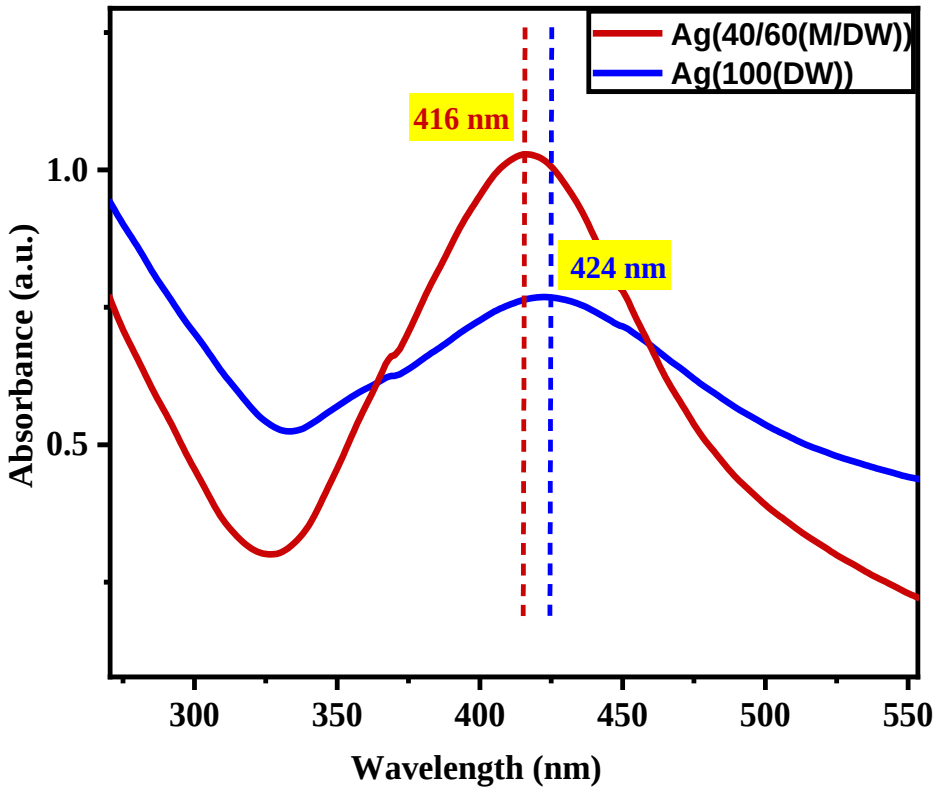

Figure 4.12 UV-Vis spectra of Green synthesized AgNPs

The absorbance spectrum of colloidal sample was obtained in the range of 200-800 nm. The red brown colour of spectra AgNPs (40/60 (M/DW)) shows absorbance of stable AgNPs in the solution of 40/60 (M/DW) solvent at 416 nm wavelength before centrifugation. The blue colour AgNPs (Powder) shows UV-Vis spectra in the wavelength of 424 nm. The nanoparticles are formed by collecting nanoparticles using moisture removal and then centrifugation. The absorption peaks shifted towards the higher wavelength for the powdered sample from (416-424 nm). This might be due to an increase in particle aggregation. As the diameter of AgNPs increases, the energy required to excite the SPR electron decreases. The increase of the agglomeration of particle is due to stabilizing and capping agents of plant extract.

4.5.2 X-RAY Diffraction

The phase evaluation of AgNPs produced at different pH (pH-5 and pH-7), the crystalline grain size was investigated from X-ray diffraction graph sown as figure 4.13.

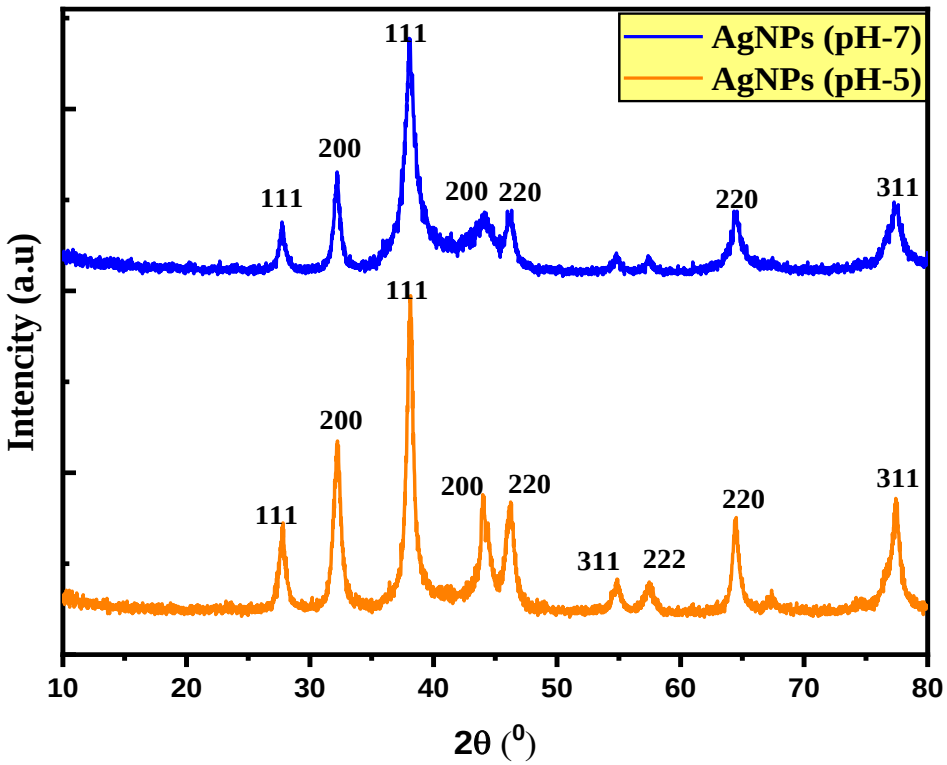

Figure 4. 13 X-ray diffraction of AgNPs synthesized at PH-7 and pH-5

The XRD pattern showed four intense peaks in the whole spectrum of 2θ values ranging from 27^0 to 80^0 .A comparison of the obtained XRD spectrum with the standard confirmed that the silver particles formed in the four intense peaks appeared at 38.109, 44.14°, 64.47°, 77.37° for pH-5 and 38.0946°, 44.4385° 64.494°, 77.349° for pH-7. However, peaks at 27 °, 32°, 46°, 54°, 57°, shows for AgO nanoparticles. This AgNPs results were agreed with the green synthesis of AgNPs using *G. ofcinalisw* plant extract. The XRD peaks in degrees 2θ appear at 38.0946°, 41.4385° 64.494°, 77.349° this can be attributed to the planes (111) (200) (220) (311) and (222) sets of lattice planes consistent crystal structure of silver reported (Manosalva et al., 2019). The distance between two planes was calculated using Bragg's equation using the data illustrated in Table 4.2. The d-spacing of Ag synthesized at pH-5 is 0.031A° and for Ag synthesized at pH-7 was 0.21A°. The average crystal size of Ag nanoparticles with pH-5 (original sample) and pH-7 was calculated by using scherrer equation from the data gathered from the origin, as illustrated in Table 4.3. The crystalline size of Ag for pH-5 was 7.04 nm and pH-7 was 4.26 nm.

Table 4.2 Indexed consecutive peaks of AgNPs

2 theta(2θ)	Peak position in Radian	D=$\lambda/2sin\theta$	Average D-Spacing
pH-5			
27.768°	0.242321513	0.018477	
32.210°	0.281091385	0.0213	
38.109°	0.332563762	0.025138	
44.140°	0.385194166	0.028932	**0.031095 A°**
46.181°	0.403013105	0.030199	
54.829°	0.478473288	0.035453	
64.470°	0.562606884	0.041071	
77.370°	0.675180621	0.048128	
Ph-7			
27.763°	0.24227788	0.321072583	
32.1895°	0.28090638	0.277859323	
38.0946°	0.332438099	0.236035939	
44.4385°	0.361619131	0.217728578	**0.210514 A°**
46.1825°	0.403018341	0.196406578	

54.804°	0.478255122	0.167372553
64.494°	0.562816324	0.144367124
77.349°	0.674997362	0.123268658

Table 4.3 AgNPs crystalline size calculated from intense peaks

2 theta(2θ)	Theta(θ)	FWHM (β)	Crystalline size (nm)	Average Size (nm)
For pH-5				
38.109°	19.054	0.775	9.6854	
44.140°	22.07	3.602	2.038	7.045
64.47°	32.235	0.638	10.507	
77.37°	38.685	1.04	5.950	
For pH-7				
38.0946°	19.0473	1.092	6.872	
44.01°	20.7192	11.348	0.656	4.266
64.494°	32.247	1.151	5.832	
77.349°	38.6745	1.673	3.706	

4.5.3 Fourier Transferred Infrared Radiation

FT-IR spectroscopy is used to investigate the organic chemical composition on the surface of AgNPs. This chemical composition was carried out to identify the potential biomolecules responsible for the reduction of the Ag ions and capping or efficient stabilization of the AgNPs synthesized using *V. amygdalina* leaves extract. The result of FT-IR analysis of AgNPs at pH-7 and plant extract for comparison was showed on figure 4.14. The FT-IR spectrum showed absorption bands at 3390 cm^{-1}, 2919 cm^{-1}, 2842 cm^{-1}, 1714 cm^{-1}, 1600 cm^{-1}, 1369 cm^{-1}, 1247 cm^{-1}, 1041 cm^{-1},825 cm^{-1}, 608, 531 cm^{-1} indicates the presence of capping agents with AgNPs.

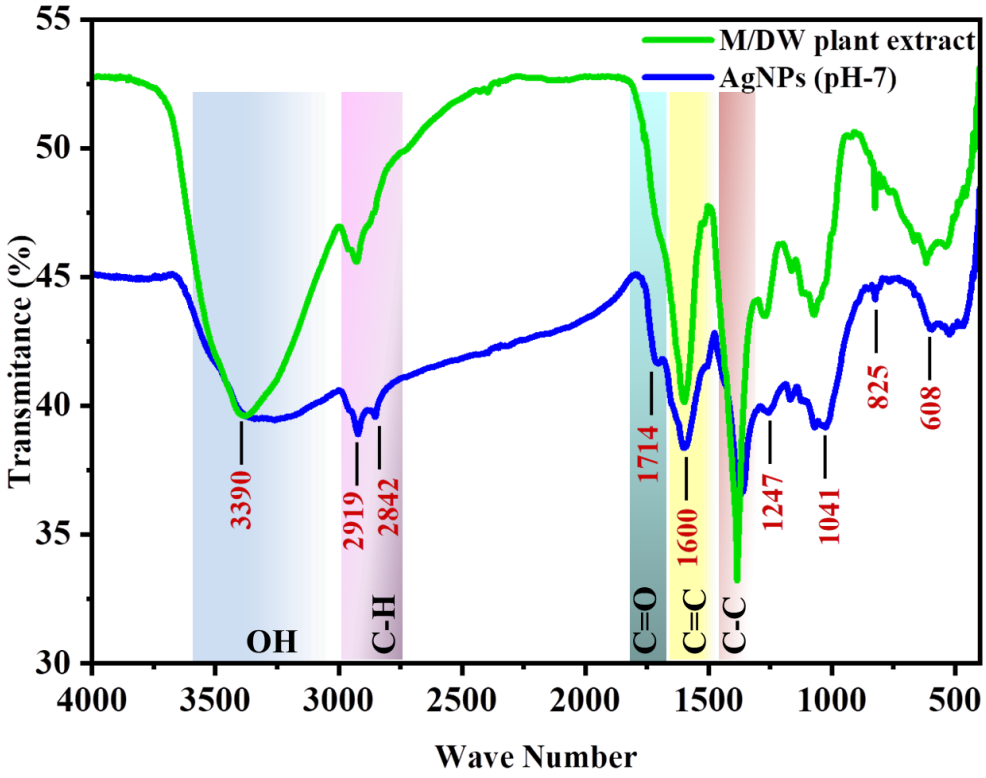

Figure 4.14 FTIR analysis of AgNPs and plant extract

The FTIR spectrum of AgNPs showed bands at 3335 cm^{-1}, this showed O-H stretching vibration of phenolic and alcoholic compounds. The absorption peaks located at 2919 $cm^{-1}$and 2842 cm^{-1} are region arising from C-H stretching of alkenes. Peak at 1714 cm^{-1} was assigned as C=O ester stretching. The peaks at 1600 cm^{-1} showed stretching of aromatic compounds of

C=C (non-conjugated) Stretching. The peak near 1369 cm^{-1} corresponds to the starching vibration of C-C stretching.

The FT-IR spectra of AgNPs showed two new major peaks different from plant extract. The peaks at 2842 cm^{-1} and peaks at 1714 cm^{-1}, which are the starching of CH_2 and C=O bonds due to the flavonoids of functional groups. Also there is a change on the intensity peaks at 1600 cm^{-1} and 1369 cm^{-1} were showed corresponding to the stretching of C=C band and C-C bond of aromatic groups. From the FT-IR analysis and phytochemical screened preformed of *V. amygdalina* plant extract compounds the presence of Saponins, Tannins, Flavonoids and phenolic compounds provide the extra stability to the nanoparticles. This result was also argued with green synthesis of AgNPs using Cannonball Leaves. It shows different stretches of bonds shown at different peaks; 3432.94, 2777.28, 2676.19, 2071.75, 1637.58 and 1121.56 cm^{-1} peaks of O-H Stretching, C-H Stretching, -C≡C, -C=C and –C=O. also the peak near 833 cm^{-1} assigned to $C=CH_2$ and the peaks near 677 cm^{-1} and 651.96 cm^{-1} assigned to C-H out of plane bending vibrations are substituted ethylene systems –CH=CH (Preetha et al., 2013).

4.5.4 Antimicrobial Activity of AgNPs

Antimicrobial effect of greenly synthesized AgNPs using *V. amygdalina* were tested against Gram negative bacteria (*E.coli* and *p. aurugonosa*) and Gram positive bacteria species (*S. pyogen* and *S. aureus*) using disk diffusion assay. Greenly synthesized AgNPs were prepared at pH-5 and pH-7 and the prepared nanoparticles with different concentration of sample (75, 50, and 25 µg/mL) and Ciprofloxacin was used as reference drug to test the antimicrobial activity. The zone of inhibition was indicated on the Table 4.1 and figuratively as shown on figure 4.15

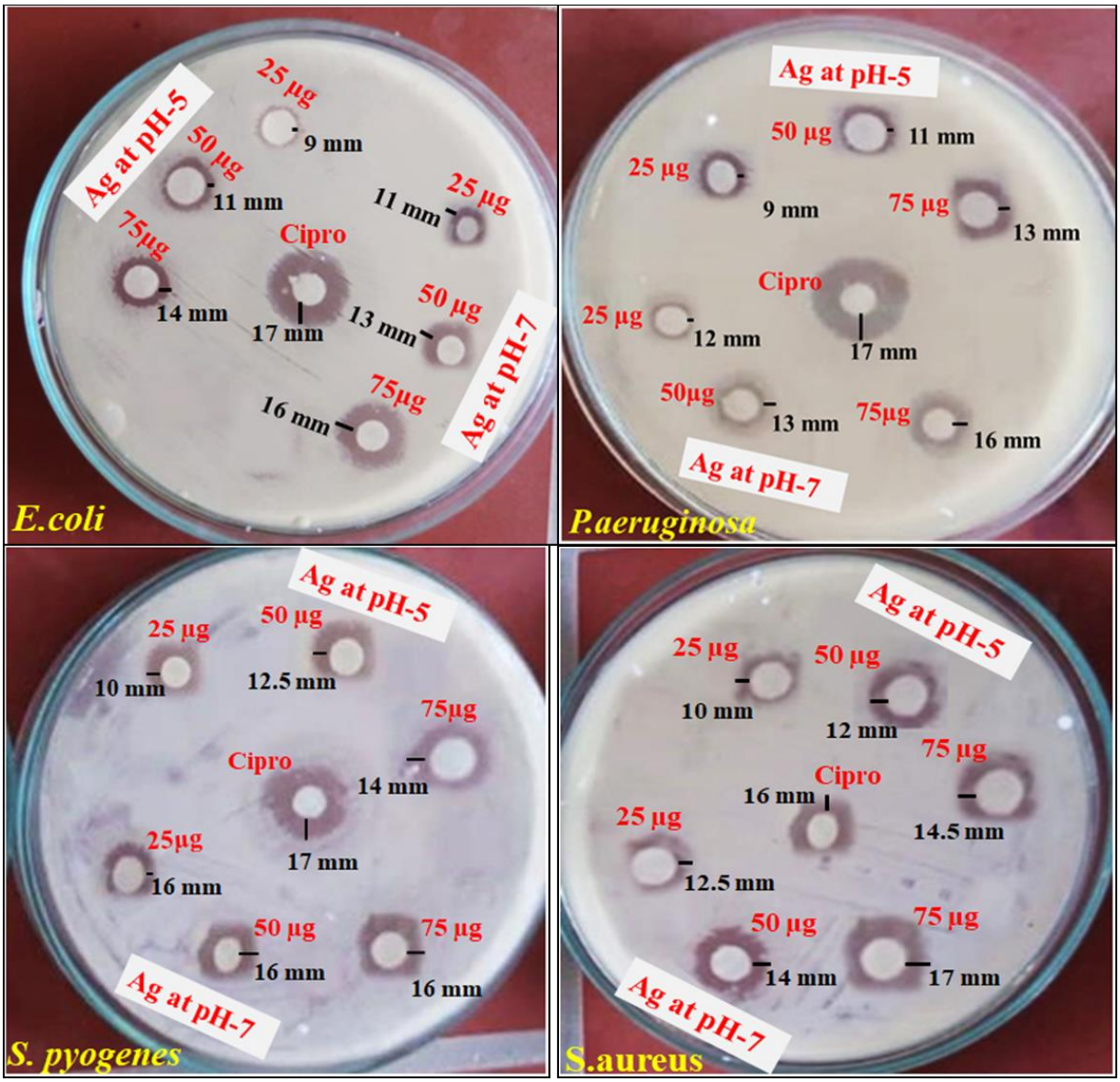

Figure 4. 15 Zone of inhibition produced by AgNPs against four pathogens

Among synthesized nanoparticles at different pH values (pH-5 and pH-7) bacteria test was investigate. pH-5 showed moderate inhibition activities against Gram-negative, *E.coli* with 14, 11, 9 mm for concentration of 75, 50, 25 µg/mL respectively compared to standard drug Ciprofloxuein (17mm). *P. aeruginosa* also shows comparable inhibitions 13, 11, 9 mm. pH-5 also showed good implication against Gram-positive bacteria. As indicated in the figure 4.15 at pH- 5 a broad spectrum antimicrobial activity were found against Gram-positive bacteria.

AgNPs synthesized at pH-7 showed higher inhibitory activities against Gram-positive bacteria of *S. pyogenes and S. aureus* with zone of inhibition 17, 15, 13 mm and 17, 14, 12.5 mm respectively for the concentrations 75, 50, 25µg/mL. The results of this investigation are consistent with those found in the literature. For example, against *S. aureus*, *E. coli*, and Candida albicans, AgNPs produced using *Talinum triangulare* showed inhibitory zones of 2.35, 2.55 and 1.65 mm, respectively (Nurul Aini et al., 2019).

Table 4.4 Anti-bacteria activity (inhibition zone) of AgNPs

		Zone of inhibition an mm (mm)			
		Gram-negative		**Gram-positive**	
	Concentration	***E.coli***	***P.aeruginosa***	***S.pyogenes***	***S.aureus***
pH- 5	75 µg/mL	14	13	14	14.5
	50 µg/mL	11	11	12.5	12
	25 µg/mL	9	9	10	10
pH- 7	75 µg/mL	16	16	17	17
	50 µg/mL	13	13	15	14
	25 µg/mL	11	12	13	12.5
Ciprofloxacin		17	17	17	16

From both of AgNPs synthesized with different pH. pH-7 showed higher antimicrobial activity on both Gram-negative and Gram-positive bacteria than AgNPs synthesized at pH-5. Generally when the concentration of AgNPs increased the zone of inhebitition produced also increased.

4.6 Characterization of Synthesized AgNPs/GLY-LAC Bio-conjugates

The prepared 3-armed GLY-LAC macromolecule from the condensation reaction of Lactic acid and Glycerol at 190^0C for 8 h is viscous and has light yellow colour. After AgNPs were dispersed at a concentration (0.1%, 1%, 3%) into GLA-LAC bio-conjugate assisted using Ultrasonicator the colour of GLY-LAC was changed to dark brown colour.

4.6.1 UV-Vis Spectroscopy

The UV-Vis absorbance spectra were recorded for GLY-LAC bio-conjugate and AgNPs/GLY-LAC bio-conjugate as indicated on the figure 4.16. The absorbance peak of 1% AgNPs /GLY-LAC was observed at 420 nm, which represent transmission of AgNPs in the fluid. The GLY-LAC by itself didn't show any intense peaks.

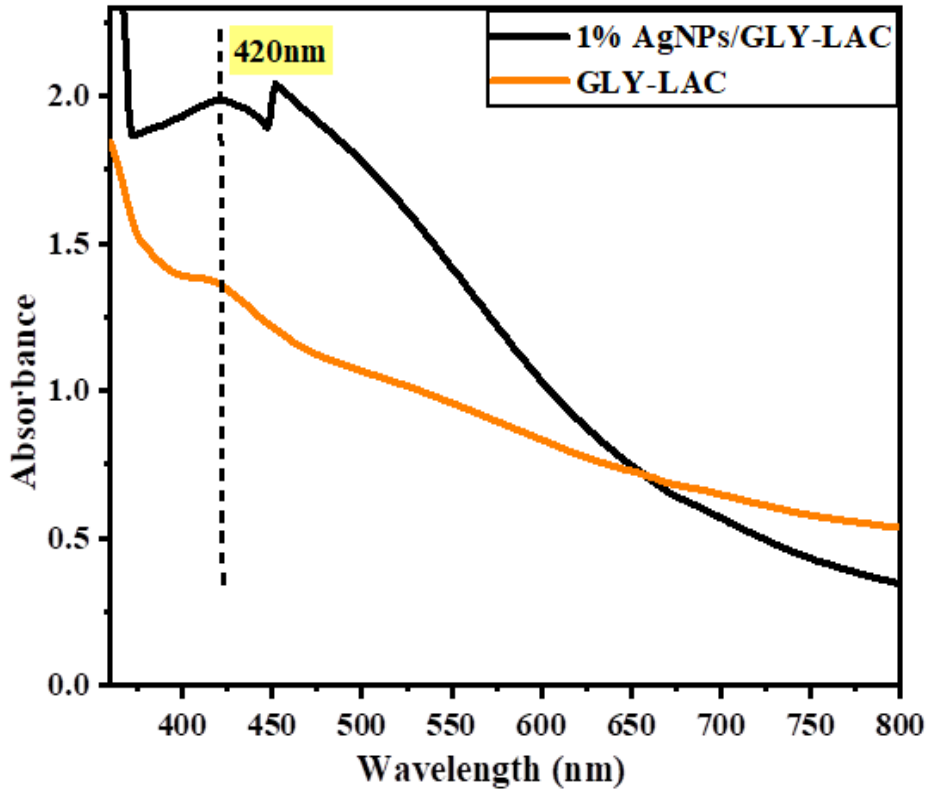

Figure 4. 16 UV-Vis spectra of AgNPs/GLY-LAC and GLY-LAC bio-conjugate

4.6.2 Fourier Transferred Infrared Radiation

The Fourier transform infrared (FTIR) result for the synthesized GLY-LAC and 1% AgNPs/GLY-LAC bio-conjugate was analyzed on the figure 4.17. Here when the reaction was done between the three OH groups of Glycerol and 3- molecules of lactic acid via condensation reaction there will be a possible increased C=O bond formation. This ester functional group supported by the formation of a broad peak at 1746 cm^{-1}. Likewise approximately same intense peak was observed at 1639 cm^{-1} there is a hump peak was observed, due to weak Vander walls interaction of C=O bond on the glycerol core with OH group found at the end chain. Other peak was found at 1040 cm^{-1} is for C-O stretching in secondary OH group of glycerol. Also the peaks observed at 989 and 935 cm^{-1} was for the C-O stretching on the hydroxyl group in glycerol. A black colour of FT-IR peak showed that 1% AgNPs incorporated in the GLY-LAC macromolecule. Here also a C=O bond observed at 1746 cm^{-1}, however the intensity peak of C=O interaction with OH decreased as showed at 1636 cm^{-1}

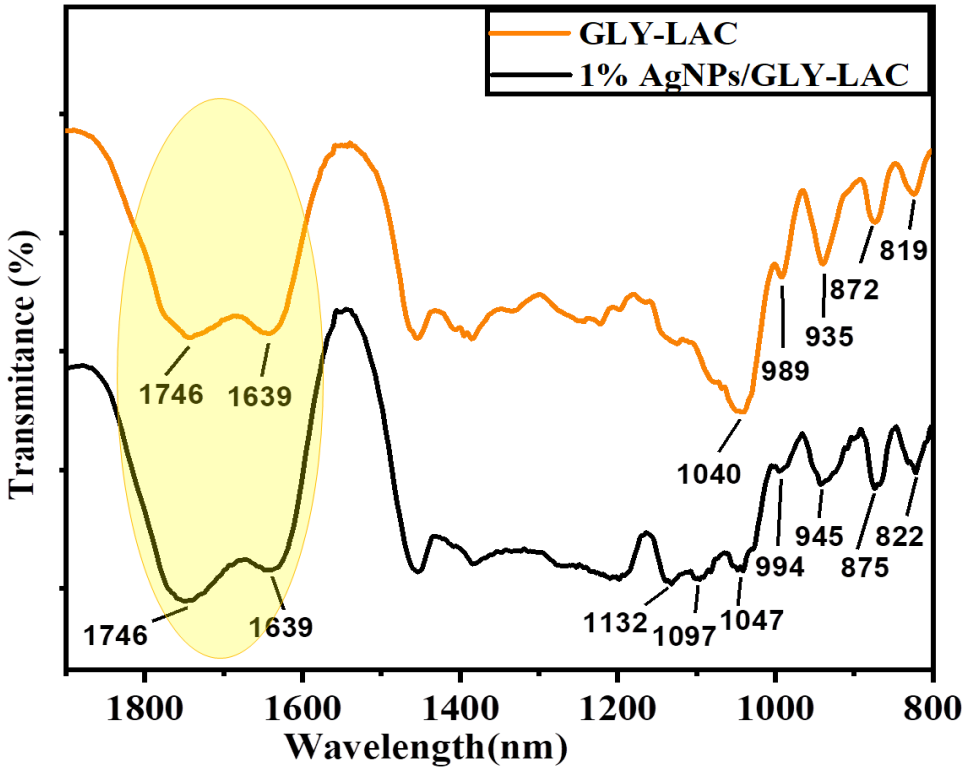

Figure 4. 17 Functional group analysis for GLY-LAC and AgNPs/GLY-LAC

When AgNPs introduced in the bio conjugate AgNPs suppressed the interaction between OH and C=O bond of macromolecule. The OH groups from the glycerol core may circle AgNPs, due to this the intensity of peak at 1639 cm^{-1} were decreased. Peaks observed at 1132, 1097 and 1047 cm^{-1} showed C-O stretching. Additionally peak shifting observed at 1047, 994, 945, 875, and 822 cm^{-1} due to the addition of AgNPs.

4.6.2 Antimicrobial Activity

Due to the high antimicrobial activities of AgNPs, The antimicrobial activities of prepared bio-Conjugate were investigated at different concentrations of 500 mg/mL and 1 mg/mL. The antimicrobial activities were tested against Gram positive and Gram negative bacteria, selected from greenly synthesized AgNPs which showed higher inhibition zones from four bacteria. Figure 4.18 showed a clear zone of inhibition produced by using AgNPs/GLY-LAC, where AgNPs dispersed with (0.1%, 1%, and 3wt %). Hereafter ensuring stable nanoparticles dispersion in the conjugate, the antibacterial activity with the diameter zone of inhibition was observed by the conjugate.

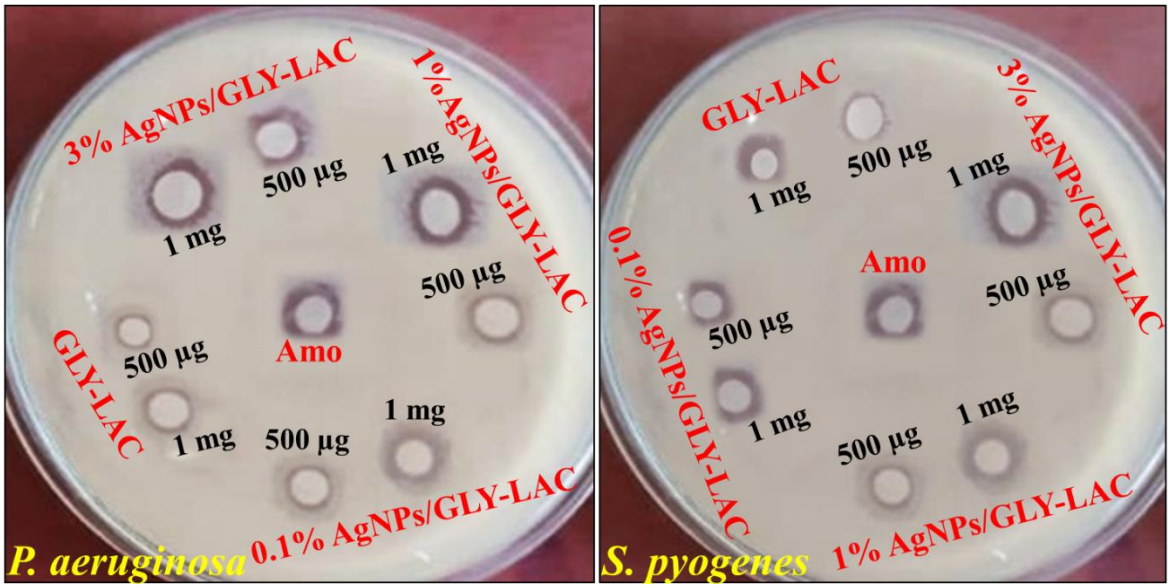

Figure 4. 18 zone of inhibition produced by bio conjugate againest two pathogens; (*Pseudomonas aeruginosa* and *Streptococcus pyogenes*)

The synthesized 1:12 bio-conjugate showed antimicrobial activities for both of Gram-positive (*S.pyogenes*) and Gram negative (*P.aeruginosa*) bacteria by disk diffusion assay at different concentration (500 µg/mL and 1 mg/mL). Amoxicillin were used as a reference drug. Net GLY-LAC bio-conjugate showed 9, 10 mm and 10, 11.5 mm zone of inhibition at 500 µg/mL and 1mg/mL, respectively. However, after adding 0.1%, 1% and 3% AgNPs into the GLY-LAC macromolecule, the inhibition zone was increased to 10.5, 13 and 14 mm at 500µg and 12.5, 13.5 and 16 mm at 1mg for the *P. aeruginosa* bacteria. Also, for bacteria *S. pyogenes,* after adding 0.1%, 1% and 3% AgNPs into the GLY-LAC macromolecule, the inhibition zone increases to 11, 12.5 and 14 mm at 500µg and 13.5, 14 and 17 at 1mg. Increasing the compound of AgNPs/GLY-LAC from 500µg/mL to 1mg/mL increased the antibacterial activities also as shown in Table 4.5.

Table 4.5 Anti-bacteria activity (inhibition zone) of GLA-LAC and GLA/LAC-Ag bio-conjugate

Compound	**Concentration**	**Zone of inhibition an mm**	
		P. aeruginosa **ATCC27853**	***S. pyogen*** **ATCC19615**
GLY-LAC	500 µg/mL	9	10
GLY-LAC	1mg/mL	10	11
0.1% AgNPs/GLY-LAC	500 µg/mL	10.5	11.5
0.1% AgNPs/GLY-LAC	1mg/mL	12.5	13.5
1% AgNPs/GLY-LAC	500 µg/mL	13	13.5
1% AgNPs/GLY-LAC	1mg/mL	13.5	14
3% AgNPs/GLY-LAC	500 µg/mL	14	14.5

3% AgNPs/GLY-LAC	1mg/mL	16	17
Amoxicillin		**13**	**13**

As compared to the inhibition zones of 13 mm for Amoxicillin, the 500 µg/mL and 1mg/mL compounds of 3% AgNPs/GLY-LAC have better antimicrobial properties for both pathogens. The ant-bacterial activities of synthesized bio-conjugate are enhanced with AgNPs, in which nanoparticles are well dispersed.

4.7 Characterization of AgNPs/GLY-LAC/PLA Biofilm

4.7.1 Antimicrobial Activity

The effect of PLA biofilms with GLY-LAC and AgNPs/GLY-LAC bio-conjugate was measured based on the halo formed around the 6mm film (disk). The clear zone of inhibition was observed for both *P. aeruginosa* and *S. pyogenes* has showed on the figure 4.19.

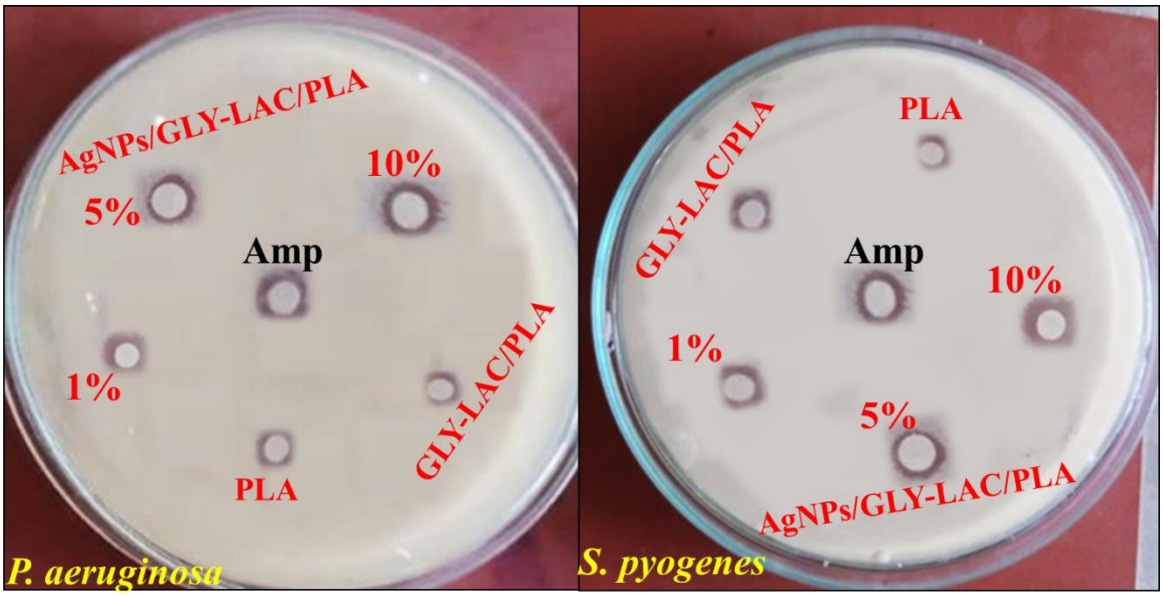

Figure 4. 19 Zone of inhebition produced by PLA based biofilm againest *P.aeruginosa* and *S.pyogenes*

The diameter of halo formed by the PLA film and GLY-LAC/PLA film were 7 and 8 mm for bacteria *P. aeruginosa* respectively, also 8 and 9.5 mm were showed for bacteria *S.pyogenes* respectively. All the 3 different percent of AgNPs are dispersed in bio-conjugate has inhibitory effect. As the well dispersed and stable AgNPs /GLY-LAC bio-conjugate. 1wt% AgNPs/GLY-LAC)/PLA, 5wt% (AgNPs/GLY-LAC)/PLA and 10wt% (AgNPs/GLY-LAC-AgNPs)/ PLA were incorporated in the film the antibacterial activities were increased 10, 12.5 and 13 mm *for P. aeruginosa* and 11, 12.5 and 13.5 mm for *S. pyogenes*. The antibacterial activates of the film increased as the concentration of the AgNPs were increased. Generally the antibacterial activities of AgNPs against Gram positive bacteria and Gram negative bacteria found that AgNPs were more active against gram positive bacteria. As seen on the Table 4.6 the antibacterial activities of the AgNPs/GLY-LAC/PLA against *S.pyogenes* (Gram positive) were higer than *P.aeruginosa* (Gram negative bacteria). Generally this study clearly demonstrates that AgNPs show good antibacterial activites, specially in gram positive bacteria.

Table 4.6 Anti-bacteria activity (inhibition zone) of PLA based film

Compounds	Bacteria strains and Zone of Inhibition in (mm)	
	***P. aeruginosa* (ATCC27853)**	***S. pyogenes* (ATCC19615)**
PLA	7	8
PLA/GLY-LAC	8	9.5
1%(AgNPs/GLY-LAC)/PLA	10	11
5%(AgNPs/GLY-LAC)/PLA	12	12.5
10%(AgNPs/GLY-LAC)/PLA	13	13.5
Ampicillin	12	12

CHAPTER FIVE

5. Conclusion and Recommendation

5.1 Conclusion

Green synthesis method of silver nanoparticles (AgNPs) achieved using *V. amygdalina* leaves extract as a reducing and stabilizing agent. The effect of different operational parameters like concentration of precursor, ratio of $AgNO_3$/plant extract, Temperature, Time and pH, including solvent type and ratio for extraction, were investigated. The plant extract phytochemical components were characterized using the preliminary phytochemical screening method and FT-IR analysis responsible for the reduction. Greenly synthesized and purified AgNPs characterized using XRD and FT-IR. The preliminary photochemical screening of plant extract showed the presence of phenolic, saponins, flavonoids and Tannins. This was also confirmed using FT-IR analysis. The UV-Vis spectra showed specific Surface Plasmon Resonance (SPR) absorption peaks for AgNPs between 411 nm- 430 nm for synthesized AgNPs at optimum conditions. The XRD peaks showed for AgNPs were around 38^0, 44^0, 64^0, 77^0 and the d-spacing between two planes were $0.031A^0$ (for pH-5) and $0.21A^0$ (for pH-7). The FT-IR results confirmed the presence of O-H, C-H, C=O, C=C bonds due to the presence of phytochemical components capping the AgNPs. The synthesized AgNPs showed antimicrobial activity with a clear zone of inhibition against Gram-negative bacteria (*E. coli* and *P. aeruginosa*) and Gram-positive bacteria species (*S.pyogen* and *S. aureus*). AgNPs synthesized at pH-7 showed higher inhibitory activates than AgNPs synthesized at pH-5. The inhibition zone was increased when the concentration of AgNPs increased from 25-75µg. The use of plant extracts as an effective reducing agent and stabilizing agent in AgNPs shows their potential values to use AgNPs for further applications, especially in medical applications.

The greenly synthesized AgNPs are applicable on the polymer matrixes to enhance the antimicrobial activities of the matrix. 3-armed GLY-LAC bio-conjugate plasticizer helps to homogenously disperse AgNPs using ultra-sonication. The antimicrobial activity of GLY-LAC macromolecule was enhanced/ increased (0.1 % AgNPs/GLY/LAC < 1 % AgNPs/GLY/LAC < 3 % AgNPs/GLY/LAC) AgNPs/GLY-LAC as the concentration of

AgNPs in the matrix was increased. When compared with inhibition zones of 13 mm for Amoxicillin, The zone of antibacterial activity increased 16 mm and 17 mm for *S. pyogenes* and *P. aeruginosa*, respectively.

1% AgNPs/GLY-LAC at different concentrations was used as filler to enhance the antibacterial activities of PLA biofilm. The antibacterial activities of the film were examined against *S.pyogenes* and *P.aeruginosa*. The zone of inhibition increases as the concentration (1% < 5% < 10%) AgNPs /GLY-LAC incorporated in PLA matrix was increased. Generally, the antibacterial activities of AgNPs found that AgNPs were more active against both gram-positive and gram negative bacteria.

5.2 Recommendation

In this research work, AgNPs were greenly synthesized using *V. amygdalina* as a reducing and stabilizing agent. Then the different effect of operational parameters was investigated to get high concentration of AgNPs. Well dispersed and AgNPs in GLY-LAC bio-conjugate and used as a filler to enhance the antimicrobial activities of the conjugate and PLA bio-films. The biocompatibility, Non-toxicity, and stability of Green methods and AgNPs high electrical conductivity, Thermal and optical properties make them a versatile application. Some recommendations for future work were opportunities are as follows:-

- Since operational parameters for the synthesis of AgNPs has effects on the Morphology and particle size of nanoparticles, the synthesized AgNPs may investigate using SEM (nm) and TEM.
- Due to the good antibacterial activities of AgNPs in the films, it is good if the Anti-fungal activities and shelf life in the food packaging application may be investigated in detail.
- AgNPs are stable in the GLY-LAC macromolecule; this is promising as a thermal Nano fluid or engineered fluids.
- Due to the physical, chemical and higher conductivity properties of AgNPs in the biofilm Nano-composite. It may be applicable for bio-packaging, bio-sensor, wound dressings, implantation, electrical and thermal applications. This is an area where further research might be done.
- Further study can be explored on toxicity and the migration of AgNPs from the bio-film.

6. Reference

aBashir, R. A., aMukhtar, Y., bChimbekujwo, I. B., cAisha, D. M., cFatima, S. U. & cSalamatu, S. U. (2020). Phytochemical Screening and Fourier Transform Infrared Spectroscopy (FT-IR) Analysis of Vernonia amygdalina Del . (Bitter leaf) Methanol Leaf Extract. *FUTY Journal of the Enviroment*, *14*(2), 35–41.

Abbasi, E., Milani, M., Fekri Aval, S., Kouhi, M., Akbarzadeh, A., & Tayefi Nasrabadi, H. (2014). Silver nanoparticles: synthesis, properties, bio-applications and limitations. *Crit Rev Microbiol*, *1*.

Abdeen, Z. I., El Farargy, A. F., & Negm, N. A. (2018). Nanocomposite framework of chitosan/polyvinyl alcohol/ZnO: preparation, characterization, swelling and antimicrobial evaluation. *Journal of Molecular Liquids*, *250*, 335–343.

Adewumi, O., Oluyomi, S., & Grace, A. (2018). *Exploring the Effect Effect of of Operational Operational Factors Factors and and Characterization Characterization Imperative Imperative to to the the Synthesis Synthesis of of Silver Silver Nanoparticles*. https://doi.org/10.5772/intechopen.76947

Ahmed A. Moosa1, A. M. R. and M. A.-K. (2015). w . m . *International Journal of Multidisciplinary and Current Research*, *3*, 966–975.

Ahmed, J., Hiremath, N., & Jacob, H. (2017). Antimicrobial efficacies of essential oils/nanoparticles incorporated polylactide films against L. monocytogenes and S. typhimurium on contaminated cheese. *International Journal of Food Properties*, *20*(1), 53–67.

Aisida, S. O., Ugwu, K., Akpa, P. A., Nwanya, A. C., Nwankwo, U., Botha, S. S., Ejikeme, P. M., Ahmad, I., Maaza, M., & Ezema, F. I. (2019). Biosynthesis of silver nanoparticles using bitter leave (Veronica amygdalina) for antibacterial activities. *Surfaces and Interfaces*, *17*, 100359.

Ajitha, A. R., Aswathi, M. K., Maria, H. J., Izdebska, J., & Thomas, S. (2016). Multilayer

polymer films. In *Multicomponent polymeric materials* (pp. 229–258). Springer.

Akbarzadeh, A., Rezaei-sadabady, R., Davaran, S., Joo, S. W., & Zarghami, N. (2013). Liposome : classification , prepNew aspects of liposomesaration , and applications. *Nanoscale Research Letters*, *8*(102), 1–9. http://www.nanoscalereslett.com/content/8/1/102

Alaqad, K., & Saleh, T. A. (2016). Gold and silver nanoparticles: synthesis methods, characterization routes and applications towards drugs. *J. Environ. Anal. Toxicol*, *6*(4), 525–2161.

Alara, O. R., Abdurahman, N. H., Ishmael, C., & Kabbashi, N. A. (2019). *Extraction and characterization of bioactive compounds in Vernonia amygdalina leaf ethanolic extract comparing Soxhlet and microwave-assisted extraction techniques*. *3655*. https://doi.org/10.1080/16583655.2019.1582460

Ali, M., Diso, S. U., Waiya, S. A., & Abdallah, M. S. (2020). *Phytochemical Screening and Antibacterial Activity of Bitter Leaf (Vernonia Phytochemical Screening and Antibacterial Activity of Bitter Leaf (Vernonia amygdalina). January*.

Ambrogi, V., Donnadio, A., Pietrella, D., Latterini, L., Proietti, F. A., Marmottini, F., Padeletti, G., Kaciulis, S., Giovagnoli, S., & Ricci, M. (2014). Chitosan films containing mesoporous SBA-15 supported silver nanoparticles for wound dressing. *Journal of Materials Chemistry B*, *2*(36), 6054–6063. https://doi.org/10.1039/c4tb00927d

Anderson, S. D., Gwenin, V. V, & Gwenin, C. D. (2019). Magnetic functionalized nanoparticles for biomedical, drug delivery and imaging applications. *Nanoscale Research Letters*, *14*(1), 1–16.

Arfat, Y. A., Ahmed, J., Hiremath, N., Auras, R., & Joseph, A. (2017). Thermo-mechanical, rheological, structural and antimicrobial properties of bionanocomposite films based on fish skin gelatin and silver-copper nanoparticles. *Food Hydrocolloids*, *62*, 191–202.

Arya, A., Mishra, V., & Chundawat, T. S. (2019). Green synthesis of silver nanoparticles from green algae (Botryococcus braunii) and its catalytic behavior for the synthesis of

benzimidazoles. *Chemical Data Collections*, *20*, 1–7. https://doi.org/10.1016/j.cdc.2019.100190

Ashraf, S., Abbasi, A. Z., Pfeiffer, C., Hussain, S. Z., Khalid, Z. M., Gil, P. R., Parak, W. J., & Hussain, I. (2013). Protein-mediated synthesis, pH-induced reversible agglomeration, toxicity and cellular interaction of silver nanoparticles. *Colloids and Surfaces B: Biointerfaces*, *102*, 511–518.

Bhat, R., Deshpande, R., Ganachari, S. V, Huh, D. S., & Venkataraman, A. (2011). Photo-irradiated biosynthesis of silver nanoparticles using edible mushroom Pleurotus florida and their antibacterial activity studies. *Bioinorganic Chemistry and Applications*, *2011*.

Bhosale, M. A., Chenna, D. R., & Bhanage, B. M. (2017). Ultrasound assisted synthesis of gold nanoparticles as an efficient catalyst for reduction of various nitro compounds. *ChemistrySelect*, *2*(3), 1225–1231.

Bordoloi, M., Sahoo, R. K., Tamuli, K. J., Saikia, S., & Dutta, P. P. (2020). Plant Extracts Promoted Preparation of Silver and Gold Nanoparticles: A Systematic Review. *Nano*, *15*(02), 2030001.

Carbone, M., Donia, D. T., Sabbatella, G., & Antiochia, R. (2016). Silver nanoparticles in polymeric matrices for fresh food packaging. *Journal of King Saud University - Science*, *28*(4), 273–279. https://doi.org/10.1016/j.jksus.2016.05.004

Chhatre, A., Solasa, P., Sakle, S., Thaokar, R., & Mehra, A. (2012). Color and surface plasmon effects in nanoparticle systems: Case of silver nanoparticles prepared by microemulsion route. *Colloids and Surfaces A: Physicochemical and Engineering Aspects*, *404*, 83–92.

Coativy, G., Misra, M., & Mohanty, A. K. (2016). Microwave Synthesis and Melt Blending of Glycerol Based Toughening Agent with Poly(lactic acid). *ACS Sustainable Chemistry and Engineering*, *4*(4), 2142–2149. https://doi.org/10.1021/acssuschemeng.5b01596

Dada, A. O., Inyinbor, A. A., Idu, E. I., Bello, O. M., Oluyori, A. P., Adelani-Akande, T. A., Okunola, A. A., & Dada, O. (2018). Effect of operational parameters, characterization

and antibacterial studies of green synthesis of silver nanoparticles using Tithonia diversifolia. *PeerJ*, *6*, 1–17. https://doi.org/10.7717/peerj.5865

Dorjnamjin, D., Ariunaa, M., & Shim, Y. K. (2008). Synthesis of silver nanoparticles using hydroxyl functionalized ionic liquids and their antimicrobial activity. *International Journal of Molecular Sciences*, *9*(5), 807–820.

Ekam, V. S., Ebong, P. E., & Umoh, I. B. (2010). *PHYTOCHEMICAL SCREENING OF ACTIVITY DIRECTED EXTRACTS OF VERNONIA AMYGDALINA LEAVES*. *16*(1), 151–154.

El Shafey, A. M. (2020). Green synthesis of metal and metal oxide nanoparticles from plant leaf extracts and their applications: A review. *Green Processing and Synthesis*, *9*(1), 304–339.

Eya'ane Meva, F., Segnou, M. L., Ebongue, C. O., Ntoumba, A. A., Kedi, P. B. E., Deli, V., Etoh, M.-A., & Mpondo, E. M. (2016). Spectroscopic synthetic optimizations monitoring of silver nanoparticles formation from Megaphrynium macrostachyum leaf extract. *Revista Brasileira de Farmacognosia*, *26*, 640–646.

Films, N., Chi, H., Xue, J., Zhang, C., Chen, H., Li, L., & Qin, Y. (2018). *High Pressure Treatment for Improving Water Vapour Barrier Properties of Poly (lactic acid)/ Ag*. 1–11. https://doi.org/10.3390/polym10091011

Fu, Y., Pang, X.-X., Wang, Z.-Q., Chai, Q., & Ye, F. (2019). A highly sensitive and selective fluorescent probe for determination of Cu (II) and application in live cell imaging. *Spectrochimica Acta Part A: Molecular and Biomolecular Spectroscopy*, *208*, 198–205.

Gahlawat, G., & Choudhury, A. R. (2019). A review on the biosynthesis of metal and metal salt nanoparticles by microbes. *RSC Advances*, *9*(23), 12944–12967.

Gama, M. R., & Bottoli, C. B. G. (2018). Nanomaterials in liquid chromatography: recent advances in stationary phases. *Nanomaterials in Chromatography*, 255–297.

Goyal, S., Hernández, N. B., & Cochran, E. W. (2021). An update on the future prospects of

glycerol polymers. *Polymer International*, *70*(7), 911–917. https://doi.org/10.1002/pi.6209

Gul, R., Jan, S. U., Faridullah, S., Sherani, S., & Jahan, N. (2017). Preliminary Phytochemical Screening, Quantitative Analysis of Alkaloids, and Antioxidant Activity of Crude Plant Extracts from Ephedra intermedia Indigenous to Balochistan. *Scientific World Journal*, *2017*(Figure 1). https://doi.org/10.1155/2017/5873648

Habtamu, A., & Melaku, Y. (2018). Antibacterial and Antioxidant Compounds from the Flower Extracts of Vernonia amygdalina . *Advances in Pharmacological Sciences*, *2018*, 1–6. https://doi.org/10.1155/2018/4083736

Haddad, N., Ayadi, Z. Ben, & Djessas, K. (2018). Synthesis and characterization of antimony doped tin oxide aerogel nanoparticles using a facile sol–gel method. *Journal of Materials Science: Materials in Electronics*, *29*(1), 721–729.

Hassan, B., Chatha, S. A. S., Hussain, A. I., Zia, K. M., & Akhtar, N. (2018). Recent advances on polysaccharides, lipids and protein based edible films and coatings: A review. *International Journal of Biological Macromolecules*, *109*, 1095–1107.

Hassan, I. A., Nasiru, I. A., Malut, A. M., Ibrahim Abdulkadir, S., & Ali, A. S. (2015). Phytochemical studies and thin layer chromatography of leaves and flower extracts of senna siamea lam for possible biomedical applications. *Journal of Pharmacognosy and Phytotherapy*, *7*(3), 18–26. https://doi.org/10.5897/JPP2014.0337

Heydari-Majd, M., Ghanbarzadeh, B., Shahidi-Noghabi, M., Najafi, M. A., & Hosseini, M. (2019). A new active nanocomposite film based on PLA/ZnO nanoparticle/essential oils for the preservation of refrigerated Otolithes ruber fillets. *Food Packaging and Shelf Life*, *19*, 94–103.

Iconaru, S. L., Chapon, P., Le Coustumer, P., & Predoi, D. (2014). Antimicrobial activity of thin solid films of silver doped hydroxyapatite prepared by sol-gel method. *The Scientific World Journal*, *2014*. https://doi.org/10.1155/2014/165351

Igile, G. O., Oleszek, W., Jurzysta, M., Burda, S., Fafunso, M., & Fasanmade, A. A. (1995).

Errata: Flavonoids from vernonia amygdalina and their antioxidant activities (Journal of Agricultural and Food Chemistry (1994) 42(11) (2445–2448) (10.1021/jf00047a015)). *Journal of Agricultural and Food Chemistry*, *43*(5), 1420. https://doi.org/10.1021/jf00053a053

Ilyas, S. U., Pendyala, R., & Marneni, N. (2017). Stability of Nanofluids. In *Topics in Mining, Metallurgy and Materials Engineering*. https://doi.org/10.1007/978-3-319-29761-3_1

Islam, N. U., Amin, R., Shahid, M., & Amin, M. (2019). Gummy gold and silver nanoparticles of apricot (Prunus armeniaca) confer high stability and biological activity. *Arabian Journal of Chemistry*, *12*(8), 3977–3992.

Ivanova, N., Gugleva, V., Dobreva, M., Pehlivanov, I., Stefanov, S., & Andonova, V. (2018). Silver nanoparticles as multi-functional drug delivery systems. In *Nanomedicines*. IntechOpen.

Jain, S., & Mehata, M. S. (2017). Medicinal plant leaf extract and pure flavonoid mediated green synthesis of silver nanoparticles and their enhanced antibacterial property. *Scientific Reports*, *7*(1), 1–13.

Jamkhande, P. G., Ghule, N. W., Bamer, A. H., & Kalaskar, M. G. (2019). Metal nanoparticles synthesis: An overview on methods of preparation, advantages and disadvantages, and applications. *Journal of Drug Delivery Science and Technology*, *53*, 101174.

Kahsay, M. H. (2021). Synthesis and characterization of ZnO nanoparticles using aqueous extract of Becium grandiflorum for antimicrobial activity and adsorption of methylene blue. *Applied Water Science*, *11*(2), 1–12. https://doi.org/10.1007/s13201-021-01373-w

Kraśniewska, K., Galus, S., & Gniewosz, M. (2020). Biopolymers-based materials containing silver nanoparticles as active packaging for food applications–A review. *International Journal of Molecular Sciences*, *21*(3), 698.

Kregiel, D., Berlowska, J., Witonska, I., Antolak, H., Proestos, C., & Babic, M. (n.d.). *Saponin-Based , Biological-Active Surfactants from Plants*.

Krull, S., Brock, S., Prüße, U., & Kuenz, A. (2020). Hydrolyzed agricultural residues—low-cost nutrient sources for l-lactic acid production. *Fermentation*, *6*(4). https://doi.org/10.3390/FERMENTATION6040097

Kumavat, S. R., & Mishra, S. (2021). Green synthesis of silver nanoparticles using Borago officinalis leaves extract and screening its antimicrobial and antifungal activity. *International Nano Letters*, *0123456789*. https://doi.org/10.1007/s40089-021-00345-x

Li, W., Zhang, C., Chi, H., Li, L., Lan, T., Han, P., Chen, H., & Qin, Y. (2017). Development of antimicrobial packaging film made from poly (lactic acid) incorporating titanium dioxide and silver nanoparticles. *Molecules*, *22*(7), 1170.

Lim, S. H., Ahn, E.-Y., & Park, Y. (2016). Green synthesis and catalytic activity of gold nanoparticles synthesized by Artemisia capillaris water extract. *Nanoscale Research Letters*, *11*(1), 1–11.

Liu, H., Zhang, H., Wang, J., & Wei, J. (2017). Effect of temperature on the size of biosynthesized silver nanoparticle : Deep insight into microscopic kinetics analysis. *Arabian Journal of Chemistry*. https://doi.org/10.1016/j.arabjc.2017.09.004

Liu, X., Iocozzia, J., Wang, Y., Cui, X., Chen, Y., Zhao, S., Li, Z., & Lin, Z. (2017). Noble metal–metal oxide nanohybrids with tailored nanostructures for efficient solar energy conversion, photocatalysis and environmental remediation. *Energy & Environmental Science*, *10*(2), 402–434.

Loiseau, A., Asila, V., Boitel-Aullen, G., Lam, M., Salmain, M., & Boujday, S. (2019). Silver-based plasmonic nanoparticles for and their use in biosensing. *Biosensors*, *9*(2), 78.

Lu, P. J., Fang, S. W., Cheng, W. L., Huang, S. C., Huang, M. C., & Cheng, H. F. (2018). Characterization of titanium dioxide and zinc oxide nanoparticles in sunscreen powder by comparing different measurement methods. *Journal of Food and Drug Analysis*, *26*(3), 1192–1200.

Manosalva, N., Tortella, G., Cristina Diez, M., Schalchli, H., Seabra, A. B., Durán, N., &

Rubilar, O. (2019). Green synthesis of silver nanoparticles: effect of synthesis reaction parameters on antimicrobial activity. *World Journal of Microbiology and Biotechnology*, *35*(6), 1–9. https://doi.org/10.1007/s11274-019-2664-3

Mansour, D. A., & Atiya, E. G. (2016). *Application of UV / Vis Spectroscopy to Assess the Stability of Oil-Based Nanofluids*. 671–674.

Martínez-Abad, A., Ocio, M. J., Lagarón, J. M., & Sánchez, G. (2013). Evaluation of silver-infused polylactide films for inactivation of Salmonella and feline calicivirus in vitro and on fresh-cut vegetables. *International Journal of Food Microbiology*, *162*(1), 89–94.

Minatel, I. O., Borges, C. V., Borges, C. V., Alonzo, H., Hector, G., Gomez, G., Chen, C. O., Chen, C. O., Pace, G., & Lima, P. (2017). Phenolic compounds: functional properties, impact of processing and bioavailability, Phenolic Compounds - Biological Activity. *Open Science*, 1–24.

Monteiro, M. R., Kugelmeier, C. L., Pinheiro, R. S., Batalha, M. O., & da Silva César, A. (2018). Glycerol from biodiesel production: Technological paths for sustainability. *Renewable and Sustainable Energy Reviews*, *88*(November 2017), 109–122. https://doi.org/10.1016/j.rser.2018.02.019

Moodley, J. S., Krishna, S. B. N., Pillay, K., & Govender, P. (2018). Green synthesis of silver nanoparticles from Moringa oleifera leaf extracts and its antimicrobial potential. *Advances in Natural Sciences: Nanoscience and Nanotechnology*, *9*(1), 15011.

Moosa, A. A., Ridha, A. M., & Allawi, M. H. (2015). *Green Synthesis of Silver Nanoparticles using Spent Tea Leaves Extract with Atomic Force Microscopy*. *5*(5), 3233–3241.

Mourdikoudis, S., Pallares, R. M., & Thanh, N. T. K. (2018). Characterization techniques for nanoparticles: comparison and complementarity upon studying nanoparticle properties. *Nanoscale*, *10*(27), 12871–12934.

Muller, J., González-Martínez, C., & Chiralt, A. (2017). Combination of poly (lactic) acid and starch for biodegradable food packaging. *Materials*, *10*(8), 952.

Murugesan, S., Bhuvaneswari, S., & Sivamurugan, V. (2017). Green Synthesis, Characterization of Silver Nanoparticles of a Marine Red Alga Spyridia Fusiformis and Their Antibacterial Activity. *International Journal of Pharmacy and Pharmaceutical Sciences*, *9*(5), 192. https://doi.org/10.22159/ijpps.2017v9i5.17105

Nebu, J., Devi, J. S. A., Aparna, R. S., Aswathy, B., Lekha, G. M., & Sony, G. (2018). Fluorescence turn-on detection of fenitrothion using gold nanoparticle quenched fluorescein and its separation using superparamagnetic iron oxide nanoparticle. *Sensors and Actuators B: Chemical*, *277*, 271–280.

Nurul Aini, A., Al Farraj, D. A., Endarko, E., Rubiyanto, A., Nur, H., Al Khulaifi, M. M., Hadibarata, T., & Syafiuddin, A. (2019). A new green method for the synthesis of silver nanoparticles and their antibacterial activities against gram-positive and gram-negative bacteria. *Journal of the Chinese Chemical Society*, *66*(7), 705–712. https://doi.org/10.1002/jccs.201800412

Odukoya, J., Charles, U., & Odukoya, J. (2019). Response of Nutritional and Phytochemical Constituents of Bitter Leaf to Some Drying Methods. *International Research Journal of Pure and Applied Chemistry*, 1–10. https://doi.org/10.9734/irjpac/2019/v18i230086

Ogidi, O. I., George, D. G., & Esie, N. G. (2019). *Ethnopharmacological properties of Vernonia amygdalina (Bitter Leave) medicinal plant*. *7*(2), 175–181.

Pansara, C., Mishra, R., Mehta, T., Parikh, A., & Garg, S. (2020). Formulation of Chitosan Stabilized Silver Nanoparticle-Containing Wound Healing Film: In Vitro and In Vivo Characterization. *Journal of Pharmaceutical Sciences*, *109*(7), 2196–2205. https://doi.org/10.1016/j.xphs.2020.03.028

Piszczek, P., & Radtke, A. (2018). Silver nanoparticles fabricated using chemical vapor deposition and atomic layer deposition techniques: properties, applications and perspectives: review. *Noble and Precious Metals; Seehra, MS, Bristow, AD, Eds*, 187–213.

Preetha, D., Arun, R., Kumari, P., & Aarti, C. (2013). Synthesis and characterization of silver

nanoparticles using cannonball leaves and their cytotoxic activity against Mcf-7 cell line. *Journal of Nanotechnology*, *2013*, 1–5.

Press, D. (2016). *Biomimetic synthesis of antimicrobial silver nanoparticles using in vitro-propagated plantlets of a medicinally important endangered species : Phlomis bracteosa*. 1663–1675.

Rafique, M., Rafique, M. S., Kalsoom, U., Afzal, A., Butt, S. H., & Usman, A. (2019). Laser ablation synthesis of silver nanoparticles in water and dependence on laser nature. *Optical and Quantum Electronics*, *51*(6), 1–11.

Rao, B., & Tang, R. C. (2017). Green synthesis of silver nanoparticles with antibacterial activities using aqueous Eriobotrya japonica leaf extract. *Advances in Natural Sciences: Nanoscience and Nanotechnology*, *8*(1). https://doi.org/10.1088/2043-6254/aa5983

Rose, G. K., Soni, R., Rishi, P., & Soni, S. K. (2019). Optimization of the biological synthesis of silver nanoparticles using Penicillium oxalicum GRS-1 and their antimicrobial effects against common food-borne pathogens. *Green Processing and Synthesis*, *8*(1), 144–156. https://doi.org/10.1515/gps-2018-0042

Roy, P., Das, B., Mohanty, A., & Mohapatra, S. (2017). Green synthesis of silver nanoparticles using Azadirachta indica leaf extract and its antimicrobial study. *Applied Nanoscience*, *7*(8), 843–850.

Samuel, A. J. S. J., Vimala, A. G. K. A., & Dakshanamurthy, D. (2021). Antibacterial Activity of Ananas comosus Fruit Extract against Clinically Isolated Bacteria from Urinary Tract Infected Patients. *Journal of Pharmaceutical Research International*, *33*(February 2019), 61–70. https://doi.org/10.9734/jpri/2021/v33i24b31442

Saxena, J., Sharma, P. K., Sharma, M. M., & Singh, A. (2016). Process optimization for green synthesis of silver nanoparticles by Sclerotinia sclerotiorum MTCC 8785 and evaluation of its antibacterial properties. *SpringerPlus*, *5*(1). https://doi.org/10.1186/s40064-016-2558-x

Seifipour, R., Nozari, M., & Pishkar, L. (2020). Green Synthesis of Silver Nanoparticles using

Tragopogon Collinus Leaf Extract and Study of Their Antibacterial Effects. *Journal of Inorganic and Organometallic Polymers and Materials*, *30*(8), 2926–2936. https://doi.org/10.1007/s10904-020-01441-9

Seku, K., Hussaini, S. S., Golla, N., Rapolu, S., Bandi, R., & Reddy, B. (2020). Microwave-assisted synthesis of palladium nanoparticles using Frankincense resin and evaluation of their catalytic properties. *Materials Letters*, *278*, 128427.

Selvamani, V. (2018). Stability Studies on Nanomaterials Used in Drugs. In *Characterization and Biology of Nanomaterials for Drug Delivery: Nanoscience and Nanotechnology in Drug Delivery*. Elsevier Inc. https://doi.org/10.1016/B978-0-12-814031-4.00015-5

Shabina, S., Gaurav, S., Irfan, A. M., & Sarmad, M. (2020). Green nanotechnology: A review on nanomedicinal potential and green synthesis of silver nanoparticles (ag-np's). *Research Journal of Biotechnology*, *15*(10), 177–187.

Shah, A., Hussain, I., & Murtaza, G. (2018). Chemical synthesis and characterization of chitosan/silver nanocomposites films and their potential antibacterial activity. *International Journal of Biological Macromolecules*, *116*, 520–529.

Siddique, S., & Chow, J. C. L. (2020). Gold nanoparticles for drug delivery and cancer therapy. *Applied Sciences*, *10*(11), 3824.

Srikhao, N., Kasemsiri, P., Ounkaew, A., Lorwanishpaisarn, N., Okhawilai, M., Pongsa, U., Hiziroglu, S., & Chindaprasirt, P. (2021). Bioactive nanocomposite film based on cassava starch/polyvinyl alcohol containing green synthesized silver nanoparticles. *Journal of Polymers and the Environment*, *29*(2), 672–684.

Swamy, M. K., Sudipta, K. M., Jayanta, K., & Balasubramanya, S. (2015). *The green synthesis , characterization , and evaluation of the biological activities of silver nanoparticles synthesized from Leptadenia reticulata leaf extract*. 73–81. https://doi.org/10.1007/s13204-014-0293-6

Taurozzi, J. S., Hackley, V. A., & Wiesner, M. R. (2010). *Ultrasonic dispersion of nanoparticles for environmental , health and safety assessment – issues and*

recommendations. 1–19. https://doi.org/10.3109/17435390.2010.528846

Tham, M. W., & Liew, K. C. (2014). Influence of different extraction temperatures and methanol solvent percentages on the total phenols and total flavonoids from the heartwood and bark of Acacia auriculiformis. *European Journal of Wood and Wood Products*, *72*(1), 67–72. https://doi.org/10.1007/s00107-013-0743-y

Titus, D., Samuel, E. J. J., & Roopan, S. M. (2019). Nanoparticle characterization techniques. In *Green synthesis, characterization and applications of nanoparticles* (pp. 303–319). Elsevier.

Usunobun, U., & Ngozi, O. (2016). Phytochemical analysis and proximate composition of Vernonia amygdalina. *International Journal of Scientific World*, *4*(1), 11. https://doi.org/10.14419/ijsw.v4i1.5845

Velusamy, P., Kumar, G. V., Jeyanthi, V., Das, J., & Pachaiappan, R. (2016). Bio-inspired green nanoparticles: synthesis, mechanism, and antibacterial application. *Toxicological Research*, *32*(2), 95–102.

Verma, A., & Mehata, M. S. (2016). Controllable synthesis of silver nanoparticles using Neem leaves and their antimicrobial activity. *Journal of Radiation Research and Applied Sciences*, *9*(1), 109–115.

Vivehananthan, K., & De Silva, W. H. (2021). Effect of Different Process Parameters on the formation of Silver Nanoparticles using Crude and Modified Neem (Azadirachta indica) Leaf Extracts. *Advances in Technology*.

Wang, M., Marepally, S. K., Vemula, P. K., & Xu, C. (2016). Inorganic Nanoparticles for Transdermal Drug Delivery and Topical Application. *Nanoscience in Dermatology*, 57–72. https://doi.org/10.1016/B978-0-12-802926-8.00005-7

Widyaningtyas, A. L., Yulizar, Y., & Apriandanu, D. O. B. (2019). Ag2O nanoparticles fabrication by Vernonia amygdalina Del. leaf extract: Synthesis, characterization, and its photocatalytic activities. *IOP Conference Series: Materials Science and Engineering*, *509*(1). https://doi.org/10.1088/1757-899X/509/1/012022

Yuan, T., Zeng, J., Wang, B., Cheng, Z., Gao, W., Xu, J., & Chen, K. (2021). Silver nanoparticles immobilized on cellulose nanofibrils for starch-based nanocomposites with high antibacterial, biocompatible, and mechanical properties. *Cellulose*, *28*(2), 855–869.

Zienkiewicz-Strzałka, M., Błachnio, M., Deryło-Marczewska, A., Kozakevych, R. B., Bolbukh, Y. M., & Tertykh, V. A. (2017). Silver nanoparticles deposited on pyrogenic silica solids: Preparation and textural properties. *Adsorption Science and Technology*, *35*(7–8), 714–720. https://doi.org/10.1177/0263617417707599

Zulina, N. A., Pavlovetc, I. M., Baranov, M. A., & Denisyuk, I. Y. (2017). Optical, structural and nonlinear optical properties of laser ablation synthesized Ag nanoparticles and photopolymer nanocomposites based on them. *Optics & Laser Technology*, *89*, 41–45.

Appendix 1- Pictures of some laboratory works

AgNPs synthesized with diferent solvents

UV-Vis Spectroscopy

1%,5% and 10% AgNPs/GLYLAC/PLAFilm

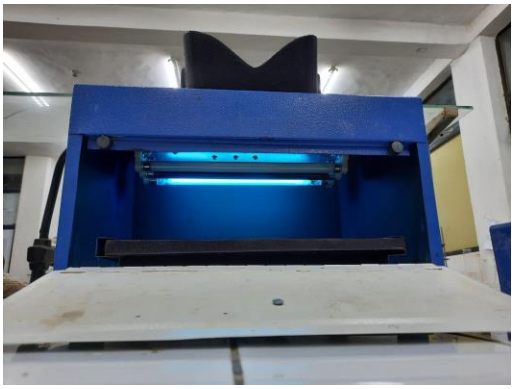

UV-Cabinet for TLC analysis